Real Time Estimation of Possible Production at Nysted

Public Version

Stephane A. Eisen

M.Sc Thesis

Technical University of Denmark
Department of Mechanical Engineering
Section of Fluid Mechanics
September 2007

ABSTRACT

This paper proposes a model for real time estimation of possible production at the Nysted Wind Plant. The model employs nacelle wind speed measurements and a power curve with an empirical correction for local flow effects about the nacelle anemometer and a dynamic wake model to account for changes in individual turbine wakes during plant regulation. An alternative control strategy that employs power rather than the nacelle wind speed measurements and requires no corrections is also presented.

Results from the model are compared with operational data from the 165 MW Nysted Offshore Wind Plant in southern Denmark and indicate an improvement in the estimate of possible production during down-regulation. The largest improvement is gained from correction of the wind speed measurement error. The wake correction contributes relatively little. Simulation results indicate that the alternative control strategy successfully estimates possible plant production. However, the overall down-regulation capability is limited to 50% since only half the turbines participate in down-regulation.

TABLE OF CONTENTS

TABLE OF APPENDICES

TABLE OF FIGURES

TABLE OF TABLES

1 INTRODUCTION

As large wind power plants grow increasingly in capacity and number compared to traditional electrical production units, they will begin to participate more actively in control of the electric power system. As such, newly developed large wind power plants are required to provide control services similar to those in traditional power plants. Providing these control services successfully requires knowledge of the wind power plant's maximum possible production to ascertain both the operational state of the plant and the financial cost of lost production during various plant control actions. A distinct difference between a traditional power plant and a wind power plant however, is that the maximum possible production of the traditional plant is known; whereas, a wind power plant's maximum possible production depends not only on the current wind conditions but also on the operational state of the wind plant.

This project investigates two different strategies for estimating possible plant production during plant control actions at the Nysted Wind Plant in Denmark. The first strategy, denoted the power curve method, is an extension of current practice at Nysted which employs Nacelle Wind Speed (NWS) measurements and a power curve to estimate possible production. To extend the performance a NWS measurement correction is developed, to account for changes in local flow effects near the NWS anemometer during down-regulation. A dynamic wake model is also proposed to account for changes in turbine wakes between normal and down-regulated operation. Attention is also given to the power curve, to improve its performance in different ambient wind conditions.

The performance of the power curve method is compared with an alternative control strategy that employs power rather than the NWS measurements and requires no corrections. This strategy splits the wind plant into two separate grids, using one grid to estimate the total plant production while the other is down-regulated to meet the desired plant output. The approach is advantageous in its simplicity, an important factor for successful implementation of a real time controller. However, an obvious drawback is that the plant regulation is limited to 50% of the possible production or less depending on the down-regulation limitations of each turbine.

A simulation model of the Nysted Wind Plant is also developed to facilitate evaluation of both estimation methods during down-regulation. It employs representation of the individual turbines at Nysted, the as-built wind plant controller, stochastic wind speed input for each turbine, stochastic plant wind direction input and includes a wake model to simulate the wind speed deficits throughout the wind plant due to individual turbine wakes. An alternative version of the simulation model, incorporating pitch-regulated turbines based on the historic 2MW Tjaereborg turbine, has also been developed to evaluate differences in performance between pitch and stall regulated wind plants.

2 PROJECT OBJECTIVES

The objective of this project is to investigate two methods for real time estimation of the possible production of a large wind plant during down-regulation. The first method employs a power curve and the Nacelle Wind Speed (NWS) measurements from each turbine to estimate the possible plant production. This method employs corrections to the NWS measurement to account for the changes in local flow effects around the NWS anemometer and wake effects throughout the wind plant during down-regulation. The second method divides the wind plant into two separate grids; using one grid to estimate the total plant production while the other is down-regulated to meet the desired plant output. The performance of both methods is characterized using historic time history measurements from the Nysted Wind Plant and simulation results.

3 NYSTED WIND PLANT DESCRIPTION

The 165.6 MW Nysted Wind Plant is located approximately 10km south of the town of Nysted, on the island of Lolland in Denmark and was commissioned in 2003. It is owned by DONG Energy A/S (80%) and E.ON Sweden (20%) and is operated by DONG (1) . It consists of 72 Siemens Wind Power (formally BONUS Wind Energy) 2.3MW Combi-Stall wind turbines arranged in a parallelogram with 9 rows and 8 columns. Power from each turbine is collected at an offshore transformer platform via a 33kV inter-array network. The voltage level is then increased to 132kV and power is transmitted via a submerged cable to an onshore point of common coupling. The plant is configured with a wind plant controller (WPC) which communicates with each turbine at all times. It receives measurement and status data from each turbine and sends control commands as necessary.

The geographical location of the Nysted Wind Plant is depicted in Figure 3-1 showing the 72 turbines in a regular parallelogram pattern 10 km south of the Lolland coast. Figure 3-2 depicts the wind plant layout in more detail and highlights the compass directions in which turbines are aligned in single rows.

Figure 3-1: Geographical Location of Nysted Wind Plant (maps taken from Google Earth, plant scale and location approximate)

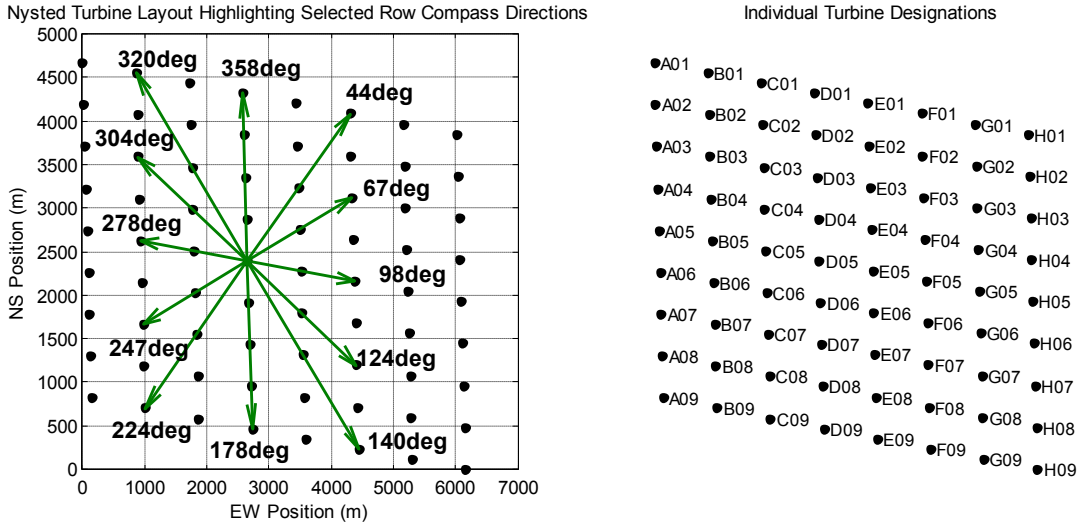

Figure 3-2: Detailed Layout of Nysted Highlighting the Compass Directions for Selected Rows.

3.1 SIEMENS 2.3MW WIND TURBINES

The Siemens 2.3MW Combi-Stall wind turbine is a 3 blade upwind machine with an 84 meter diameter rotor and 69 meter hub height. It employs active stall regulation for power limitation above rated power and a below rated power pitch angle schedule for power optimization. Additionally, it employs 2 generators; a 6 pole induction machine rated at 400kW and a 4 poles induction machine rated at 2335kW intended to optimize the rotor performance for low and high wind speed conditions, respectively. A representative power curve is provided in Figure 3-3 as a single power curve including both modes of operation.

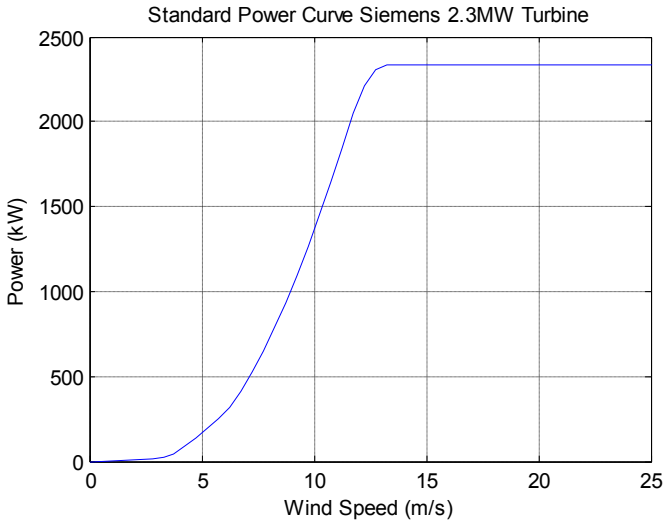

Figure 3-3: Standard Power Curve of Siemens 2.3MW Turbine

The turbine employs active stall regulation for power limitation above rated power. With this concept the rotor is increasingly pitched to stall (increasing overall angle of attack of the blades) as the wind speed increases above rated power. The pitch angle measurement data and the trajectory required for normal power limitation is depicted in Figure 3-4 and includes the below rated (wind speeds < ~ 13.5 m/s) pitch angle schedule for power optimization. A significant result of the stall regulation strategy is the limited pitch angle changes required to maintain rated power in above rated wind conditions.

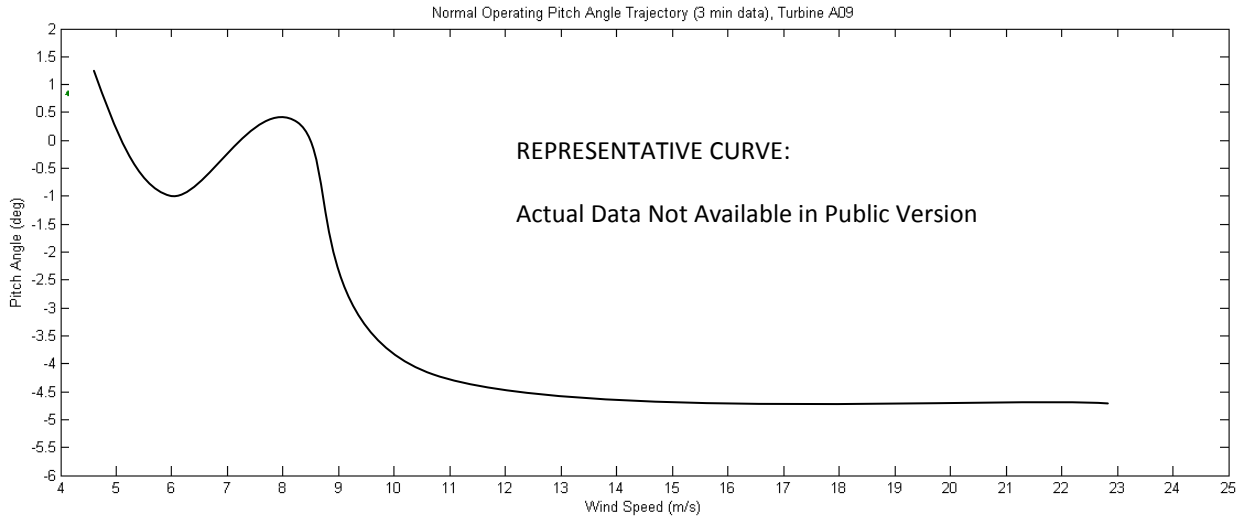

Figure 3-4: Pitch Angle Trajectory for Normal Operation

The Siemens 2.3MW turbine employs a turbine control system that provides all supervisory control functions and actively commands all turbine actuation systems such as blade pitching, nacelle yawing, high speed rotor brake, etc. The turbine control system communicates turbine measurement data and status and receives control commands from the WPC. Turbine measurement data are provided every 1 sec to the WPC and are recorded in a database for further analysis. Salient measurement quantities used throughout this present work include:

- Turbine Status
- Generator Status
- Blade Pitch Angle
- Generator Power
- Nacelle Wind Speed
- Yaw Angle

The turbine status and generator status data consist of integer values corresponding to a specific turbine conditions. Table 3-1 lists the possible status values and Table 3-2 the generator values. These values are used extensively in this present work to effectively sort measurement data for analysis.

Turbine Status				
Value	Description	Transition Criteria	Transition	Shutdown Type
0	Online	N/A	N/A	N/A
1	Startup / Synchronization	Startup / Synchronization Complete	0	N/A
2	Waiting for Release to Run	Release to Run Command	1	N/A
3	Waiting for Wind	Sufficient Wind	3	N/A
4	Pitch Bearing Greasing	Completion	3	Power Ramp to Zero then Disconnect
5	Cable Unwind	Completion	3	Power Ramp to Zero then Disconnect
6	High Wind Stop	10 min avg wind < 18 m/s	3	Power Ramp to Zero then Disconnect
7	Grid Failure	Returned Grid	3	Generator Disconnected Immediately
8	Fault	Automatically Cleared	3	Generator Disconnected Immediately
9	Fault	Manually Cleared	3	Generator Disconnected Immediately
10	Stop	Cleared	3	Power Ramp to Zero then Disconnect
11	Remote Stop	Cleared	3	Power Ramp to Zero then Disconnect

Table 3-1: Possible Turbine Status Values

Generator Status			
Value	Description	Transition Criteria	Transition to
0	Offline	N/A	2,4
1	Small Generator Connected	N/A	0
2	Small Generator Connecting	N/A	1
3	Large Generator Connected	N/A	5
4	Large Generator Connecting	N/A	3
5	Large/Small Generator Disconnecting	Generator Power < 0	0

Table 3-2: Possible Generator Status Values

3.2 WIND PLANT CONTROLLER

The wind plant controller (WPC) is the primary means of controlling the wind plant for power regulation and maintenance activities. It receives all measurement and status data and issues start/stop, set-point and maintenance commands from/to each turbine as necessary. It can also provide primary and secondary network control services if configured to do so, similar to a conventional power plant, to help support the electrical network at the point of common coupling (PCC). Primary control supports frequency stability, and secondary control supports the balance of power exchanges in a control area of the plant (2) . These control services are provided by controlling active and reactive power output of the wind plant (in this present work reactive power control is not considered). In practical terms, the local transmission system operator (TSO) or plant operator can issue control commands to the WPC, and the WPC responds by issuing active and reactive set-point commands to the individual turbines. This occurs in a controlled manner so that the aggregated plant output meets the desired control objectives. The overall control envelop is constrained by the ambient wind conditions, the individual turbine operating limitation and the turbine availability.

The available control actions available at Nysted to achieve primary and secondary control include:

Absolute Limitation Control – During periods of reduced transmission capacity the TSO may request that the overall wind plant production be limited to an absolute maximum value. Figure 3-5 depicts simulation results of absolute limitation control. At time 100 minutes the absolute limitation control is activated and the plant production set-point is reduced to the limit value to 120MW. Subsequent production is limited to this value regardless of the possible production. The absolute limitation is deactivated at time 500 minutes.

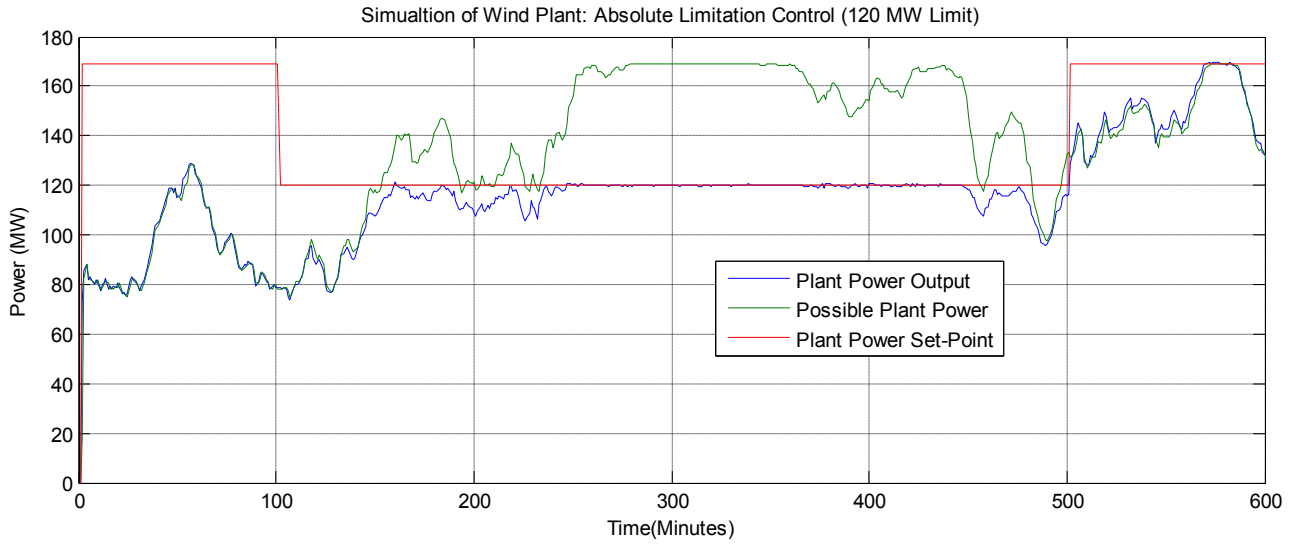

Figure 3-5: Example of Absolute Limitation Control

Delta Control – During some periods the wind plant may be operated as a spinning reserve. In this case the WPC maintains the plant production at an adjustable number of MWs below the total possible production. Figure 3-6 depicts simulation results of delta control. At time 100 minutes the delta control is activated and the plant production set-point is reduced 20MW below the possible production and maintained until the delta control is deactivated at time 500 minutes.

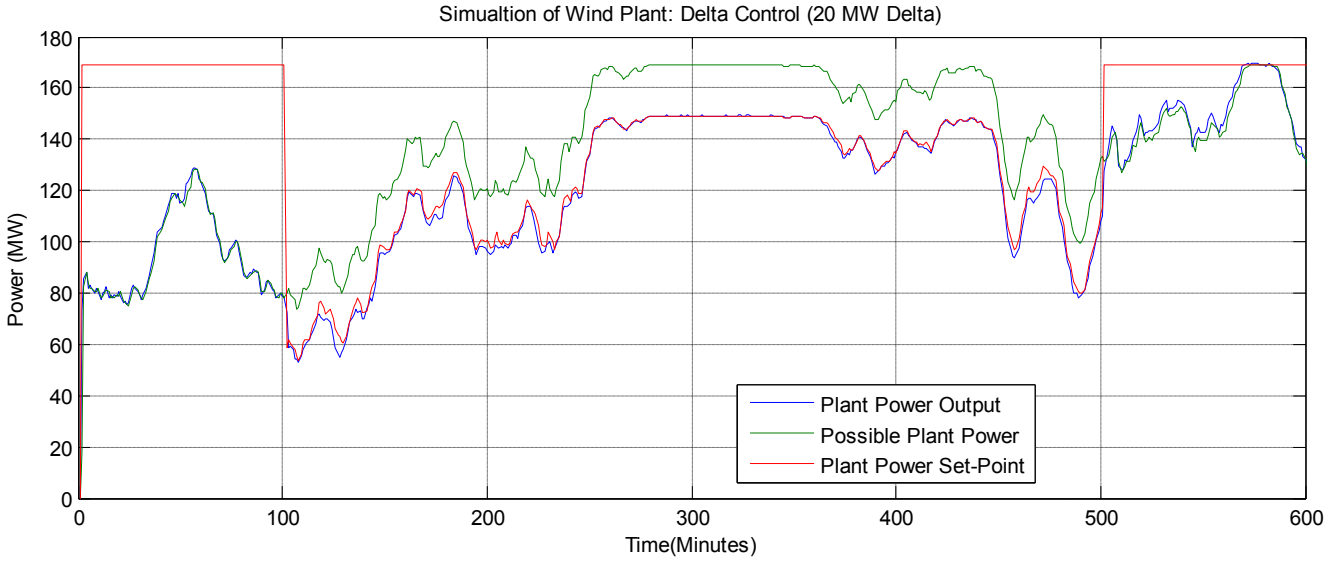

Figure 3-6: Example of Delta Control

Rate Limitation Control – During periods of fast power output variations, caused predominately by passing weather fronts, the WPC can limit the positive power production rate. Figure 3-7 depicts simulation results of rate limitation control. At time 100 minutes the rate limitation control is activated and the plant production set-point is follows the possible production but limits the positive power rate to 1MW/min The rate limitation control is deactivated at time 500 minutes.

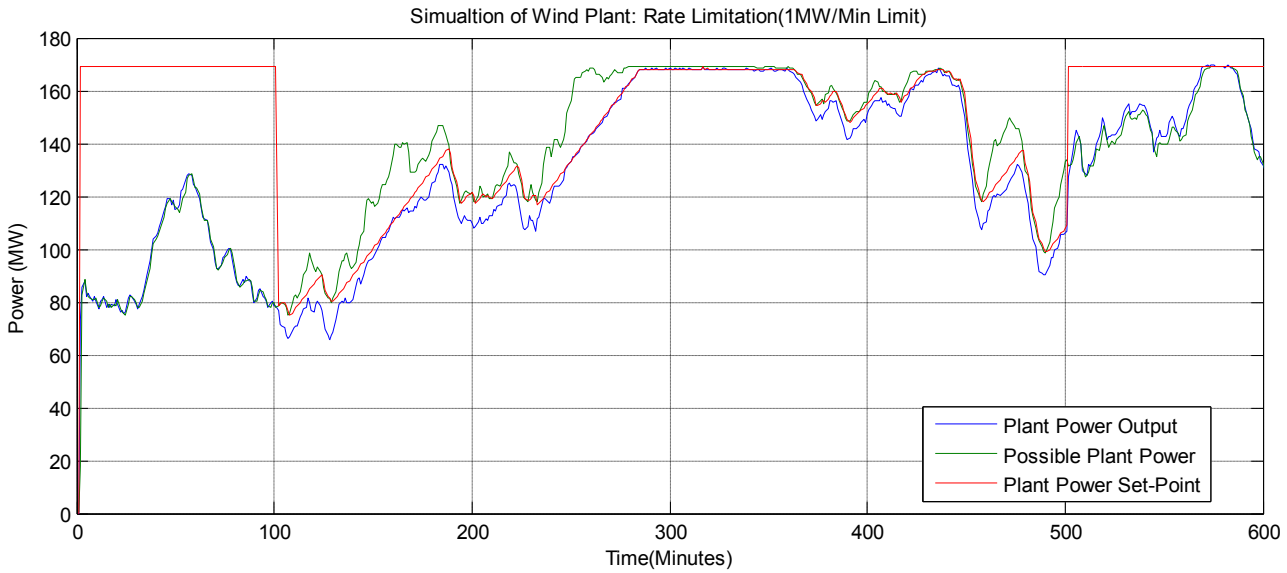

Figure 3-7: Example of Rate Limitation Control

Balance Control – During certain periods the TSO may request a specific production schedule to help maintain the local power exchanges in the area. Figure 3-8 depicts simulation results of balance control. At time 250 minutes a 120 MW dispatched order is issued. A 90 MW dispatch order is subsequently requested at 330 minutes. The orders are canceled at 425 and 500 minutes respectively.

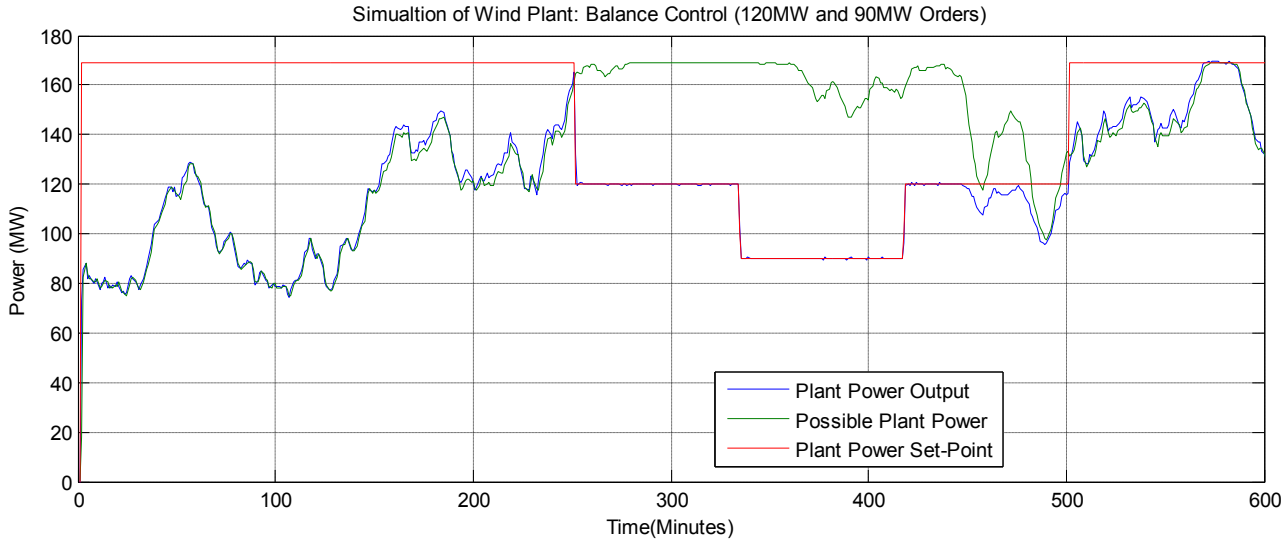

Figure 3-8: Example of Balance Control

Frequency Control – During certain periods the wind plant may participate in frequency control of the network. The WPC responds to network frequency deviations by adjusting the active production on a proportional basis. Figure 3-9 depicts the general relationship between frequency deviation and the active production response. To effectively provide frequency control the wind plant must operate with a delta value so that the production can be both down and up-regulated to respond to both over and under frequency conditions.

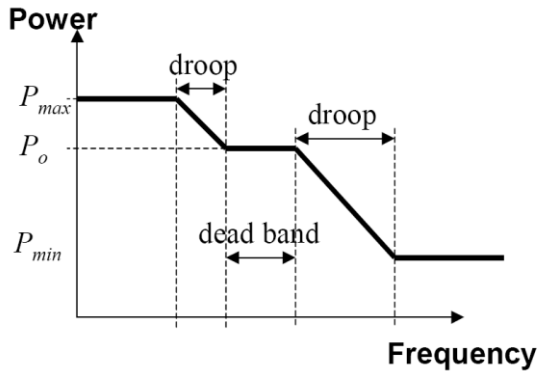

Figure 3-9: Proportional Relationship between Frequency and Plant Power (taken from ref XX)

Voltage Control – During certain periods the wind plant may participate in voltage control at the PCC. The WPC responds to voltage deviations (measured at the PCC) by adjusting the reactive power production of the plant (voltage control is not considered in this present work).

The preceding control actions determine the overall plant production set-point. The WPC however, must also distribute the overall set-point values to the individual turbines. The algorithm used to determine the distribution of individual turbine set-points is depicted in Figure 3-10 and is derived from the as-built WPC controller specification (3). The basic idea behind the algorithm is to only adjust the individual set-points of the turbines that have possible production greater than the mean desired set-point value (plant set point divided by the number of turbines online). The set-point controller iterates to ensure that the number of turbines which are above the mean desired set-point value does not change when the new set-point values are calculated.

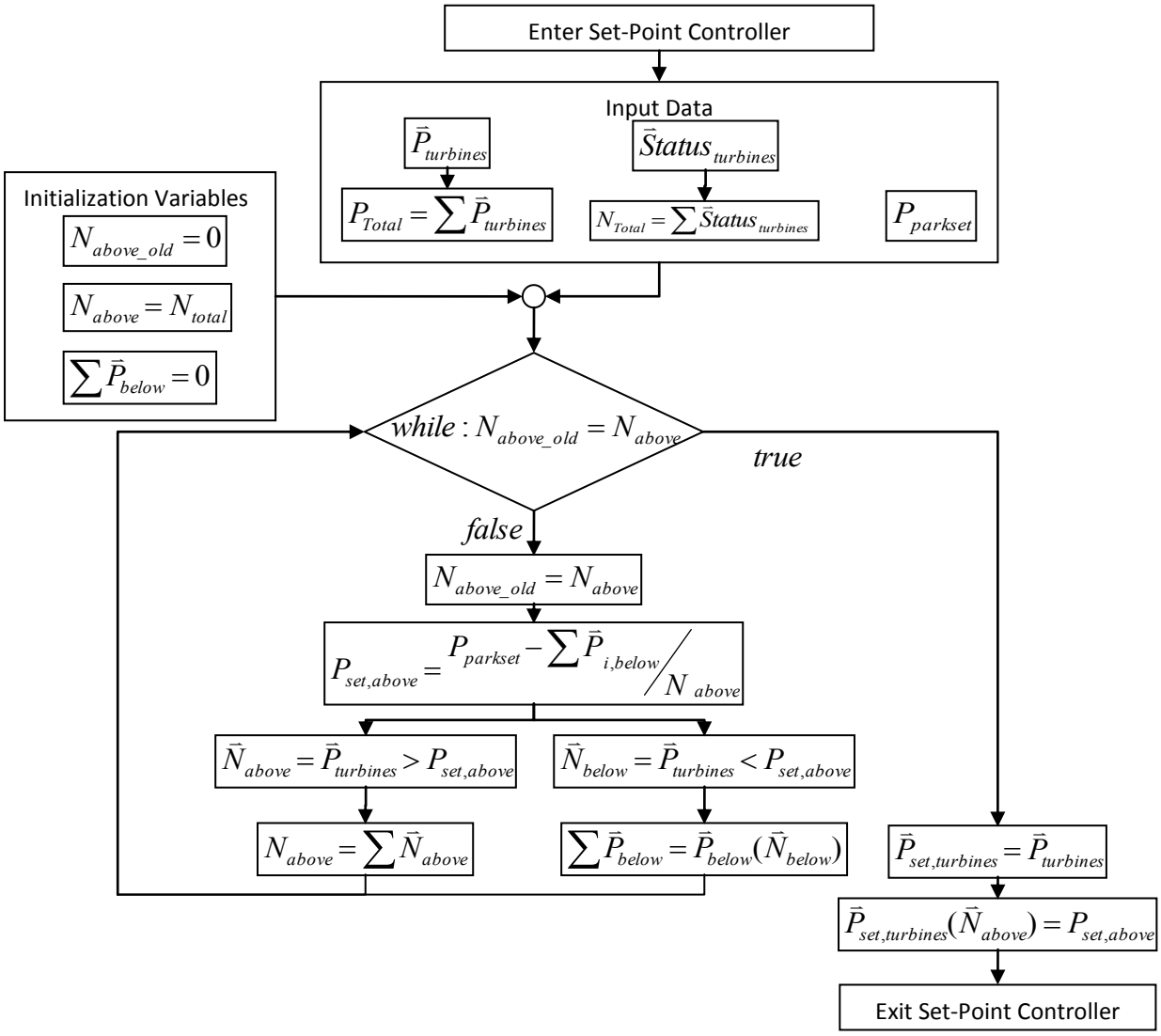

Figure 3-10: Turbine Set-Point Distribution Algorithm

To successfully execute the plant control actions the WPC requires an estimate of the total possible production during operation. During normal operation the total possible production is the actual production since all turbines are producing their maximum power. During regulation at Nysted the WPC calculates the total possible production as a sum of the possible production from the individual turbines, employing a unique power curve for each turbine and the corresponding nacelle wind speed measurement. The unique power curves for each turbine are continually updated using 10 second mean power and wind speed values. As new mean values are added the oldest values are discarded. The power curve is only calculated during normal operation, i.e. no plant regulation so that it represents the maximum possible production for all wind speeds. The power curves are also compensated for temperature dependent air density variations. The effectiveness of the estimation of possible production is critical to achieving the WPC objectives.

4 ESTIMATION OF POSSIBLE PLANT PRODUCTION AT NYSTED

Real time estimation of possible plant production is important for successful control of wind power plants which participate actively in power system control. Estimation of a wind power plant's maximum possible production depends not only on the current wind conditions but also on the operational state of the wind plant. In this present work 2 different strategies are investigated for estimation of the possible plant production during wind plant control regulation.

The first method, denoted the power curve method, is an extension of current practice at Nysted which employs Nacelle Wind Speed (NWS) measurements and a power curve to estimate possible production. To extend the method to provide better performance during down-regulation, a NWS correction is developed to account for the changes in local flow effects in the vicinity of the NWS anemometer. A dynamic wake model is also proposed to account for changes in turbine wakes between normal and down-regulated operation. Attention is also given to the power curve, to improve its performance in different ambient wind conditions.

The power curve method is also compared to an alternative control strategy, denoted the grid method, that requires no wind speed measurement error correction or wake model development. The grid method splits the wind plant into two separate grids; one grid is used to estimate the total plant production while the other is down-regulated to meet the desired control objectives.

In this present work, all analysis of measurement and simulation data are preformed based on 3 min mean values. This provides a worst case estimate since the local TSO where Nysted is connected requires that wind plant control actions be evaluated based on 5 minute mean values measured at the PCC (4).

4.1 POWER CURVE METHOD

The power curve method is intended to estimate the possible wind plant production at Nysted during down-regulation. It employs various turbine and plant data in addition to 3 corrections to estimate the possible production of each turbine and subsequent total plant production. The input data and corrections employ in the power curve method are summarized in Table 4-1.

Input Data	Corrections
Individual Turbine NWS	NWS Correction
Individual Turbine Status	Plant Wake Correction
Individual Turbine Yaw Angle	Air Density Correction
Individual Turbine Pitch Angle	
Plant Air Temperature	
Plant Air Pressure	
Plant Humidity	

Table 4-1: *Required Input Data and Corrections for Power Curve Method*

The salient feature of the power curve method are discussed in the following sections followed by an outline of the implementation and an evaluation of the power curve methods' performance.

4.1.1 CALCULATION OF POWER CURVES

The power curves employed in the estimation of possible production with the power curve method are derived from turbine A09 at Nysted. The intent was to initially follow IEC 61400-12(5) to calculate a single standard power curve. However, this approach gives unsatisfactory results for use in real time estimation of the turbine production since (5) is intended to capture long term statistical behavior of the wind turbine and does not account for real time variations in ambient wind conditions. Additionally (5) is intended for comparing different wind turbine configurations and as such

requires a reference wind speed measurement from which comparisons can be made. The reference wind speed measurement is not the measurement employed in power curve method. A power curve based on the NWS measurement gives better correlation than a reference wind speed measurement located some distance from the turbine.

In this present work the turbulence intensity is taken as a measure of the ambient wind conditions and is included in the calculation of the power curve. The turbulence intensity is calculated directly from each NWS measurement to give an indication of the local ambient wind conditions. Subsequently, a family of power curves based on turbulence intensity, employing the A09 NWS and power measurements gives better performance for estimating the possible plant production. The measurement data consists of 3min average between 113 and 343 degrees yaw to ensure the measurements do not include wakes from surrounding turbines. The data employed in the calculation are depicted in Figure 4-1.

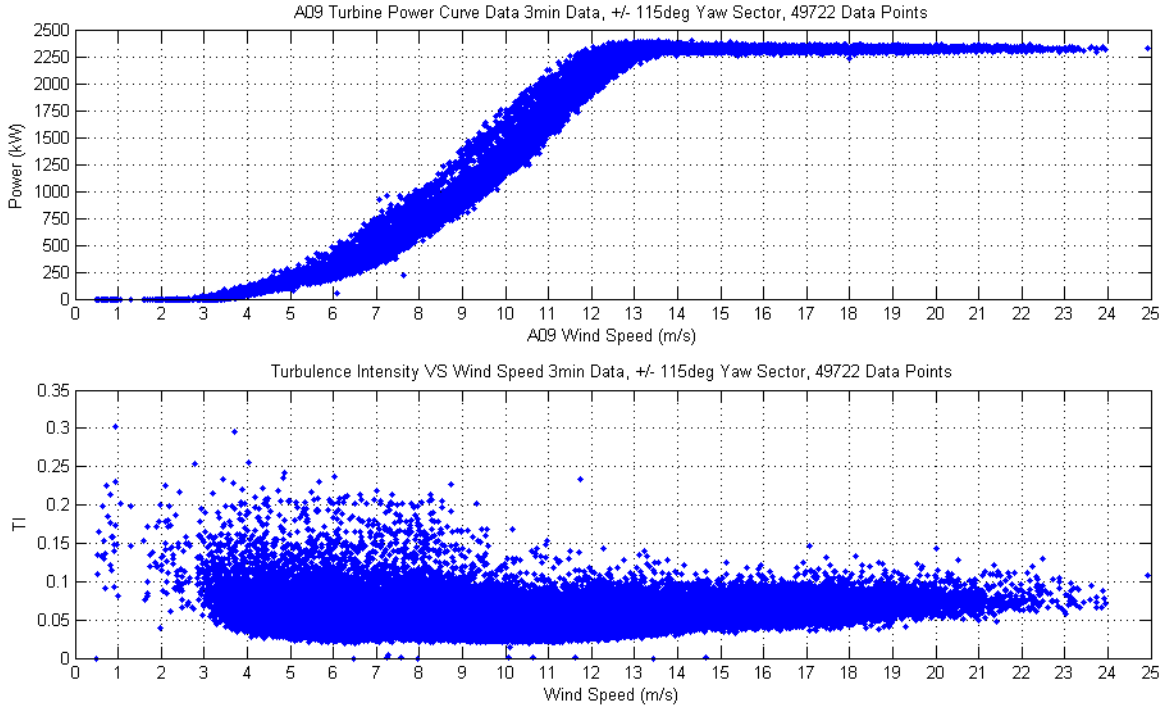

Figure 4-1: Measurement Data for Calculation of TI Based Family of Power Curves

In this present work the family of power curves are calculated as follows:

1. The raw data is decimated to 3 minute values
2. The A09 NWS is corrected to the equivalent ISO standard atmosphere with the equation 5 in (5):

$$U_{A09NWS,corrected} = U_{A09NWS} * \left(\frac{\rho}{\rho_{ref}}\right)^{1/3}$$

3. The corrected A09 NWS and power values are sorted; removing all offline data, down-regulated data, data during rain showers, and data outside yaw angles between 113 and 314 degrees.
4. The turbulence intensity is calculated as the standard deviation of the a 3 minute segment of 1 second A09 NWS values divided by the 3 minute mean value of the segment.
5. The data are binned by turbulence intensity (TI).

6. A power curve is calculated for each TI bin, applying the method of bins described in (5) for wind speeds between 4 and 14 m/s (wind speeds greater than this are not requires since the turbine reaches rater power at approximately 13.5 m/s).
7. The mean power value of all bins at 14m/s is used to linearly extrapolate the power curve to 30 m/s.

The resulting family of power curves are depicted in Figure 4-2. Note that for a given wind speed below rated power, the power varies approximately 300kW (12.9% of rated power) between the minimum and maximum turbulence intensity bins of 3% and 10% , respectively. The power curve calculated according to (5) (except for employing 3 min measurement points) is also depicted in Figure 4-2 as the "all data" curve and deviates up to 200kW (8.5% of rated power) from the TI based power curves.

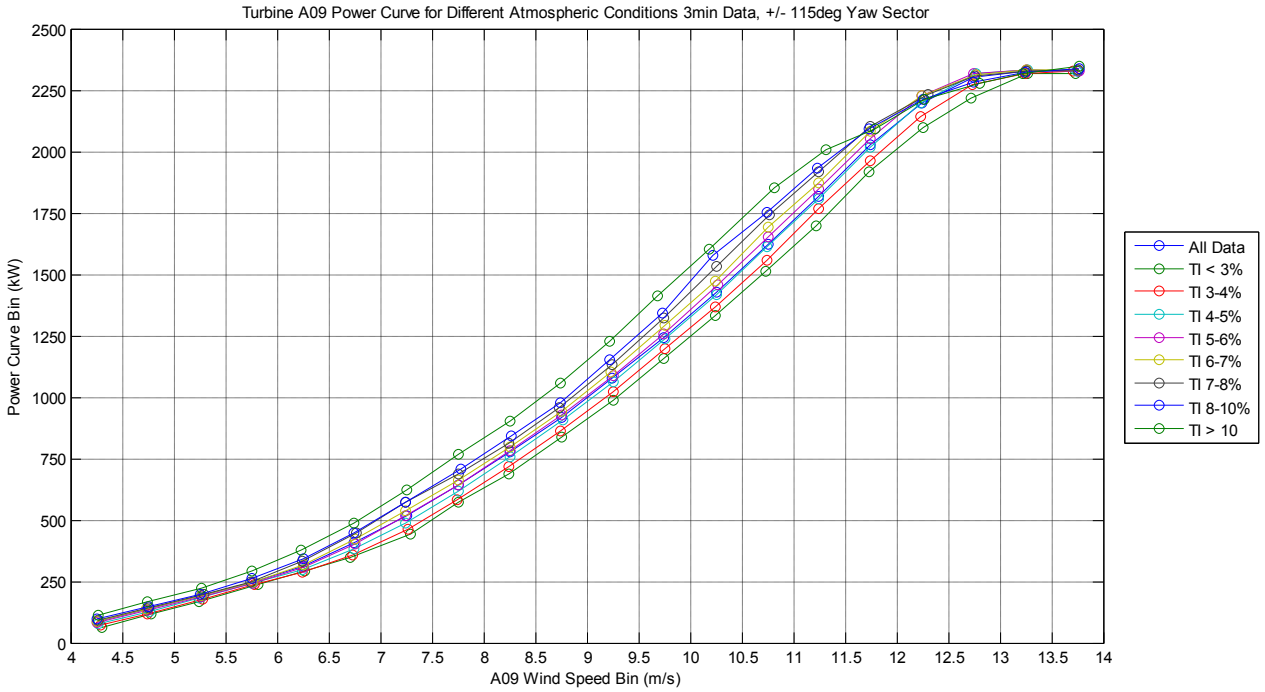

Figure 4-2: TI based Power Curves

4.1.2 NACELLE WIND SPEED CORRECTION

Estimation of the possible production based on the power curve method employs the NWS measurement of each turbine in the wind plant as primary input. The measurement consists of a nacelle mounted cup anemometer located approximately 5 meters above the rotor axis and 15 meters downwind of the rotor plane. The NWS correction accounts for changes in local flow conditions due to near wake effects generated by the rotor. Previously, near wake effects at Nysted were investigated by(6). The NWS measurement was found to "speed up" relative to a reference wind speed measurement as the blade pitch moves increasingly negative (Nysted turbines are stall regulated) during down-regulation. The "speed up" effect, caused predominantly by changes in the near rotor wake are accounted for to accurately estimate the possible production during down-regulation. The NWS correction is intended to correlate the NWS measurement to an equivalent rotor wind speed, U_{EWRS}, which represents the mean wind speed of entire rotor disk immediately upwind of the rotor. U_{EWRS} is then used as input to a power curve to subsequently estimate the possible production during down-regulation. Determination of the U_{EWRS} is depicted graphically in Figure 4-3 where U_{NWS} is the NWS measurement and θ_{blade} is the blade pitch angle of one blade (turbines at Nysted are collectively pitched).

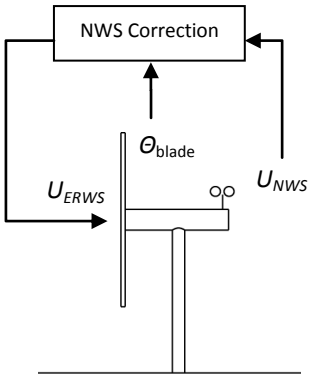

Figure 4-3: Application of the NWS Correction to U_{NWS}

In this present work the previous investigation of the NWS correction is extended to include additional analysis of limited down-regulated operating data. Afterwards a frequency analysis of the NWS and pitch angle is presented which highlights the effect of changing local flow conditions on the NWS measurement and provides a basis for investigating the alternative method for determining the NWS correction.

4.1.2.1 PREVIOUS WORK

The method previously described by (6) for determining the NWS correction and extended in this present work is derived from the following measurement data recorded at the Nysted Wind Plant: turbine A09 NWS (U_{A09}), turbine A09 blade pitch angle, and met mast MM1 69 meter (rotor hub height) wind speed (U_{mm1}). The data are limited to +/- 22.5 degrees yaw from nominal alignment between A09 and MM1 so that wake effects from surrounding turbines are excluded from the analysis. The spatial relationship between MM1 and A09 is depicted in Figure 4-4.

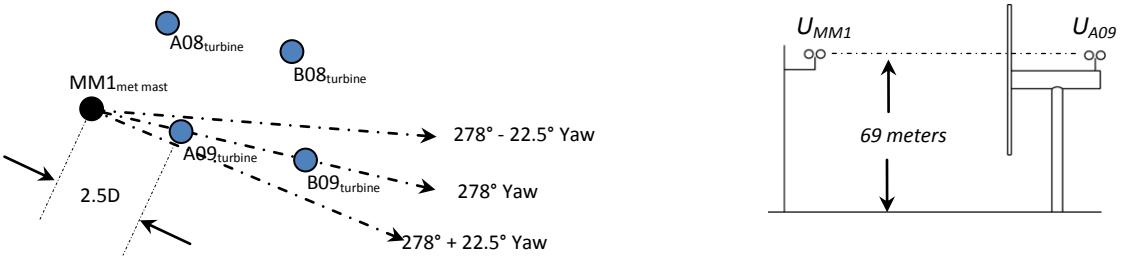

Figure 4-4 : Layout of MM1 and A09 for Calculation of the NWS Correction

The correction is calculated as the ratio between each 3min average wind speed measurement at MM1 and A09. The ratios are then binned by pitch angle to create a NWS correction lookup table as a function of pitch angle. Both the measurements and the binned values with standard deviation error bars are depicted in Figure 4-5. Notice that the very limited down-regulation data exists (pitch angle values less than -5.5 degrees during operation). The NWS Correction is applied by multiplying the NWS measurement with the correction during operation.

The NWS correction values reveal that U_{A09} "speeds up" relative to U_{mm1} during down regulation. In Figure 4-5 values greater than 1 indicate that the U_{A09} (denominator of the ratio) is less than the reference U_{mm1}. Estimation of the possible plant production ***without*** applying the NWS correction over-predicts the wind speed at each turbine approximately 4-5% at -10.0 degrees pitch. This corresponds to approximately a 12-16% over-prediction in the plant power.

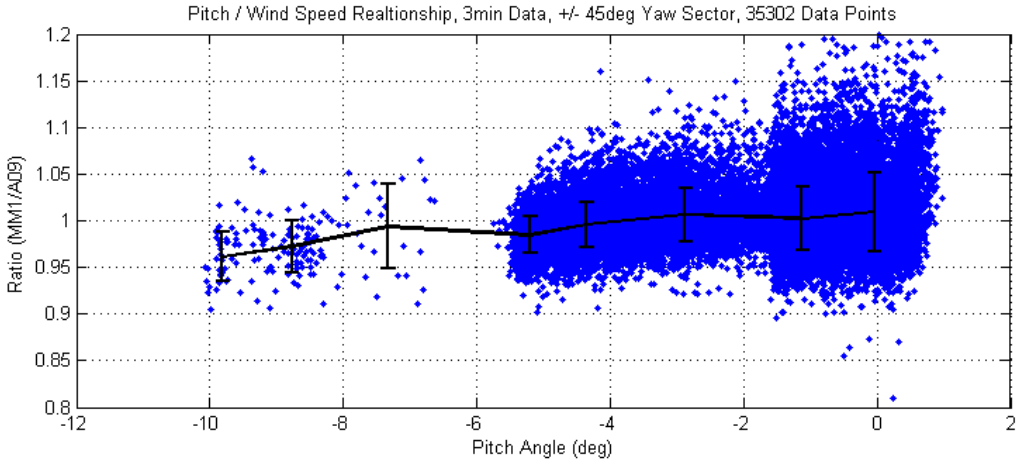

Figure 4-5: Measurement Data and Fit for the NWS Correction

A significant assumption in calculation of the NWS correction is that the A09 and MM1 wind speed measurements are well correlated. This is important since the NWS correction is calculated as:

$$NWS(\theta)_{correction} = U(\theta,t)_{A09}/U(t)_{MM1}$$

Where $U(\theta,t)_{A09}$ can be separated into a part that is solely a function of pitch angle $U(\theta)_{A09}$ and a stochastic part based only on time $U(t)_{A09}$. This implies that to isolate the effect of pitch angle changes on U_{A09}, $U(t)_{MM1}$ and $U(t)_{A09}$ should be perfectly correlated (i.e. have the same value at any time t). In practice this is not possible since the wind is both stochastic and the measurements are some distance apart compared to the distance scales of the turbulent wind structures. This results in uncertainty in the calculation of the NWS Correction.

Another consideration for employing the U_{mm1} as a reference is that a calibration error between U_{mm1} *and* U_{A09} will have a direct impact on the calculated NWS Correction ratios. The relative calibration error between MM1 and A09 is depicted in Figure 4-6. A narrow yaw sector and long averaging time was chosen to attempt to maximize the correlation between the measurements to capture their relative error. The results indicate that U_{mm1} *and* U_{A09} are within approximately 1.5% over the wind speed range of interest (7-14m/s). The bias error between U_{mm1} *and* U_{A09} is accounted for in the NWS Correction by multiplying the binned calibration ratios in Figure 4-6 with U_{A09} before calculating U_{mm1}/U_{A09}.

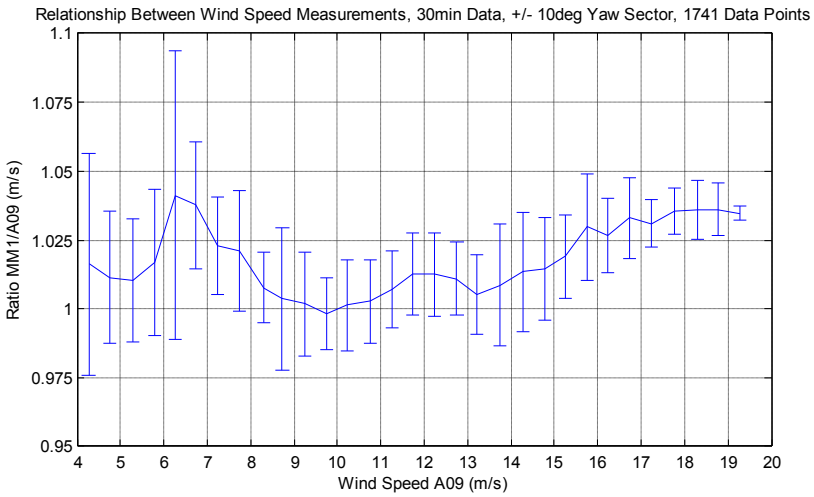

Figure 4-6: *Relationship Between the Reference Wind Speed(MM1 and NWS (A9) for varying Wind Speeds*

4.1.2.2 FREQUENCY ANALYSIS OF NWS MEASUREMENT

A frequency analysis of the NWS measurement during below rated operating highlights the effect of the pitch angle on the wind speed measurement. During below rated operation the nominal pitch angle, determined from the below rated power optimization pitch schedule, includes a superimposed square wave pitching action at a regular frequency and amplitude. This pitch action is added to facilitate continual pitch bearing lubrication. The top plot of Figure 4-7 depicts sample time history of U_{mm1} *and* U_{A09} and the pitch angle for below rated operation. The bottom plot of Figure 4-7 depicts the same measurement quantities for above rated operation which does not include a superimposed square wave. A frequency analysis of the measurements reveals that the superimposed square wave pitching actions causes a corresponding change in the U_{A09} (Figure 4-8, top). The first harmonic of the square wave is visible in both the NWS and pitch angle PSDs at 8.3mHz (precisely the square wave's fundamental frequency). The 3^{rd},5^{th},7^{th} and 9^{th} harmonics are also clearly visible in both measurements. For reference $U_{mm1}$is also included and does not include any harmonics related to the square wave pitch action. The bottom plots of Figure 4-8 shows the same frequency analysis for above rated operation. The frequency content of the U_{A09} and the pitch angle do not show the same explicit relationship. These results highlight the direct effect of pitch angle changes on U_{A09} for even small pitch angles changes and indicate that the near wake changes rapidly to pitch angle changes measured by U_{A09}.

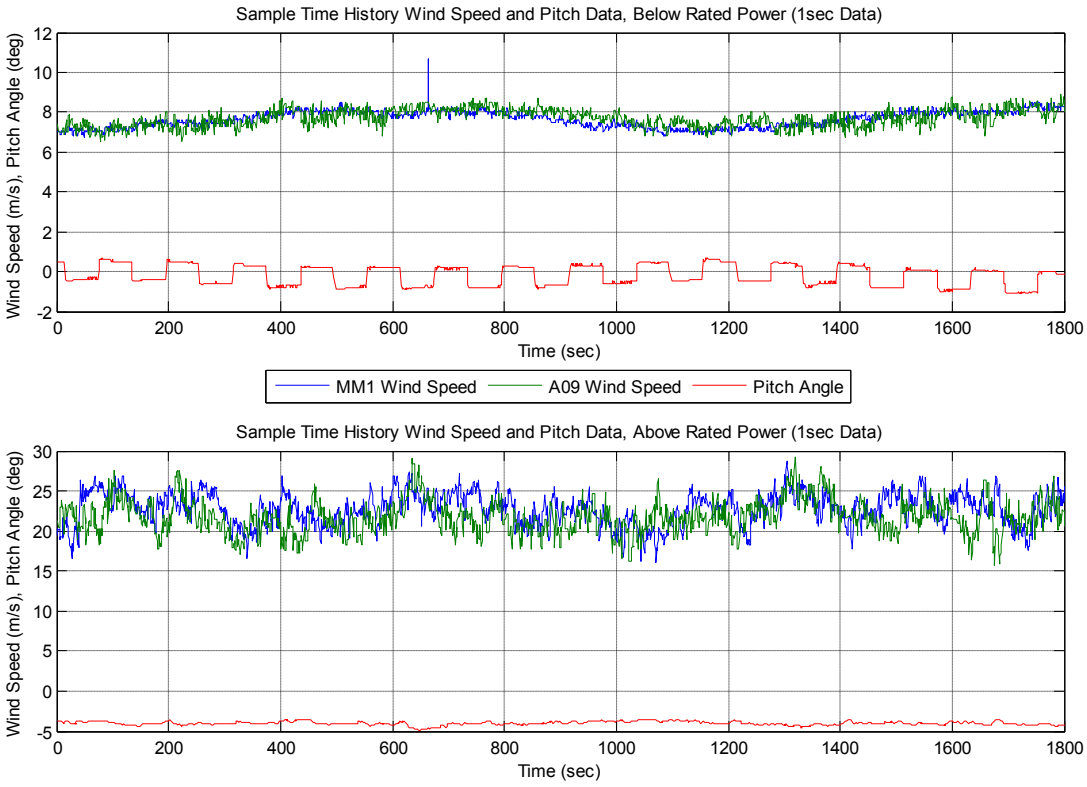

Figure 4-7: Sample Time History of MM1 and A09 Wind Speeds and Pitch Angle for Below (top plot) and Above Rated Operation

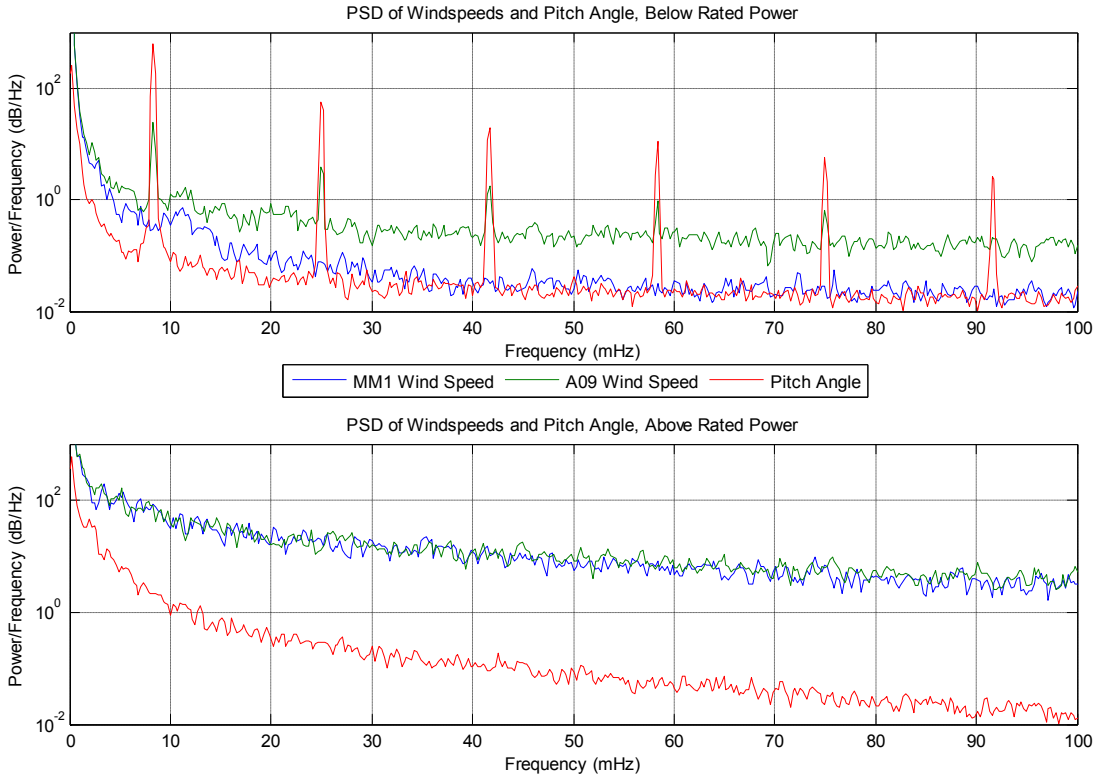

Figure 4-8: PSDs of MM1 and A09 Wind Speeds and Pitch Angle for Below (top plot) and Above Rated Operation

4.1.2.3 ALTERNATIVE METHOD

An alternative method for determining the NWS Correction is based on analysis of approximately 21000 unique turbine shut-down events recorded over 498 days of historic operating data at Nysted. This approach overcomes the 2 areas of uncertainty associated with the previously described method; a lack of statically significant measurement data and the relatively poor correlation between U_{mm1} *and* U_{A09} due to distance between them.

During a turbine shutdown the blade pitch angle is ramped towards the negative pitch limit to reduce the rotor power to zero and subsequently generate adequate negative rotor torque to absorb the rotational energy of the rotor This initial pitching action during shut-down is similar to a down-regulation event except that in this case the blade pitch continues beyond the maximum down-regulation point of approximately -15.0 degrees. The initial part of the shut-down, where the power is ramped to zero is a transient event, lasting no more than 10-15 seconds, compared to down-regulation which can last orders of magnitude longer (hours time scale). Extending the dynamic response of the NWS measurement to conditions during down-regulation is a significant assumption of this approach which requires further investigation. During the initial part of the shut-down, the NWS correction (NWS_{cor}) for varying pitch angles is determined as:

$$NWS_{correction}\ (\theta, U_{NWS\ Ref}) = U(\theta)_{NWS} / U_{NWS\ Ref}$$

Where $U_{NWS\ Ref}$ corresponds to the NWS measurement at the initiation of shut-down and $U(\theta)_{NWS}$ is the NWS measurement for varying pitch angles during the shut-down. To ensure that $U_{NWS\ Ref}$ corresponds to the initiation of shut-down the NWS measurement data are time shifted 2 second to approximate the transport time of the wind parcel affected by the pitch angle change. A two second time shift corresponds to the wind parcel traveling 15 meters at 7.5 meters per second. The approach is depicted graphically in Figure 4-9 and measurements from an actual shutdown are depicted in Figure 4-10. Variable transport should be considered in future work

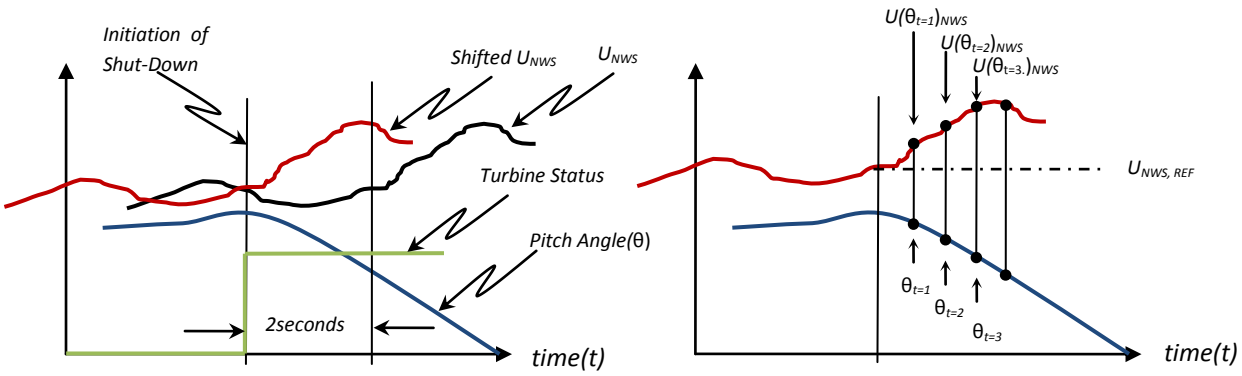

Figure 4-9: Alternative NWS Correction Approach

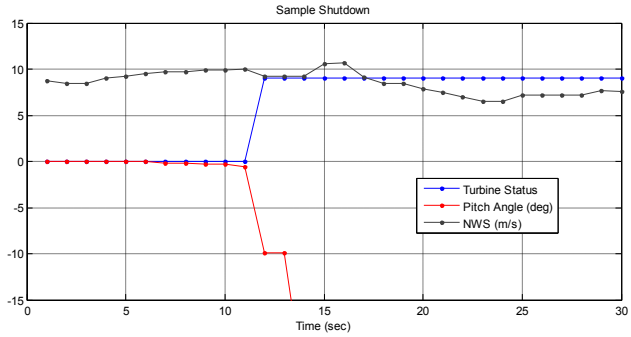

Figure 4-10: Sample Shutdown Event

During the shut-down event the stochastic ambient wind inflow results in a corresponding stochastic response of the NWS measurement to pitch angle changes relative to $U_{NWS\ Ref}$. Assuming the NWS measurements are normally distributed in the local vicinity of $U_{NWS\ Ref}$ the NWS Correction corresponds to the bias in the calculated NWS ratios for varying pitch angles. Figure 4-11 depicts the resulting NWS correction ratios, as a function of pitch angle from processing of approximately 21000 unique shut-down events at Nysted. A simple binned fit of the NWS Correction ratios is also include and shows the same trend as that found in Figure 4-5.

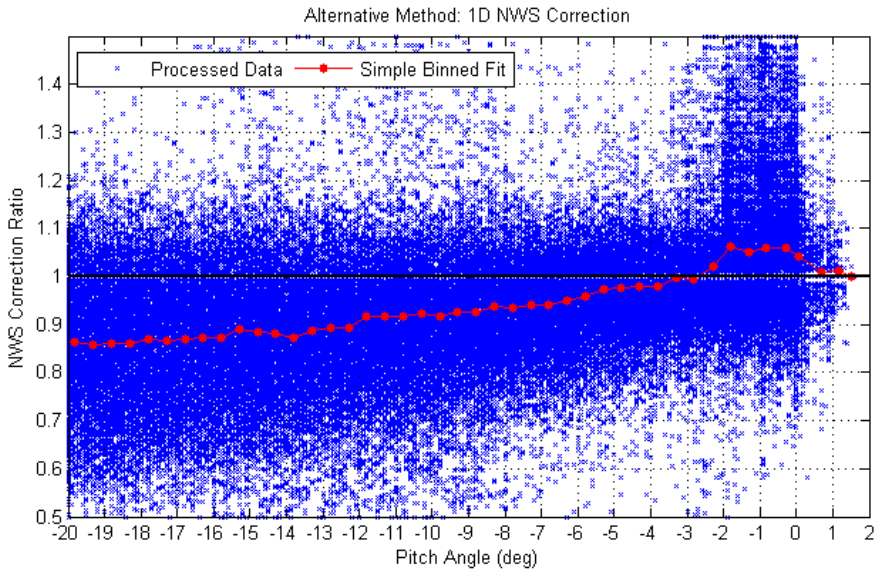

Figure 4-11: NWS Correction Ratios as a Function of Pitch Angle

An important assumption with this approach is that the pitch angle at the commencement of shutdown is always the same so that $U_{NWS\ Ref}$ can be directly compared from shut-down to shut-down. However, this is not always the case since the pitch angle can vary between approximately 1 and -3 degrees in below rated operation (the NWS correction is not relevant above rated power) so $U_{NWS\ Ref}$ does not always correspond to the same pitch angles. Future work should consider the effect of the initial pitch angle on $U_{NWS\ Ref}$.

The resulting data set is also processed as function of pitch angle and wind speed, resulting in the NWS Correction ratios depicted in Figure 4-12 as color intensity values according to the color-bar legend at the bottom of the figure. Additionally, ISO Coefficient of Thrust (C_T) contour lines, derived from blade element momentum calculations for the Nysted turbines, are overlaid in the figure. The NWS Correction ratios roughly follow the ISO C_T contour lines; where greater "speed up" of the NWS measurement corresponds to higher rotor C_T.

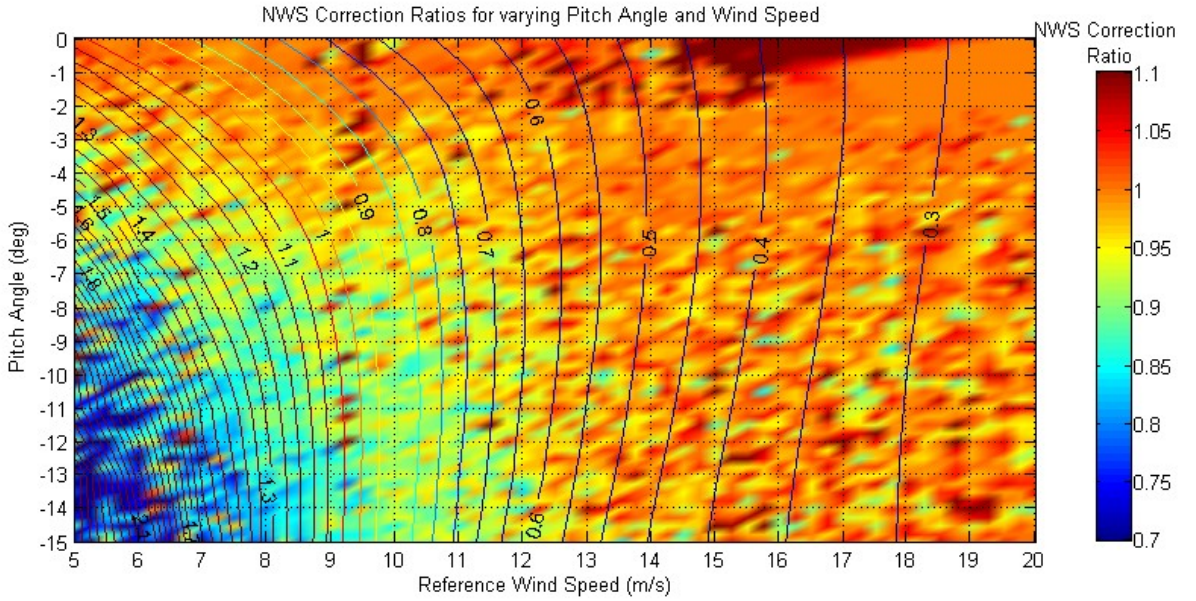

Figure 4-12: 2-D NWS Correction with Overlaid ISO Rotor C_T Contour Lines

4.1.3 DYNAMIC PLANT WAKE MODEL

The dynamic plant wake model (DWM) accounts for changes in individual turbine wakes in real time during down-regulated operation to estimate the wind speeds that would exist if no down-regulation had occurred. It is based on application of the simple wake model originally proposed by (7)and later expanded by(8). The dynamic plant wake model applies the simple wake model in both inverse and forward directions. The inverse direction removes the wind speed deficits caused by the wakes of down-regulated turbines and estimates a U_{free}. U_{free} represents the wind speed that would exist at each turbine location if no turbines (and their subsequent wakes) where actually there. U_{free} are then used as input to the forward application of the wake model which adds the wind speed deficits that would exist during normal operation. An graphical overview of the DWM is depicted in Figure 4-13.

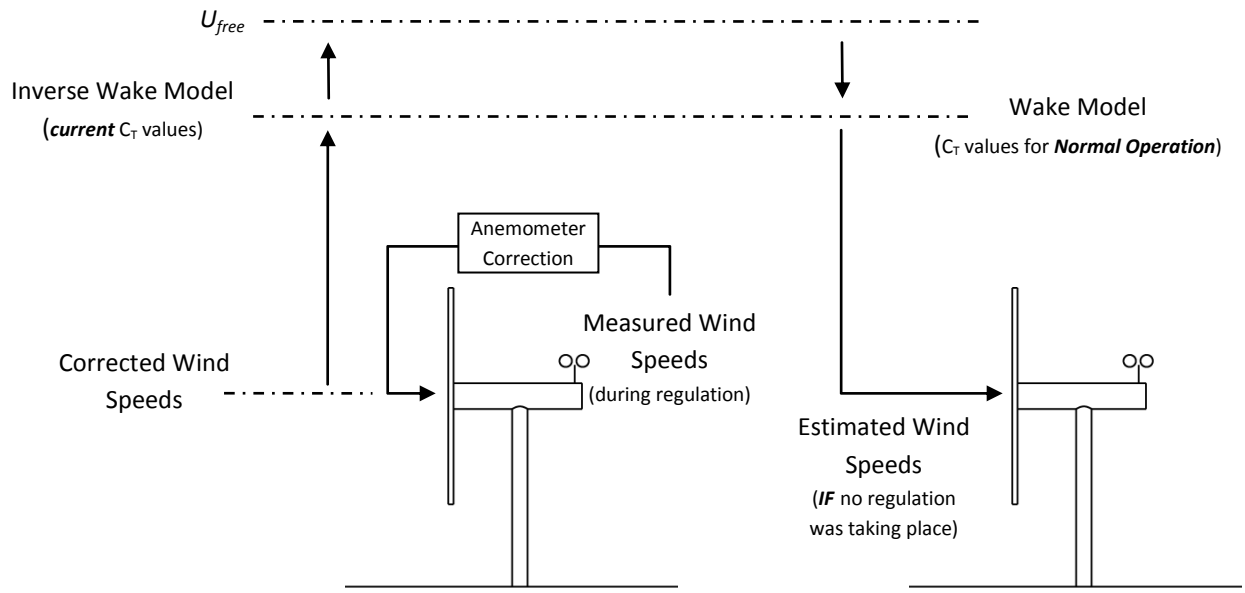

Figure 4-13: Overview of the Dynamic Wake Model

The static wake model is similar to that used in early versions of wind resource assessment software such as WASP (9),a product offered by Risoe National Laboratories in Denmark. It is a simple analytic model that employs momentum theory to calculate the down-stream wind speed deficit developed by a single wind turbine. Overlapping wind speed deficits from interacting wakes are summed energetically using a Root Square Sum approach as described in (8) which has previously shown to give good agreement with measurements.

Development of dynamic wake model is described in the following sections . It begins with a derivation of the static wake model followed by a statistical comparison with measurements from Nysted. Afterwards, the relationship between a turbine's operating state and its wake is derived so that real time operating data can be used to estimate changes in the turbine wakes during down-regulation. Finally, the implementation of the dynamic plant wake model is presented.

4.1.3.1 DERIVATION OF THE STATIC WAKE MODEL

The static wake model employed for describing the wind speed deficits throughout the wind plant is derived from early work by Jensen (7) and Katic et al (8). These models were intended primarily to provide a global estimate of the wake effects throughout the plant to help the wind plant developer estimate the energy capture, and subsequent plant revenue. Under these "normal" operating conditions the static wake model has proven quite successful for relatively small wind plant, giving good agreement with measurements. However, in this present work the model is extended to provide an estimate of the wind speed deficits during down-regulation at Nysted. During down-regulation (in addition to normal power limitation) the turbines are increasingly stalled to achieve the desired plant production output limit. As the rotor moves deeper into the stall regime, the momentum theory on which the static wake model is based begins to break-down. For this present work the wake deficits are assumed to remain constant in the operating region where momentum theory breaks-down. This is given more consideration in Section 4.1.3.3.

The derivation of the static wake model employed in this present work is given in the following sections. It begins with the derivation of a single wake from momentum theory. The orientation of the wind plant layout is then treated to facilitate calculation of the relative orientations between turbines and individual wakes. The interaction of wakes in then treated by employing a simple area overlap of individual wakes based on the down-wind distance and the skew distance (the horizontal distance between turbine rotor axes). Finally the total wind speed deficit at each turbine is calculated as the summation of the individual kinetic energy deficits from each wake.

4.1.3.1.1 SINGLE TURBINE MODEL

The wake for each turbine is derived using simple conversation of momentum within a cylindrical control volume in which the wind turbine rotor resides. Additionally, constant steady wind conditions are assumed throughout the

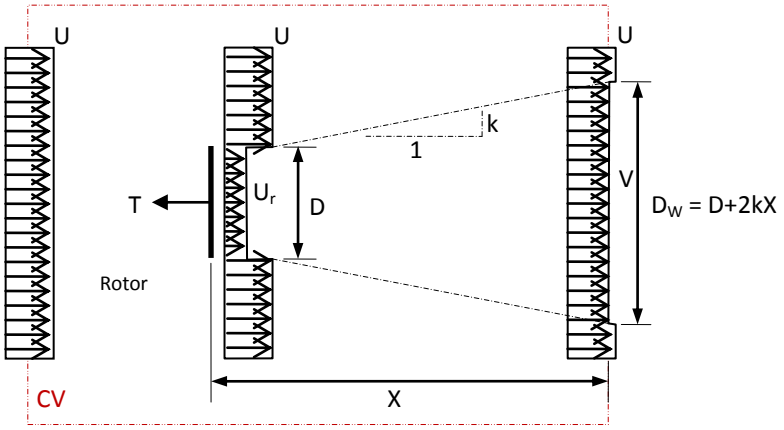

control volume. Figure 4-14 depicts the basic model.

Figure 4-14: Cylindrical Control Volume About the Turbine Rotor

The model assumes that the initial wind speed deficit occurs at the rotor plane and has a diameter equal to the rotor. From this point the wake is assumed to expand linearly and in order to maintain conversation of momentum the wind speed deficit subsequently decreases. The wind speed deficit across the wake area is assumed constant at a given distance X. The derivation of the wind speed deficit at distance X down-wind of the rotor is as follows. Beginning with conservation of momentum:

$$D^2 U_r + \left(D_w{}^2 - D^2\right)U = D_w{}^2 V$$

Defining the initial wind speed deficit(axial induction factor) as $a = 1 - U_r/U$,applying the linear wake expansion relationship (D_W = D+2kX) and rearranging gives:

$$1 - \frac{V}{U} = 2a\left(\frac{D}{D + 2kX}\right)^2$$

This equation relates the free wind speed U with the wake wind speed at distance X down-wind. However the initial axial induction factor a is also related to the rotor thrust coefficient, C_T in the classic formulation by Betz (10; 11) as:

$$C_T = 4a(1 - a)$$

Solving for a gives:

$$a = \frac{1}{2} - \frac{1}{2}\sqrt{1 - C_T}$$

Replacing a in the above equation gives:

$$1 - \frac{V}{U} = (1 - \sqrt{1 - C_T})\left(\frac{D}{D + 2kX}\right)^2$$

From this equation the wind speed deficit V, at down-wind distance X can be found. The wake expansion constant k is found experimentally and is usually taken to be 0.05 for offshore environments. It is a measure of how quickly the wake decays down-wind of the rotor. The C_T is a function of the aerodynamic and structural properties of the rotor for a

given wind speed, rotor speed and blade pitch angle. The Nysted wind turbines are treated as constant speed machines and therefore the C_T is defined by only wind speed and blade pitch angle. This relationship is discussed in Section 4.1.3.3.

4.1.3.1.2 COORDINATE TRANSFORMATION MODEL

The coordinate transformation model is employed to simplify determination of the geometric orientation between wind turbines relative to the incident wind throughout the wind plant (12). The geometric orientation is needed to determine both the extent of wake over-lap between turbines and the order of wake summation since only up wind wakes contribute to the overall wake deficit at each turbine. Figure 4-15 depicts the original turbine coordinates and a transformed coordinate systems at the Nysted Wind Plant for an incident wind direction indicated by the black arrow. In the transformed coordinate system the down-wind and skew distances are calculated directly from the transformed coordinate.

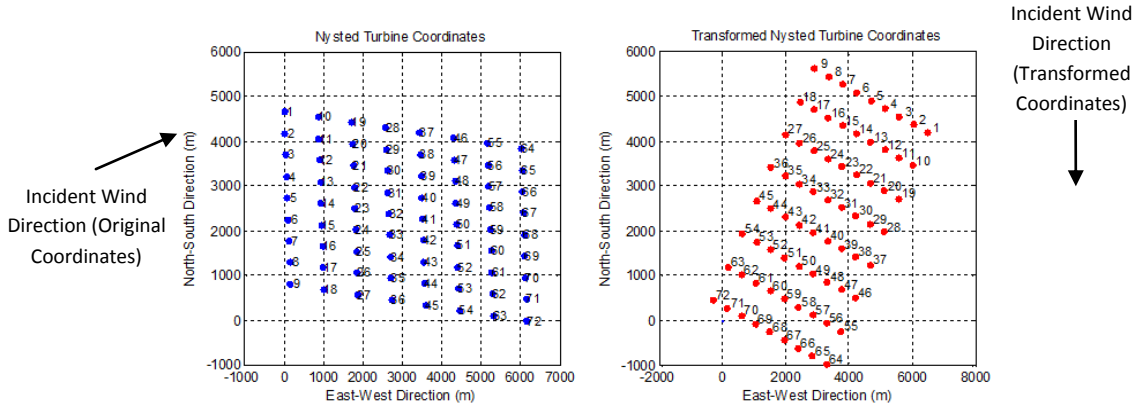

Figure 4-15: Original and Transformed Coordinate Systems

4.1.3.1.3 AREA-OVERLAP AND SUMMATION MODEL

The single turbine wake model provides both the wind speed deficit and the diameter of the wake at distances down-wind of the rotor. The area-overlap and summation models account for wake interaction and calculate the total wake deficit at each turbine from up-wind wakes. The model calculates the interaction of every wake generated throughout the wind plant with every wind turbine including the ground reflection of wakes. The ground reflection is calculated assuming an imaginary wind turbine located beneath each real turbine. The individual wake interaction at each down-wind rotor is determined as a ratio of the area-overlap of the wake and the rotor area employing a circle-circle intersection algorithm taken from (13; 12).A fully enshrouded rotor will have a 100% overlap while only partial area-overlap will give ratios less than 100%. Figure 4-16 illustrates the concept of area overlap and Figure 4-17 depicts the reflected wakes. The signal turbine wake model is modified to include the area-overlap of the upwind wake as:

$$WSR_{\mathrm{i,j}} = 1 - \frac{V_{i,j}}{U_{free}} = (1 - \sqrt{1 - C_T}) \left(\frac{D}{D + 2kX}\right)^2 \frac{A_{i,j\ overlap}}{A_{rotor}}$$

Where V is the reduced wind speed in the wake, U_{free} is the free stream wind speed, D is the rotor diameter, k is the wake decay constant (determined from fitting the simple wake model with measurements from Nysted), $X_{i,j}$ is the down-wind distance between the ith and jth turbines, $A_{i,j\ overlap}$ is the area overlap of the ith turbine's wake on the jth turbine and A_{rotor} is the area of the turbine rotor.

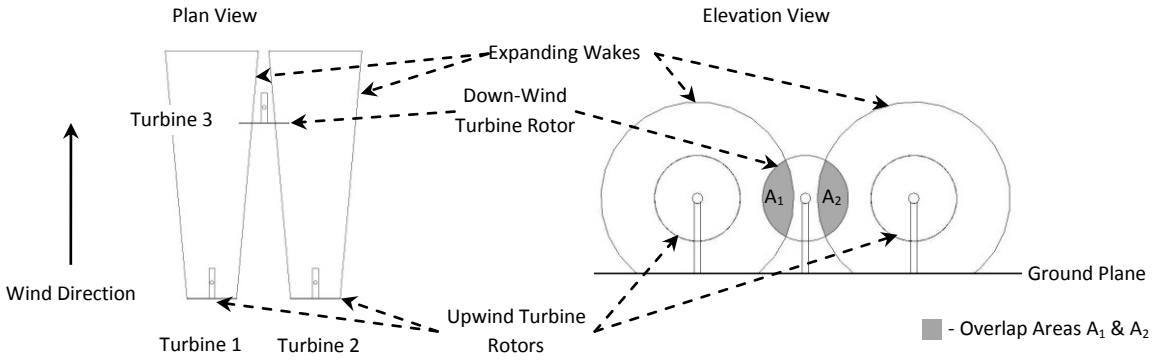

Figure 4-16: Area Overlap Visualization

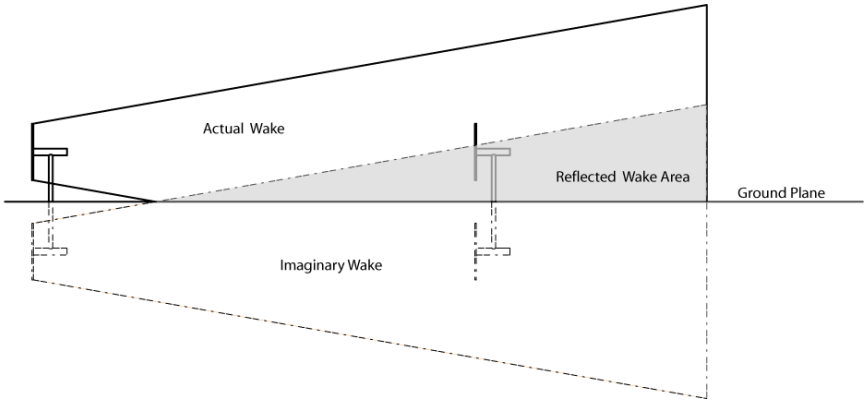

Figure 4-17: Reflected Wake Visualization

Programmatically the wake interactions of each turbine at every other turbine throughout the wind plant are calculated in matrix form as:

$$\begin{bmatrix} 1-\frac{V_{i,j}}{U} & \cdots & 1-\frac{V_{i,N}}{U} \\ \vdots & \ddots & \vdots \\ 1-\frac{V_{N,j}}{U} & \cdots & 1-\frac{V_{N,N}}{U} \end{bmatrix} = \begin{bmatrix} (1-\sqrt{1-C_{T,i}})\left(\frac{D}{D+2kX_{i,j}}\right)^2 \frac{A_{i,j}}{A_{rotor}} & \cdots & (1-\sqrt{1-C_{T,i}})\left(\frac{D}{D+2kX_{i,N}}\right)^2 \frac{A_{i,N}}{A_{rotor}} \\ \vdots & \ddots & \vdots \\ (1-\sqrt{1-C_{T,i}})\left(\frac{D}{D+2kX_{N,j}}\right)^2 \frac{A_{N,j}}{A_{rotor}} & \cdots & (1-\sqrt{1-C_{T,i}})\left(\frac{D}{D+2kX_{N,N}}\right)^2 \frac{A_{N,N}}{A_{rotor}} \end{bmatrix}$$

The resulting matrix has size N by N, where N is the number of turbines. Additionally, the interactions between imaginary and real wakes are calculated in a similar way giving second matrix with size N by N:

$$\begin{bmatrix} 1-\frac{V_{imag,i,j}}{U} & \cdots & 1-\frac{V_{imag,i,N}}{U} \\ \vdots & \ddots & \vdots \\ 1-\frac{V_{imag,N,j}}{U} & \cdots & 1-\frac{V_{imag,N,N}}{U} \end{bmatrix} = \begin{bmatrix} (1-\sqrt{1-C_{T,i}})\left(\frac{D}{D+2kX_{imag,i,j}}\right)^2 \frac{A_{imag,i,j}}{A_{rotor}} & \cdots & (1-\sqrt{1-C_{T,i}})\left(\frac{D}{D+2kX_{imag,i,N}}\right)^2 \frac{A_{imag,i,N}}{A_{rotor}} \\ \vdots & \ddots & \vdots \\ (1-\sqrt{1-C_{T,i}})\left(\frac{D}{D+2kX_{imag,N,j}}\right)^2 \frac{A_{imag,N,j}}{A_{rotor}} & \cdots & (1-\sqrt{1-C_{T,i}})\left(\frac{D}{D+2kX_{imag,N,N}}\right)^2 \frac{A_{imag,N,N}}{A_{rotor}} \end{bmatrix}$$

The resulting wind speed deficits or WSRs are summed energetically as proposed by (8) and include reflected wakes, denoted V_r, to account for wake-ground interaction. The total wind speed deficits, denoted V_t, and subsequent total wind speed ratios WSR_t at each turbine throughout the wind plant are given as:

$$\begin{bmatrix} \mathrm{WSR}_{t,1} \\ \vdots \\ \mathrm{WSR}_{t,N} \end{bmatrix} = \begin{bmatrix} 1 - \frac{V_{t,1}}{U} \\ \vdots \\ 1 - \frac{V_{t,N}}{U} \end{bmatrix} \begin{bmatrix} \sqrt{\sum_{i=1}^{N} \left(1 - \frac{V_{1,i}}{U}\right)^2 + \sum_{i=1}^{N} \left(1 - \frac{V_{r,1,i}}{U}\right)^2} \\ \vdots \\ \sqrt{\sum_{i=1}^{N} \left(1 - \frac{V_{1,N}}{U}\right)^2 + \sum_{i=1}^{N} \left(1 - \frac{V_{r,1,N}}{U}\right)^2} \end{bmatrix}$$

Where N is the total number of turbines in the plant. In summary the wind speed ratio at each turbine, for a given wind plant layout and turbine configuration, is a function of C_T and wind direction (φ):

$$WSR_{t,i} = f(C_{T,i}, \varphi)$$

In the present model configuration the wind direction is assumed to be single valued throughout the wind plant and is derived from yaw angle measurements of online (power producing) turbines. Online turbines are assumed to have prefect alignment with the inflow, i.e. no yaw error resulting in the yaw angle and wind direction being equal.

4.1.3.2 COMPARISON OF STATIC WAKE MODEL WITH MEASUREMENTS

The static wake model was compared to measurements from Nysted. Three principle wind directions were analyzed 278, 246, and 178 degrees with turbine spacing of 5.7D, 10.3D and 10.9D, respectively. The results are depicted in Figure 4-18 through Figure 4-22. Salient features of the analysis include:

1. 10 min mean data values were analyzed.
2. Both model and measurements use +/- 5 deg yaw averaging window about the principle yaw angle to calculate the deficit.
3. Only the center row for each principle direction was analyzed (analysis of the other rows are provided in Appendix D).
4. Only data where all the turbines in the row were online was analyzed.
5. Only data with where the high speed generator was operating was analyzed.
6. Data was binned into 7, 8, 9, 10 m/s wind speed bins.
7. The wind speed values were determined from the turbine power and application of the inverse standard power curve.
8. The wake decay constant was chosen as 0.055.

Overall the model and measurement show good agreement for the second turbine in each row for each principle direction. However subsequent turbines increasingly deviate from the model predications. This is most visible for the lowest wind speed (indicated by the blue trace in all plots) and for the 178 deg direction which corresponds to the minimum turbine spacing. The deviation of the measured wind speed deficits for the lowest wind speed bin of 6.5 -7.5 m/s is due primarily to a lack of data (No data for this wind speed bin exists for the 178deg wind direction). In this region the turbine operates at low speed a significant part of the time, which excluded from the analysis since the rotor C_T values are significantly different between the two operating regimes.

Results depicted in Figure 4-22 for the wind speed deficit of turbine 2 as a function of yaw angle centered on 178 degrees indicates that the measurements are not symmetrical about the principle row direction (178 degrees). Analysis of the other rows (Appendix D) about the same principle row direction show the same trend. This has not been investigated further but may be related to the distribution of the measurement data which is not symmetric about 178 degrees. Figure 4-44 depicts the distribution of the measurement data by yaw direction.

Additionally, the similar plot in Figure 4-22 for the 246 degree principle row direction indicates an offset exists between the measurements and model results. This offset is not apparent for other row directions. This has been investigated.

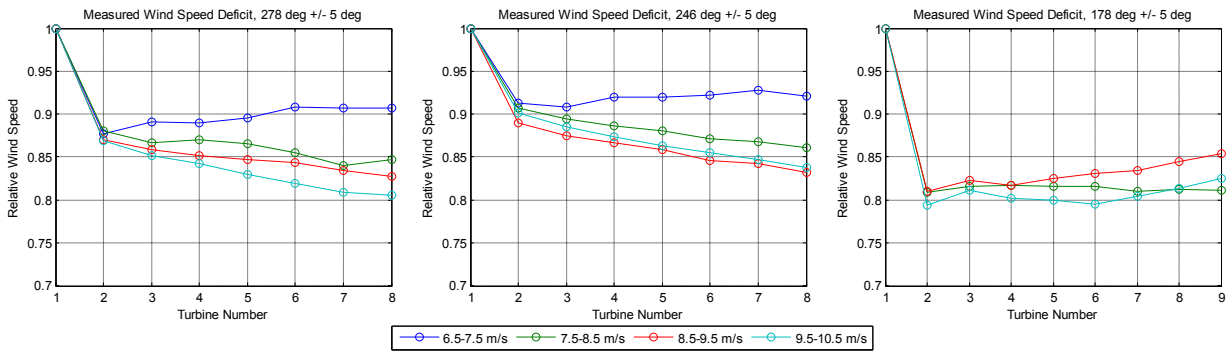

Figure 4-18: Measurement Results for Relative Wind Speed Deficits in each Row

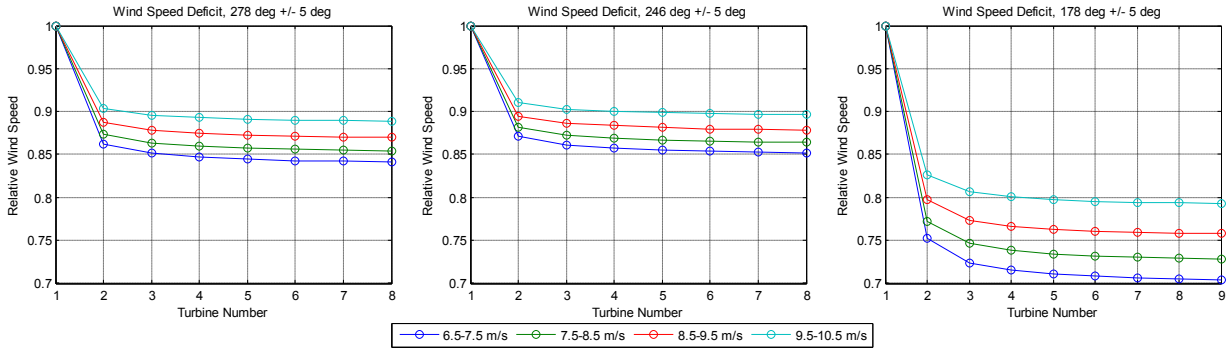

Figure 4-19: Static Wake Model Results for Relative Wind Speed Deficits in each Row

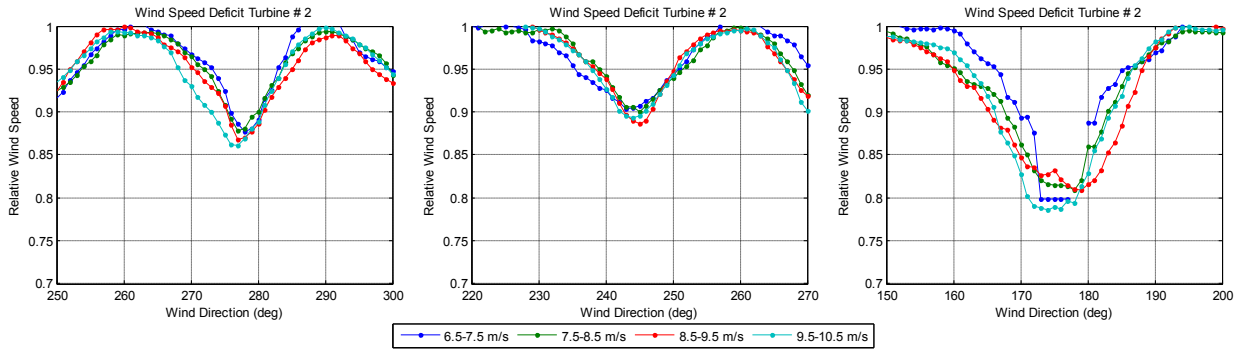

Figure 4-20: Measurement Results for Varying Wind Direction and Wind Speed at Turbine 2 in each Row

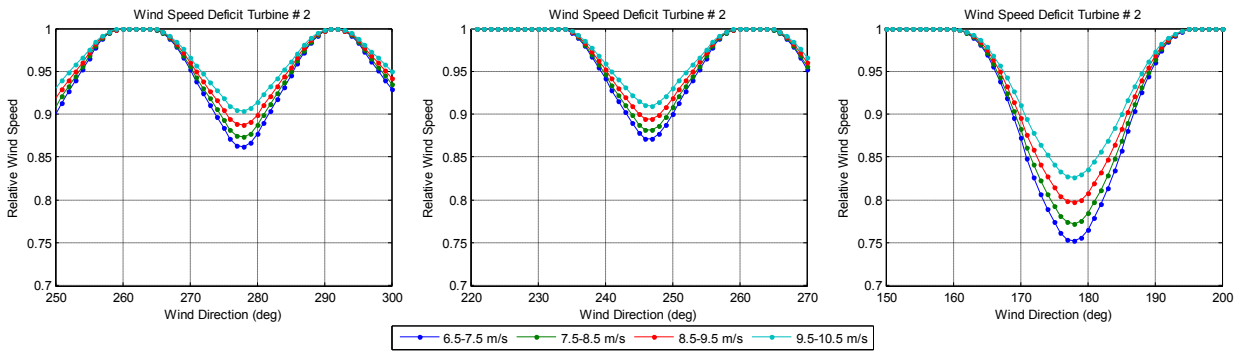

Figure 4-21: Static Wake Model Results for Varying Wind Direction and Wind Speed at Turbine 2 in each Row

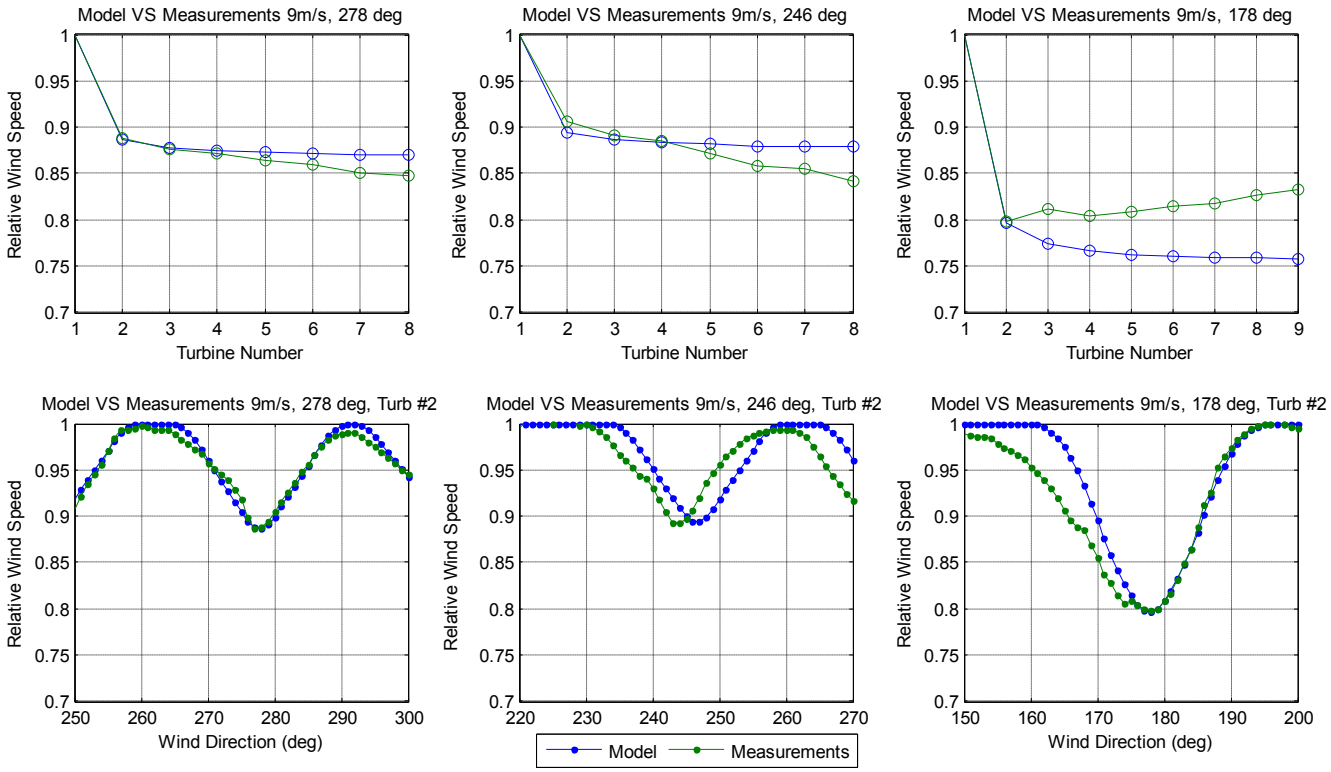

Figure 4-22: Comparison of the Relative Wind Speed Deficits for the Static Wake Model and Measurements at 9m/s

4.1.3.3 TURBINE OPERATING STATE AND ROTOR C_T

Effective application of the wake model requires knowledge of the C_T throughout the operating envelop of the turbine since the wind speed deficits are a function of C_T and wind direction. The rotor C_T values employed in the wake model are derived from steady state blade element momentum (BEM) theory calculations. For a rotor operating in steady wind with given structural and aerodynamic properties the C_T is a function of blade pitch angle, wind speed and rotor speed. In this present work the rotor speed is assumed constant to simplify calculation of C_T. The C_T is subsequently determined by table lookup using individual pitch angle and wind speed measurement data in real time. For a stall regulated turbine operating at reduced power the C_T values exceed 1.0 for certain combinations of wind speed and pitch angle (see Figure 4-25) For C_T values greater than 1, the momentum theory on which the wake model is based is no longer valid. Subsequently the relationship between C_T and the initial wind speed deficit in the wake is ill defined.. In this region, often referred to as the turbulent wake state (14; 11). Glauert's empirical correction for large axial induction (initial wind speed deficit) factors is used to augment the BEM theory and extend its validity into this operating region. It originated in early propeller/helicopter theory to extend the BEM theory for highly load rotors where the large change in momentum causes the flow at the rotor plane to become unstable (11). However it provides no indication of the structure or magnitude of the wake down-wind of the rotor. Figure 4-23 depicts rotor C_T as a function of axial induction factor for different rotor operating states for a propeller.

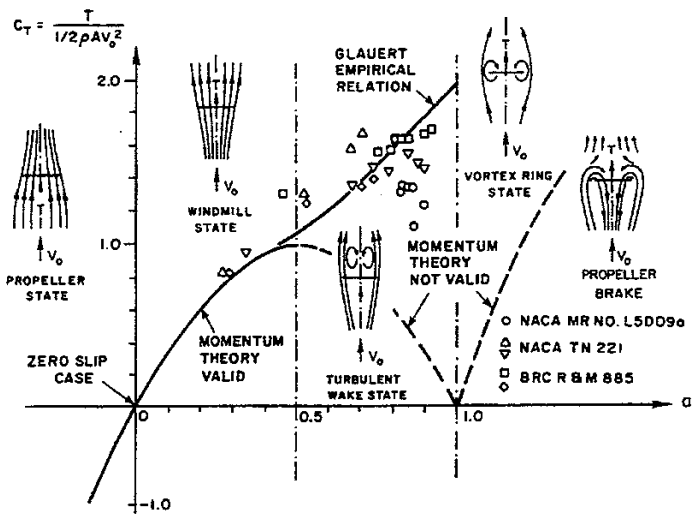

Figure 4-23: Relationship between Axial Induction Factor and Rotor C_T for Different Rotor State (taken from ref (14))

In this present work the wind speed deficit in the wake is assumed to remain constant for C_T values greater than 1 (C_T values greater than 1 are set to 1 in the model). This may be a reasonable assumption since unstable flow in the turbulent wake state helps to entrain fresh momentum from the outer flow due to turbulent eddies generated at the edge of the wake (11). Figure 4-24 depicts turbulent eddies forming in the wake. The fresh momentum may help to stabilize the wind speed deficit so that further increases in the C_T do not result in increased wind speed deficits in the wake. This is a significant assumption for application of the wake model to a heavily stalled rotor. An extend measurement campaign at Nysted was originally planned to gain insight into this relationship. The intent was to operate turbine A09 in a down-regulated state for an extend period and observe the corresponding wind speed deficits are the surrounding turbine.

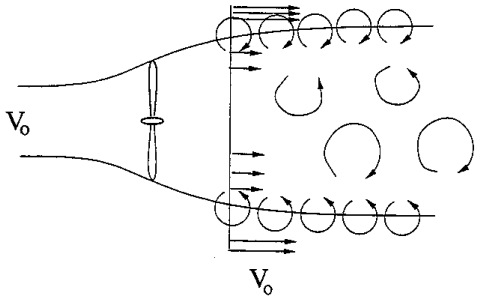

Figure 4-24: Turbulent Wake State and Turbulent Eddies for a Highly Loaded Rotor (taken from ref (11))

The operating envelop for the Nysted turbine is presented in Figure 4-25 and Figure 4-26. Figure 4-25 depicts ISO power and C_T curves for varying wind speed and pitch angle. These values are derived from BEM theory and are based on the structural and aerodynamic properties of the Nysted Turbines. The nominal pitch angle range during operation is limited between approximately 2 and -15 degrees while the nominal wind speed range is between 5 and 25 m/s.

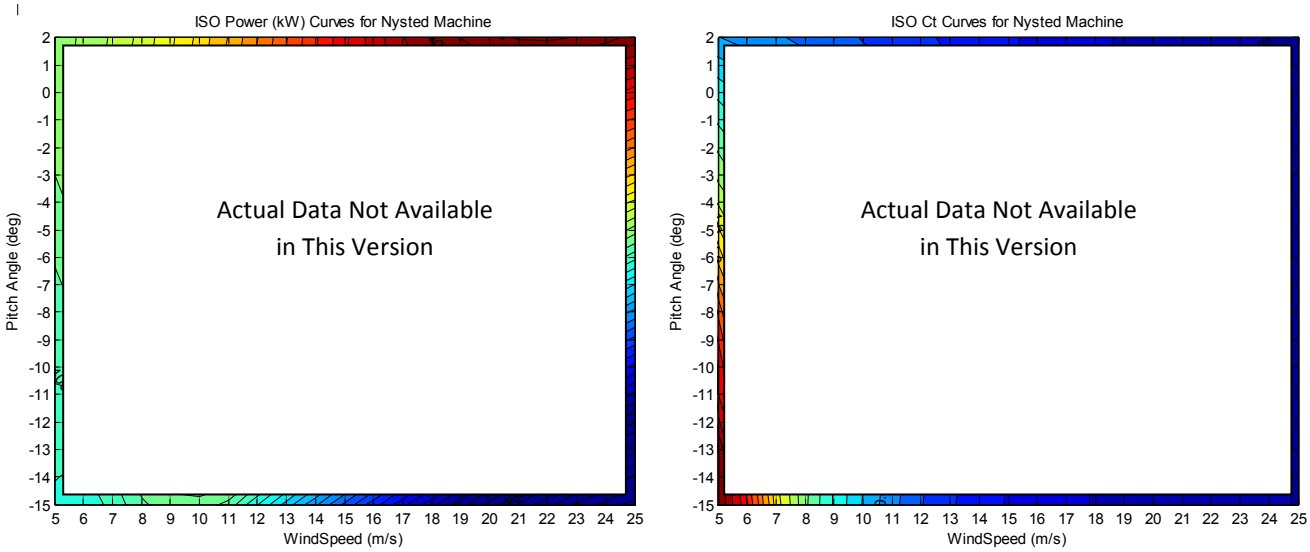

Figure 4-25: Iso Power and C_T Curves for Nysted Turbines

Figure 4-26 depicts the nominal power, pitch angle and C_T for normal operation and 25, 50, 75 and 100 percent down-regulation, where 100% down-regulation indicates zero power output over the range of wind speeds. In all cases the turbine is assumed to operate as a single speed machine. For increasing down-regulation the pitch angle is decreased to achieved the desired power output. For example, at 10m/s the nominal pitch angle for normal operation is approximately -2 degrees and must be decreased to approximately -9.5 degrees to achieve 25% down-regulation. The corresponding C_T values increase from approximately 0.75 and 0.9, indicating that the wind speed deficit in the wake ***increases*** as the rotor power is reduced during down-regulation. At first this result is counter intuitive since a reduction in the rotor power, considering the control volume defined in Figure 4-14, would imply greater power and momentum available in the wake. However, in a stall regulated configuration, the component of the lift forces acting along the rotor blade, which produce rotor torque, are not significantly reduced during down-regulation. Rather, drag forces acting along the rotor blade are dramatically increased, due to stall, and balance with the lift forces to produce an overall lower rotor torque and subsequent power. The end result is that the power extracted from the wind during down-regulation essentially generates turbulence rather than produce useful work.

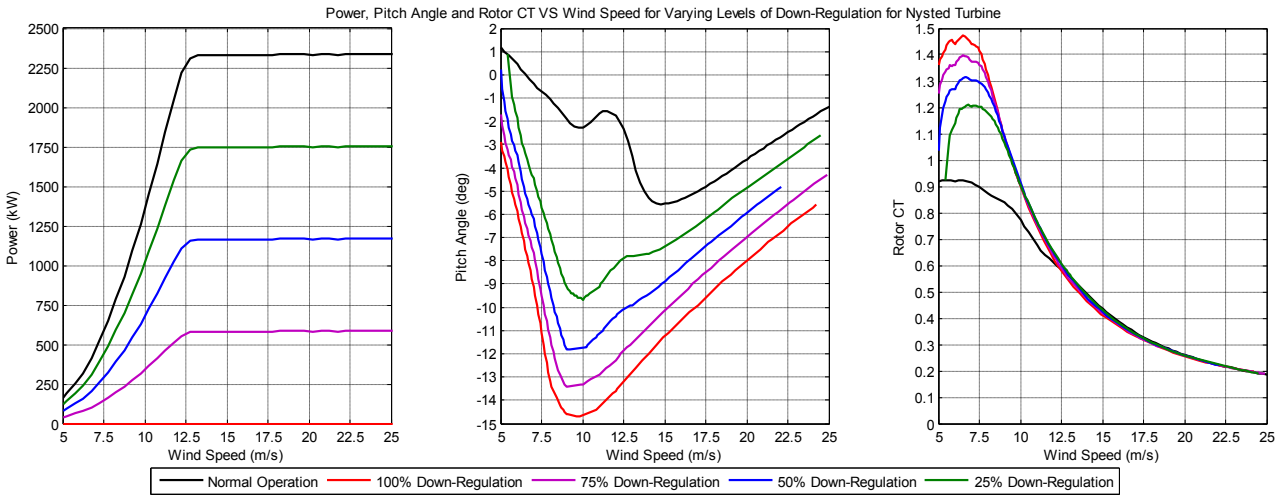

Figure 4-26: Power, Pitch Angle and C_T for Normal Operation and varying Levels of Down-Regulation

Another significant result visible in Figure 4-27 is that the C_T values (and subsequently the wind speed deficits) are essentially the same between 10 and 100 % down-regulation for a given wind speed (indicated by the vertical contour

lines in the figure). Additionally, the C_T values which are limited to 1 are indicated as a single color (red) in Figure 4-27. Further investigation of the relationship between the C_T and the corresponding wind speed deficit for heavily loaded rotors is needed to improve the performance of the wake model in this region.

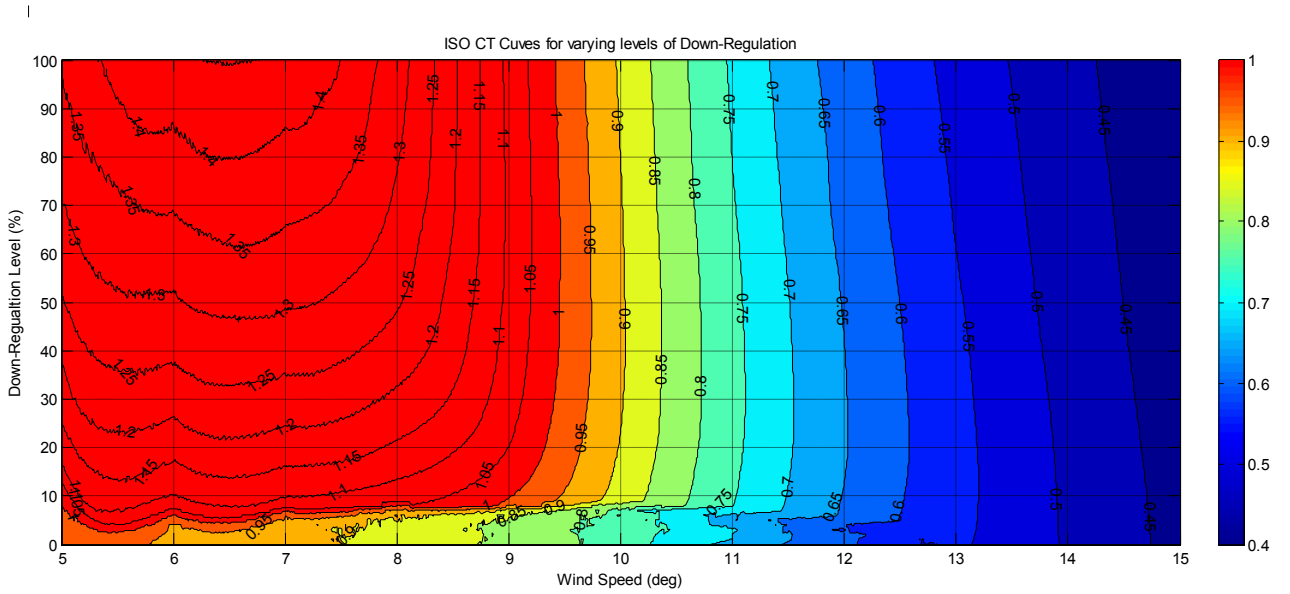

Figure 4-27: Rotor C_T Values for Varying Levels of Down-Regulation and Wind Speed

The subsequent effect of various turbine operating states on the overall wind speed ratios (WSRs) throughout the wind plant are depicted in Figure 4-28 through Figure 4-31 for varying operating conditions. Additional examples are provided in Appendix C. All the following examples are for an incident wind direction of 246 degrees at 9.4m/s. The wind direction corresponds to a principle alignment direction (see Figure 3-2) while the wind speed corresponds to the worst case change in the rotor C_T during down-regulation (see Figure 4-26). In the first example in Figure 4-28 all turbines are operating at their maximum possible power and have the same rotor C_T values (indicated in the right plot). The corresponding WSRs are indicated by color in the left plot. The example highlights that the largest drop in the WSRs are between the first to the second turbines and generally stabilizes further down-wind. In the second example in Figure 4-29 the 5th row of turbines are offline (indicated in the right plot) with corresponding rotor C_T values of zero. The corresponding down-wind turbines all see an increase in their WSRs due to the decrease in the overall wake at that position. Notice that turbine B4 (turbine designations are depicted in Figure 3-2) has a WSR of 1 since A5 is offline and there are no remaining upwind wakes. In Figure 4-30 the turbines in row 5 are down-regulated 100% with corresponding rotor C_T values of 1 (the C_T values saturate to the limit value in this case). The down-wind turbines see a decrease in their WSRs due to the increase in the wake effects from row 5 turbines. The effect of the down-regulation of row 5 propagates to all the subsequent down-wind turbines (indicated as a slight color variation from the normal case in Figure 4-28. The final example in Figure 4-31 includes a random distribution of offline and down-regulated turbines. This example simply highlights the dependence of the WSR distribution throughout the wind plant on the operating state of each turbine.

Note that in Figure 4-28 through Figure 4-31 the WSR coloring is interpolated between the turbines in both the upwind and down-wind directions. This is of course not physically possible since the wakes are only convected down-wind. This should be kept in mind when interpreting the coloring.

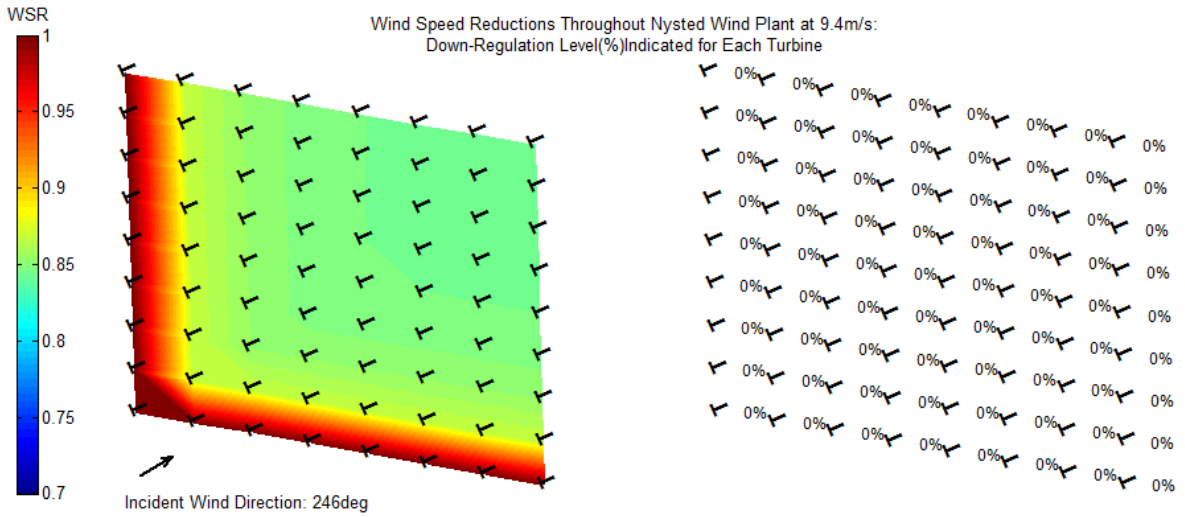

Figure 4-28 Example of Wind Speed Reductions Throughout Nysted Plant

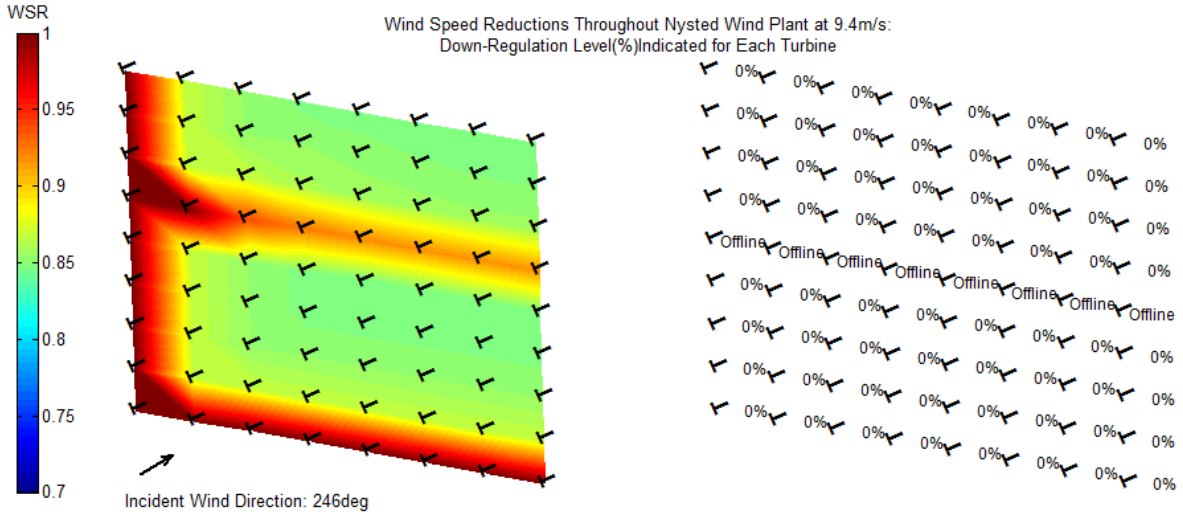

Figure 4-29: Example of Wind Speed Reductions Throughout Nysted Plant (Row 5 Turbines Offline)

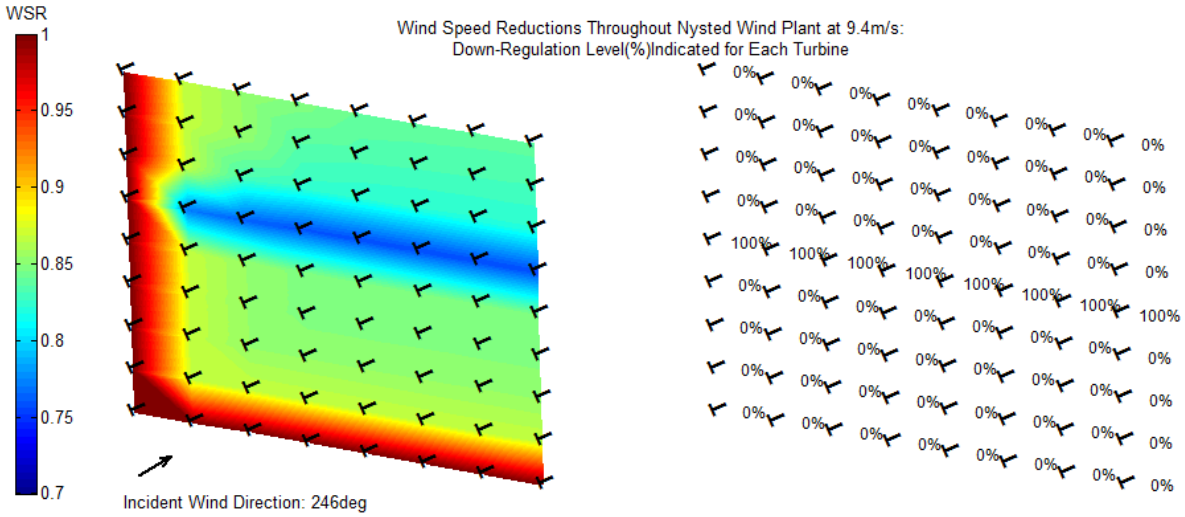

Figure 4-30: Example of Wind Speed Reductions Throughout Nysted Plant (Row 5 Turbines Down-Regulated 100%)

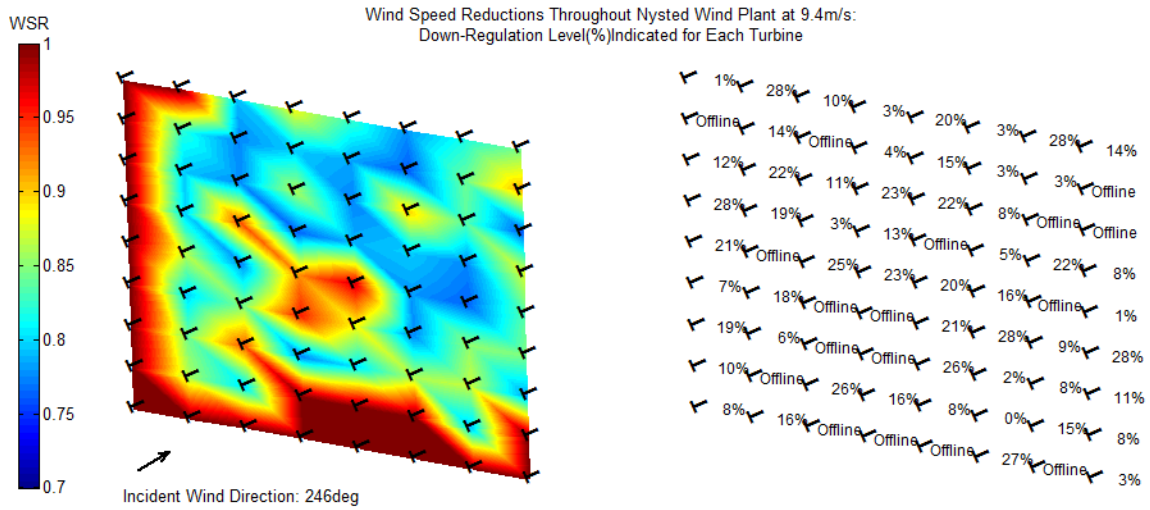

Figure 4-31: Example of Wind Speed Reductions Throughout Nysted Plant (Random Distribution of Down-Regulation Levels and Offline Turbines)

4.1.3.4 IMPLEMENTATION OF THE DYNAMIC WAKE MODEL

The dynamic wake model (DWM) is implemented in Matlab® Simulink® for use with the power curve method and the Wind Plant Production Simulation Tool (Section 5). The required measurement data and derived quantities used in the dynamic wake model are summarized in Table 4-2 and Table 4-3, respectively.

Measurement Data from Each Turbine
NWS
Blade Pitch Angle (θ)
Nacelle Yaw Angle
Status
Generator Status

Table 4-2: Measurement Data for Dynamic Wake Model

Derived Data	**Comments**
U_{ERWS} (Equivalent Rotor Wind Speed)	Derived from NWS correction and NWS measurements (Section 4.1.2.3).
C_T (θ, U_{ERWS}) - C_T Lookup Table	Derived from BEM code calculations for Nysted turbine (Section 5.1.1).
$\Theta_{norm\text{-}op}$ - Blade pitch angle trajectory for normal operation	Derived from historic operating data of Nysted turbines (Section 3.1).
Mean Nacelle Yaw Angle	Derived from Nacelle Yaw Angle of turbines that and are online (status = 0).
Wake Model Wind Speed Ratios (WSR)	Derived from Plant Wake Model with C_T values and the Mean Nacelle Yaw Angle. C_T values are set to zero for offline turbines.

Table 4-3: Derived Data for Implementation of the Dynamic Plant Wake Model

Implementation of the dynamic plant wake model consists of sub-models which apply the inverse wake model to determine the "free" wind speed throughout the wind plant and apply the normal wake model to determined the wind speed that would exist at each turbine if no down-regulation was taking place. Block diagrams of both sub-models are depicted in Figure 4-32 and Figure 4-33.

For application of the inverse wake model real time pitch angles and wind speed measurements at each turbine are first used to determine U_{ERWS}. Subsequently, the C_T values at each turbine are determined from table lookup of the pitch angle measurements and U_{free}, where U_{free} is determined by iteration of U_{ERWS} divided by WSR. Determination of the C_T values employ U_{free}, since the wake model is based on estimation of the WSRs from the free stream wind speed and not U_{ERWS} which includes wake effects from surround turbines.

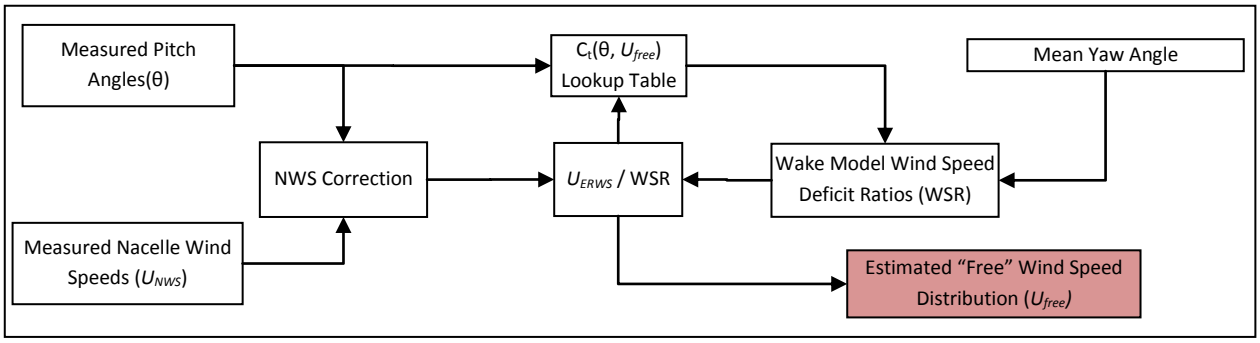

Figure 4-32: Block Diagram of the Inverse Application of the Wake Model

Application of the normal wake model requires knowledge of the pitch angle trajectory for normal operation and U_{free} to calculate the C_T values that would exist if no down-regulation was taking place. The pitch angle trajectory for normal operation is based on a simple binned fit of historic pitch angle data over the range on operating wind speeds. The measurement data and binned fit are depicted in Figure 3-4. The C_T values and the mean wind direction are then used to determine the wake model WSRs and are subsequently multiplied by U_{free} to determine the wind speed distribution at each turbine for normal operation.

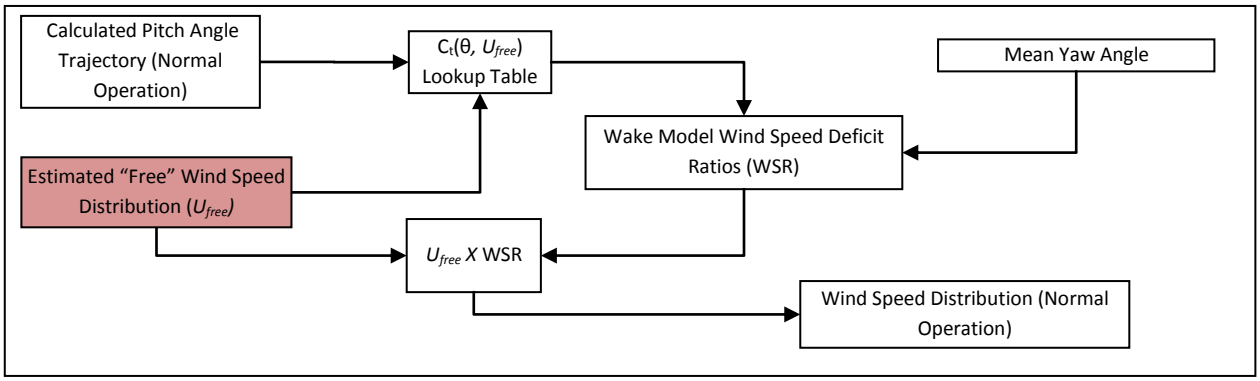

Figure 4-33: Block Diagram of the Normal Application of the Wake Model

4.1.3.5 PITCH ANGLE TRAJECTORY FOR NORMAL OPERATION

The pitch angle trajectory for normal operation and the estimated "free" wind speed distribution are required to calculate the rotor C_T and the subsequent wind speed deficits used to estimate the wind speeds at each turbine if no down-regulation had taken place. The pitch angle trajectory is derived from historic 3 min average pitch angle and NWS measurements from turbine A09 during normal operation. The measurement data and subsequent fit are depicted in Figure 3-4 in Section 3.1.

The normal operating pitch angle trajectory is important for successful implementation of the dynamic wake model since the difference between the pitch angles and subsequent rotor C_T values during down-regulation and normal operation effectively determine the level of adjustment to the NWS measurements. For down-regulations greater than 10% however the C_T essentially remains constant for over the operating range of wind speeds (see Figure 4-27)

regardless of the pitch angle. This implies that the plant wake model becomes less sensitive to pitch angle variations for increasing levels of down-regulation.

4.1.3.6 COMMENTS ON THE PLANT WAKE MODEL

An important assumption in this present work it that the changes in the wakes at each turbine are convected through the entire plant instantaneously, i.e. wake transport is not considered. This is clearly violated since the wakes are nominally convected down wind at the mean flow speed and a wake at one end of the plant may take up to 20 minutes to propagate through the entire plant. This is most severe during transient start-up or shut down of many turbines. In this present work a moving average filter is applied to each wind speed ratio (WSR) in both the inverse and forward application of the static wake model to attempt to account for the wake transport by "smearing" the change in the wind speed ratios in time.

Additionally, the dynamic wake model assumes a single value for the wind direction throughout the wind plant, derived from the online turbine yaw angle measurements. These turbines are assumed to have prefect alignment with the inflow, i.e. no yaw error and represent the mean wind direction. In reality however, the wind direction throughout the plant varies and will tend to reduce the overall wake effects since they drop off rapidly outside the principle alignment direction. Future work should attempt to include the wind direction throughout the wind plant. Only online turbines are included since offline turbine may have large yaw errors depending on the reason they are offline.

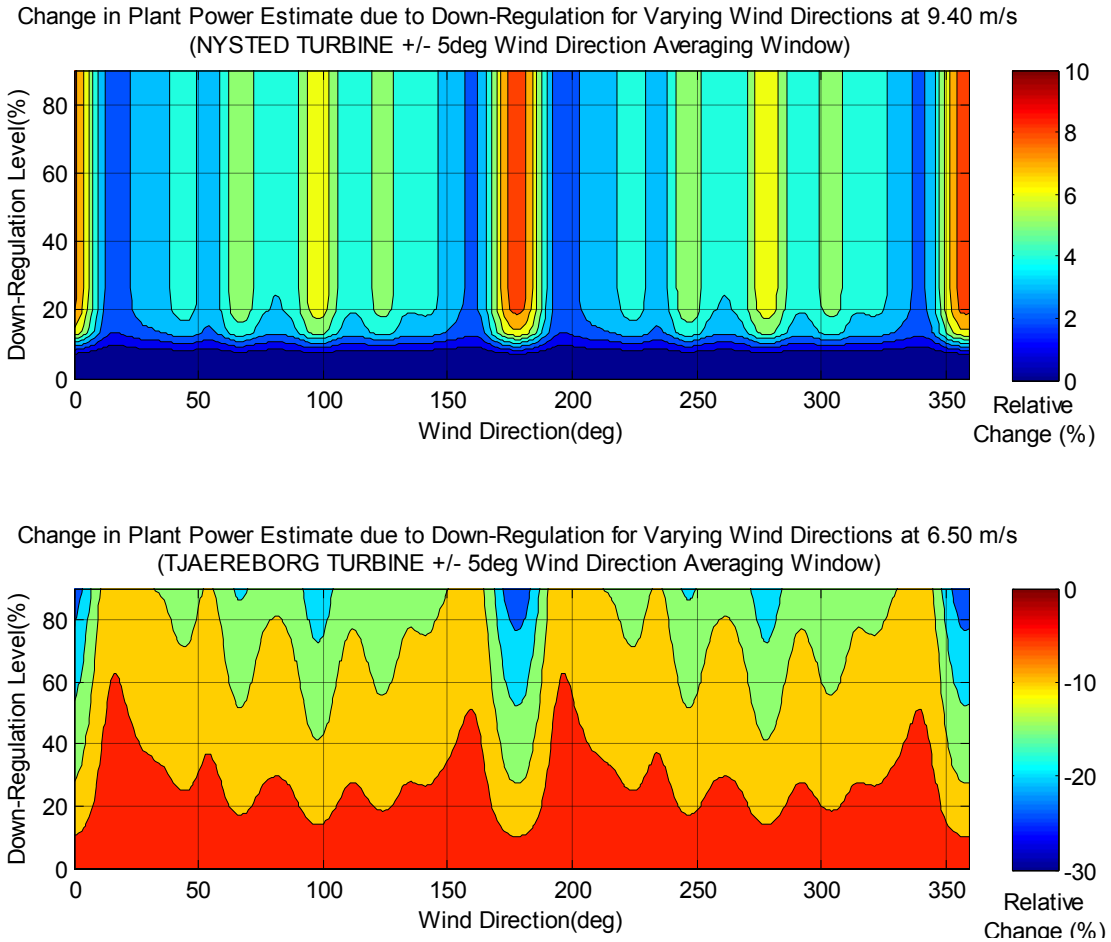

Figure 4-34: Relative Change in Plant Power Estimate for Varying Levels of Down-Regulation and Wind Direction for Nysted with the Stall-Regulated Nysted Turbine (Top Figure) and a Representative Pitch Regulated Turbine (Bottom Figure)

Finally, the error in the plant production estimate, if wake effects are not accounted for at Nysted is depicted in top plot of Figure 4-34. The plot depicts the relative change in the plant production at 9.4 m/s for varying levels of down-regulation over all wind directions. This wind speed corresponds to the maximum possible change in the rotor C_T between normal and maximum down-regulated operation. These conditions represent the worst case error in the plant production estimate due to altered wake effect during down-regulation. The plot indicates that during down regulation at Nysted the overall change in the plant production estimate between normal and down-regulated operating does not exceed 5% for most wind directions. The worst case, where the overall change approaches 10% is for a narrow yaw sector about the North-South(358deg) / South-North(178deg) direction, corresponding to the smallest turbine spacing of 5.7D. These result indicate that overall the wake effects between normal and down-regulated operation contribute a relatively small amount to the error in the estimation of possible power at Nysted.

The bottom plot of Figure 4-34 depicts the error in the plant production estimate, at 6.5 m/s for varying levels of down-regulation over all wind directions for the Nysted wind plant configured with a pitch regulated turbine. In this example the Tjaereborg turbine is used as a representative pitch regulated machine. The wind speed corresponds to the maximum possible change in the rotor C_T between normal and maximum down-regulated operation. For down-regulation of a wind plant incorporating pitch regulated turbines the wind speed reduction ***decreases*** in contrast to a wind plant with stall-regulated turbines. Additionally, the wake changes continually for increasing levels of regulation for the pitch regulated turbines rather the reaching a plateau at approximately a 25% down regulation. These results indicate that the changes in the wake effects between normal and down-regulated operation are more significant for a wind plant configured with pitch-regulated turbines.

Additional plots for other wind speeds are provided in appendix B for both stall and pitch regulated turbines.

4.1.4 AIR DENSITY CORRECTION

The air density correction is employed to adjust the reference power curves used in the estimate of the possible production to the actual air density. The reference power curves are based on an ISO standard atmosphere air density of 1.225 kg/m^3. The power produced by the wind turbine rotor is directly proportional to the air density and contributes to the estimate error if not accounted for. The air density is predominately effected by temperature, however pressure and humidity also contribute a small amount (< 0.5% combined over the expected range of values). In this present work the air density correction is calculated from temperature, pressure and humidity measured at the MM1 met mast. A constant density value is assumed throughout the entire wind plant. Pressure and humidity (15) are included since these data are readily available from the MM1 met mast. The correction is applied to the wind speed measurement rather than the power, as outlined in (5) since the turbines at Nysted employ active power control. Figure 4-35 depicts the effect of temperature and pressure on the air density over the expected temperature and pressure ranges at Nysted.

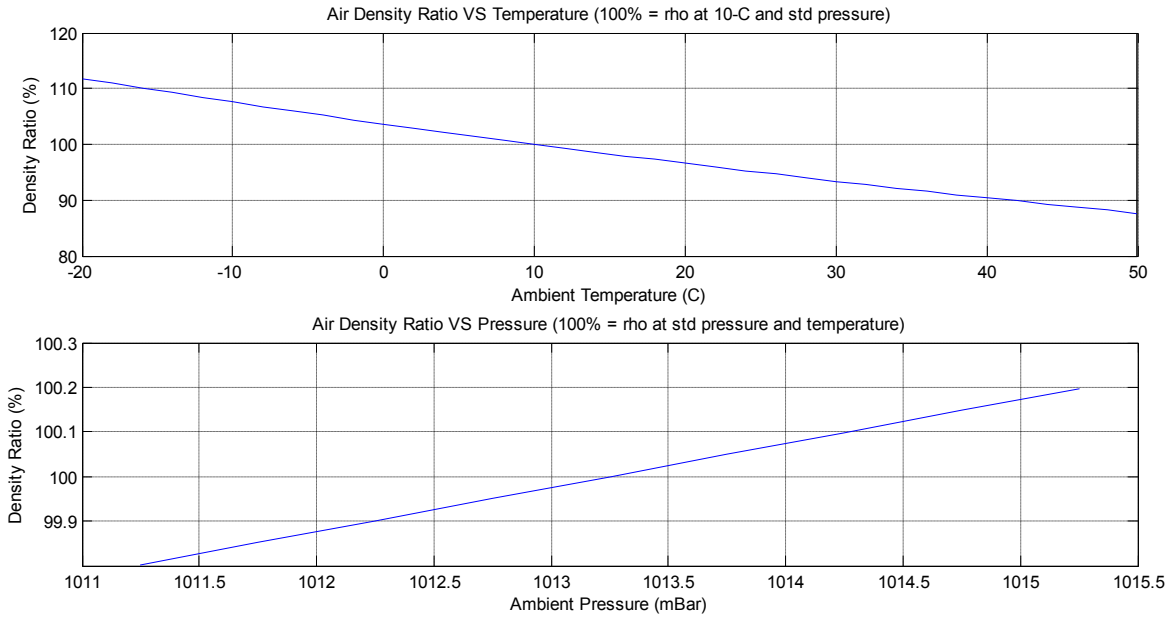

Figure 4-35: Effect of Temperature and Pressure on Air Density

4.1.5 IMPLEMENTATION OF THE POWER CURVE METHOD

The power curve method has been implemented in Matlab® Simulink® to evaluate its performance. Performance here is defined as the ability of the power curve method to accurately estimate the possible plant production. This is a straight forward analysis regarding normal operation, where the estimated production can be directly compared to the measured production. However, during down-regulation the possible production estimate can only be evaluated qualitatively since there are no control measurements available for comparison. Additionally, very limited down-regulation has occurred at Nysted (approximately 12 hours out of the 2 year of measurements employed in this present work) so only very limited data for a qualitative analysis are available. Considering that the power curve method is intended primarily for estimation of the possible production during down-regulation these results should be taken with caution until a more thorough evaluation can be completed. Nevertheless a statistical analysis is performed to ensure that the power curve method effectively predicts the plant production in normal operation; a condition for good performance but not sufficient to ensure that the method will perform during down regulation. The statistical analysis of normal operation provides at a minimum the best case performance of the power curve since the uncertainty of the estimate during down-regulation will be more significant.

The power curve method implementation is depicted graphically in Figure 4-36 where superscripts WT_i and WP indicate individual turbine values and total plant values, respectively. Subscript "meas" indicates real time measurement data values.

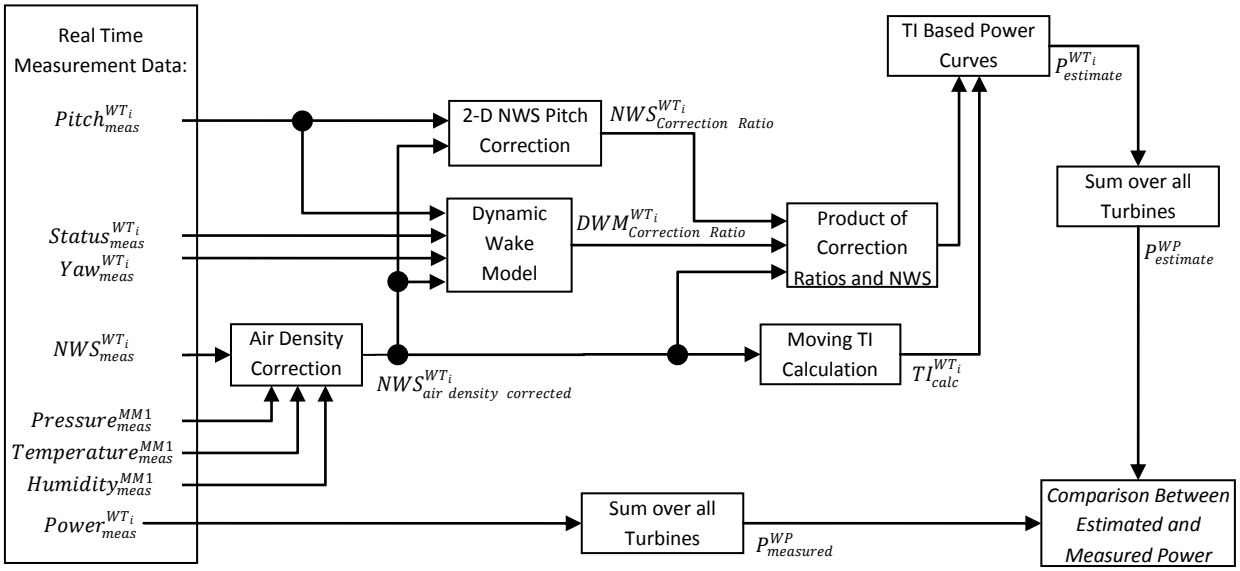

Figure 4-36: Implementation of the Power Curve Method

4.1.6 STATISICAL PERFOMANCE EVALUATION

The statistical analysis of the power curve method's overall performance applied to normal operating data with both the NWS and DWM corrections, indicates that the absolute error is within 4%, 90% of the total operating time analyzed. This analysis includes only plant operation above 25% of rated production since down-regulation below this point is not possible due to the down-regulation limitations of the individual turbines. Four different variations of the power curve method were analyzed to highlight the contribution from each component to the overall estimate error. These include:

1. The TI-Based family of power curves with both the NWS and DWM corrections.
2. The TI-Based family of power curves with only the NWS correction.
3. A single power curve (the "All Data" power curve in Figure 4-2) with no corrections. Note that this is essentially the configuration currently in place at Nysted.
4. A single power curve (the "All Data" power curve in Figure 4-2) with only the NWS correction.

Figure 4-37 depicts duration curves of the estimate error for the different variations. For all cases the estimate error is calculated as:

$$e_{estimate} = \left(\frac{P_{est} - P_{norm}}{P_{rated}}\right) * 100$$

Where P_{est} is the production estimate, P_{norm} is the measured production during normal operation and P_{rated} is the rated plant production. All the methods employ the air density correction. The results indicate that overall the TI based family of power curves with the NWS correction gives the minimum absolute estimate error (3.4%, 90% of the total operating time analyzed). Note that the NWS correction provides very little correction during normal operation as indicated by the small difference between the single power curve estimate with and without the NWS Correction. The addition of the DWM increases the absolute error by approximately 1% at 90% of the total time. The increase is due predominately to discrepancies between the calculated normal operating pitch trajectory and the actual pitch angle values during operation since there is a significant amount of scatter in the pitch angle in normal operation (depicted in Figure 3-4). Additionally, low speed operation of the turbine where the rotor C_T values are significantly different contribute to the error (the rotor C_T values for 2 speed operation are depicted in Appendix A). Three dimensional histograms of the estimate error for all 4 approaches are depicted in Figure 4-38 and Figure 4-39. The abscissa indicates

the error between the estimate and the measured power as a percentage of rated power while the ordinate indicates the plant production level. The color of each square indicates the total amount of time at that error and power level. The sum of all the square equals 100%. Note that the scale is logarithmic. These results indicate the mean error is not zero but varies for different power production levels for all approaches. Additionally, the error is biased in the negative direction implying that the estimation under predicts the possible production overall.

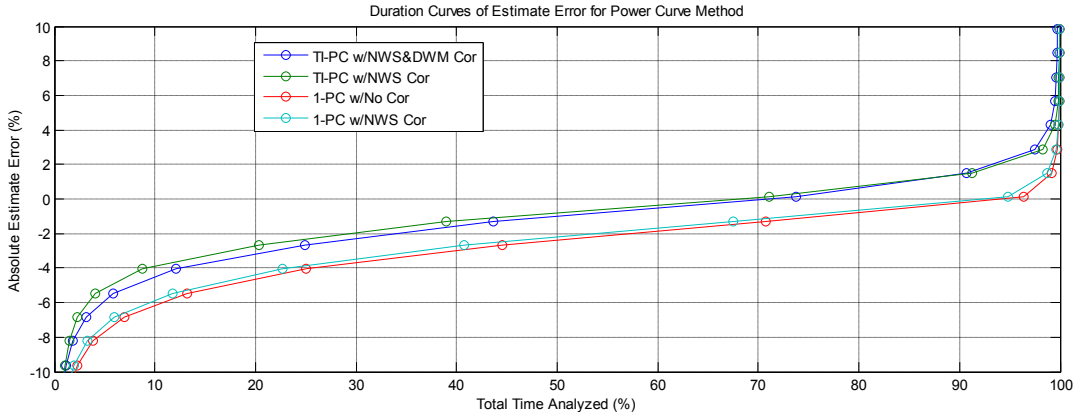

Figure 4-37: Duration Curves of the Estimate Error for the Power Curve Method for Different Approaches for Normal Operation (3 min measurement data points)

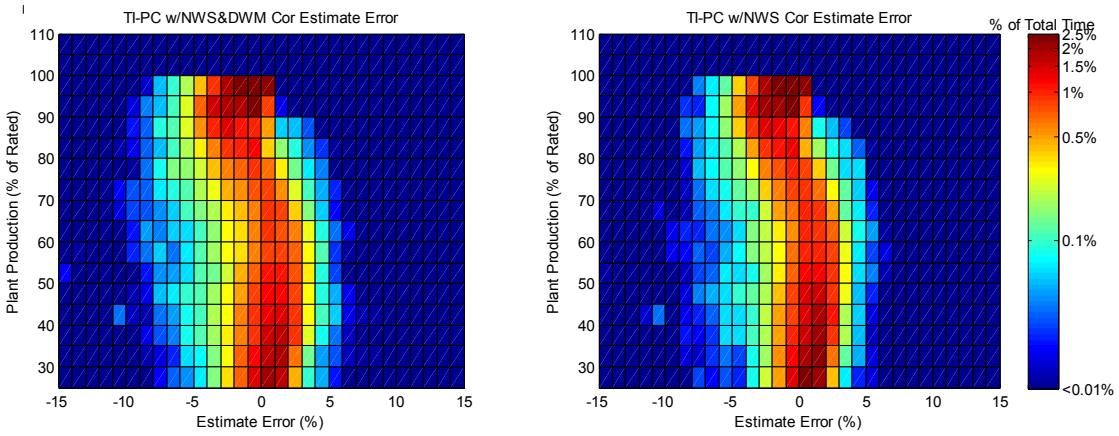

Figure 4-38: 3D Histograms of the Estimate Error for the Power Curve Method for Different Approaches (3 min measurement data points)

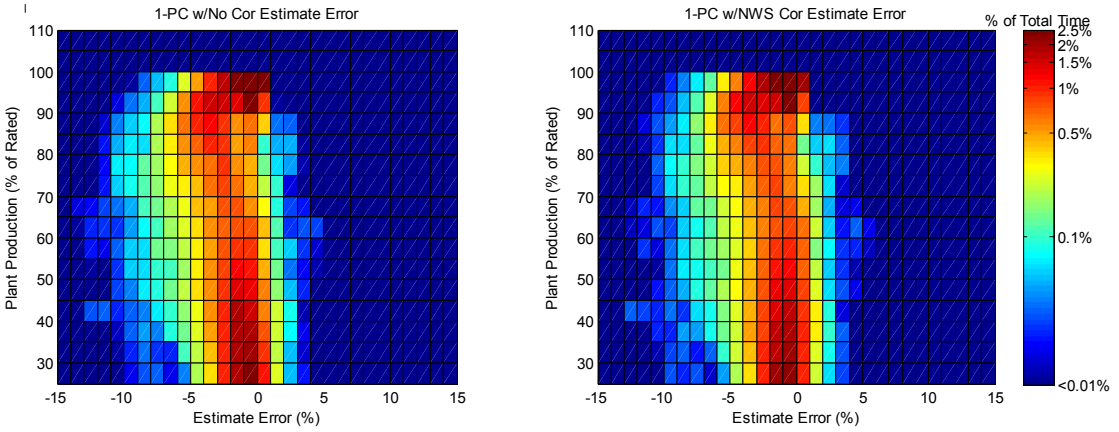

Figure 4-39: 3D Histograms of the Estimate Error for the Power Curve Method for Different Approaches(3 min measurement data points)

The addition of the DWM increases the overall error in the estimate during normal operation due to discrepancies between the calculated normal operating pitch trajectory. The error is magnified when the mean plant wind direction is along one of the principle axes. Additionally, low speed operation of the turbines are not considered in this analysis and contribute to the error due to significantly different rotor C_T values and below rated pitch angle schedule at lower wind speeds . These effects are visualized in Figure 4-40. Note that for normal operation the DWM ratios should all be 1 (No Correction).The left plot depicts the mean DWM reduction ratio varying yaw angles where the peaks correspond to principle alignment directions (Figure 3-2). The right plot depicts the mean DWM reduction for varying plant production levels and indicates large deviations from ratio 1 at low production levels.

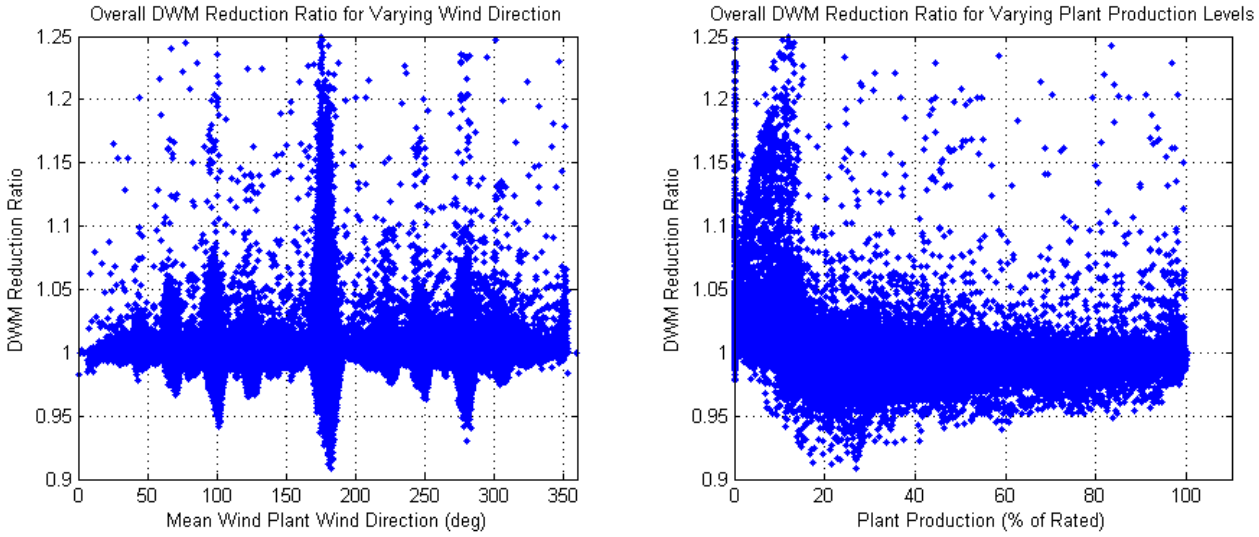

Figure 4-40: Overall DWM adjustment during Normal Operation (3 min measurement data points)

4.1.7 QUALITATIVE PERFORMANCE ANALYSIS

The power curve method applied to 3 regualtion events are depicted in Figure 4-41, Figure 4-42 and Figure 4-43. All the plots include the measured production, commanded setpoint, and three different estimations of possible produciton as indicated in the plot legend. In Figure 4-41 an absolute limit regualtion occurs at approximately 545 minutes and lasts for 10 minutes. At 560 minutes a delta regulation is then requested and lasts for 15 minutes. During the regualtion events the estimate of possible production with no corrections increases sharply while the estimates based on only the NWS correction and both the NWS and dynamic wake model (DWM) corrections seem to follow a constant slope similar to that of the actual production slope before and after the regualtion. This indicates that the corrections are qualitatively doing the right thing. However, the NWS corrrection and the NWS/DWM correction give almost the same results indicating that the DWM does not contribute much to the overall correction. Actually, the DWM is ***increasing*** the estimate of the possible production. The results indicate that the NWS correction provides the greatest improvement in the possible production estimate currently employed at Nysted (No Corrections).

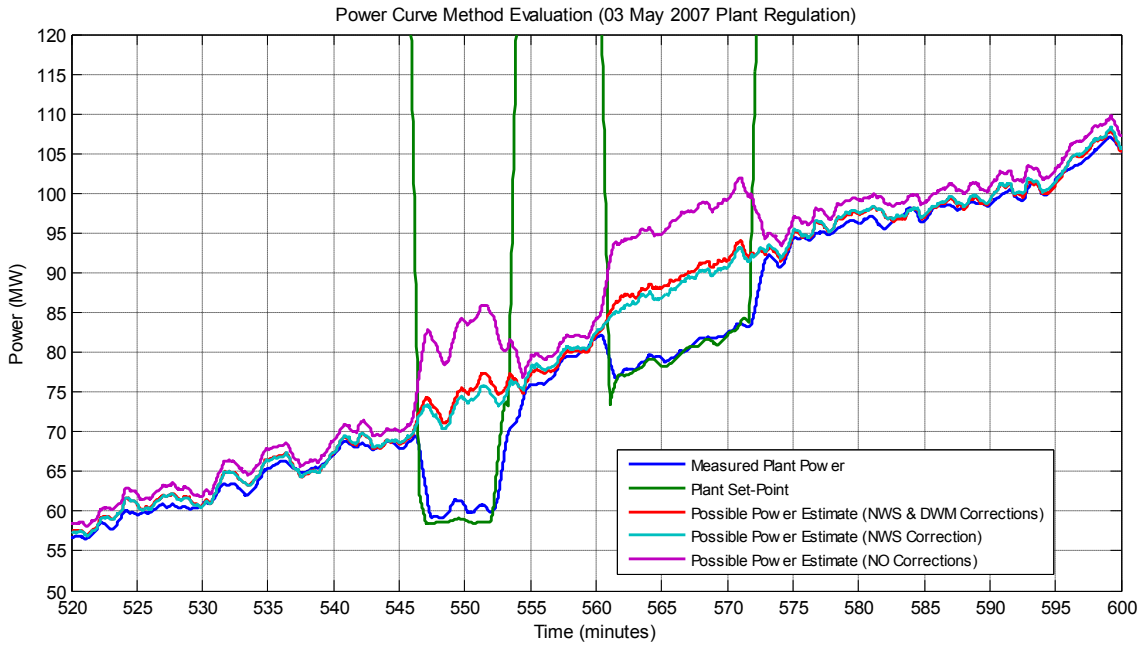

Figure 4-41: Power Curve Method Applied to Measured Down Regulation Data (3 min measurement data points)

The second regualtion event, depicted in Figure 4-42, features a absolute limitation command of approximately 93 MW at time 625 minutes. At that time the estimate with no corrections jumps approximate 15 MW; where as the estimates employing the NWS correction and the NWS and DWM correction appear not to respond to the down-regulation. At time 675 minutes the plant reaches the maximum possible production of 157 MW (less than the rated plant power of 169.2 MW due to offline turbines) and all 3 of the estimates converge as the turbines enter power limiation mode. Another interesting observation is at 725 minutes the actual power drops slightly below the plant set-point. At this point the estimates which employ the corrections almost converge with the actual power. However the estimate with no corrections indicates a possible production of 100MW and therefore if this estimate was correct, the actual production should remain at the set-point level.

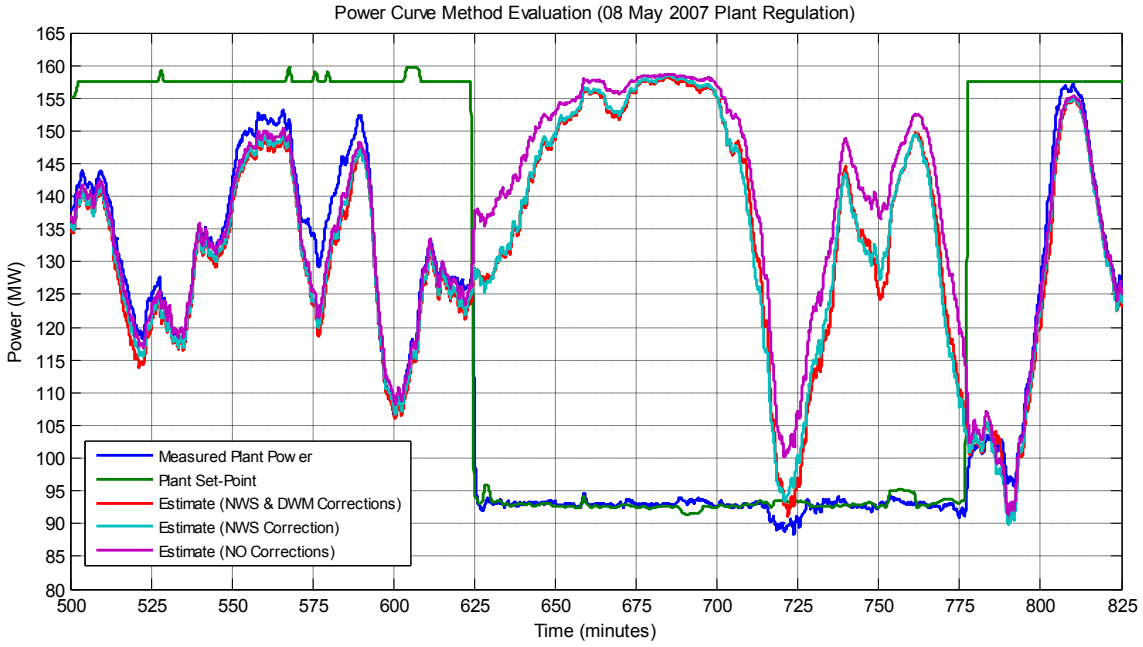

Figure 4-42: Power Curve Method Applied to Measured Down Regulation Data (3 min measurement data points)

The final regulation event depicted in Figure 4-43 is a continuation of the operation in Figure 4-42.At approximately 840 minutes an absolute regulation command of approximately 93 MW is issued. In this case the plant production is close to rated power and begins to decrease shortly after the start of the regulation. An interesting observation between approximately 860 and 870 minutes is the estimate that includes the DWM deviates from the estimate with only the NWS correction. The mean wind direction during this time is approximately 278 degrees, which corresponds to the principle West-East direction and causes in increase in wake effect. The DWM correction responds to the increased wake effect, which decreases the wind speeds throughout the wind plant by applying a positive correction to measured wind speed values.

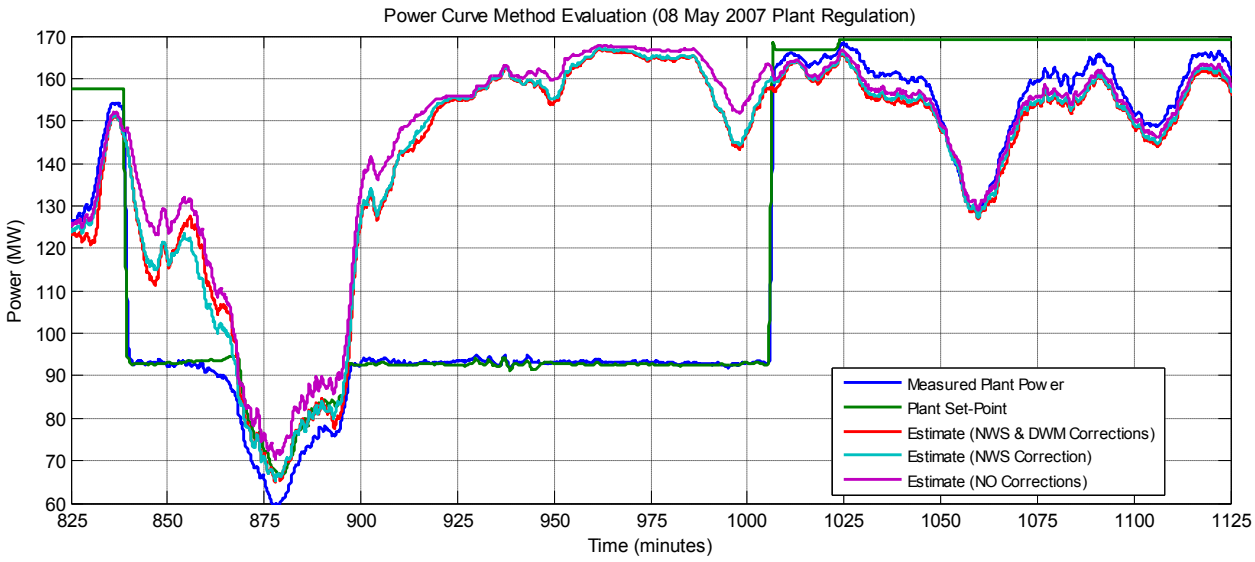

Figure 4-43: Power Curve Method Applied to Measured Down Regulation Data (3 min measurement data points)

4.1.8 COMMENTS ON THE POWER CURVE METHOD

Overall the power curve method described in this present work provides a improvement over the current method employed at Nysted during down-regulation. The major contribution to the improvement is the addition of the NWS correction. The DWM was found to not contribute significantly to the improvement during down-regulation for most operating conditions. The turbines at Nysted are stall regulated and therefore the rotor C_T, and subsequent wind speed deficit in the wake, change relatively little during down-regulation compared to a pitch regulated turbine. For the most unfavorable wind directions and wind speeds the DWM could improve the estimate error by approximately 10% (see Section 4.1.3.6 and Figure 4-34). A significant assumption in development of the DWM however, is that the wind speed deficit in the wake stabilizes for C_T values greater than 1. The only qualification of this assumption is the qualitative performance analysis of down regulated operation presented in the previous section. Additional down-regulated operation is needed to gain confidence in the DWM.

The DWM correction will be more significant for a wind plant configured with pitch regulated turbines since the rotor C_T changes more dramatically during down-regulation. Selected simulation results of down regulation of a wind plant with pitch-regulated turbines are provided in Section 5.5.

A drawback to the power curve method not considered here is the degradation of both the rotor performance and the NWS measurement over time. The rotor performance degrades overtime due to blade surface contamination. The NWS measurement degrades overtime due surface contamination of the anemometer cups and bearing friction. These effects will induce an error in the estimate of the possible production and require recalibration of power curve and the NWS correction over time to reduce the estimate error.

The measurement data employed in calculation of the TI-based family of power curves was limited between 113 and 343 degrees, which includes the prevailing wind direction, to ensure wake effects from the surrounding turbines were excluded. However, it is known from previous analysis of measurements at both Nysted (16) and Horns Rev (17) that the power curve is heavily dependent on the changes in ambient wind conditions from varying yaw sectors. This uncertainty was not investigated.

Another assumption in the calculation of TI-based family of power curves is that the power curve derived from a single turbine (A09) and can be extended to estimate the production at all other turbines. Power curves calculated from other turbines in the plant were not investigated. An improvement of the calculation of the power curve could be to include measurement data from all turbines in the wind plant with no wake effects. The resulting power curve would better represent the overall wind plant.

4.2 GRID METHODS

The grid methods are an alternative control strategy that facilitates estimation of the possible wind plant production during regulation and requires no wake model development, wind speed measurement error correction or power curve. This strategy essentially splits the wind plant into two separate grids; one grid is used to estimate the total plant production while the other is down regulated to meet the desired plant control objectives. This approach is advantageous in its simplicity, which is an important factor for successful implementation of a real time controller. Additionally, it employs the power measurement directly rather than inferring it from other measurement quantities. An obvious drawback however, is that only 50% of the possible plant production can be down-regulated or possibly less depending on the limitations of each turbine.

The underlying assumption for employing either grid method is that the average wind conditions throughout both grids are the same during both normal and down-regulated operation. This implies that if all turbines are operating in each grid their power outputs are the same. In this case one grid serves as the measurement grid, where these turbines are maintained at their maximum production and represent one half of the total possible production. The second grid is a control grid that is down-regulated to meet the desired wind plant control objective.

In this present work 2 alternative grid layouts are investigated. For both layouts, approximately 1 year of 3min measurement data from Nysted are used to compare the power output between the measurement and control grids during normal operation. The difference between the grids, referred to as the error between the grids, is calculated as:

$$error_{between\ \ grids} = \left(\frac{P_{MT} - P_{CT}}{P_{rated}}\right) * 100$$

Where: $P_{MT} = \frac{\sum_{i=1}^{N} P_{MT}^{WT\,i}}{\sum_{i=1}^{N} S_{MT}^{WT\,i}} * \sum_{i=1}^{N} S_{MT}^{WT_i}$ and $P_{CT} = \frac{\sum_{i=1}^{N} P_{CT}^{WT\,i}}{\sum_{i=1}^{N} S_{CT}^{WT\,i}} * \sum_{i=1}^{N} S_{CT}^{WT_i}$

And P_{rated} is the rated plant power, $P_{MT}^{WT_i}$,$P_{CT}^{WT_i}$ are the measured production, $S_{MT}^{WT_i}$,$S_{CT}^{WT_i}$ are the status values of the i^{th} measurement (MT) and control (C_T) turbines, respectively. N is the total number of turbines. Note that online turbines here are indicated by value 1 in contrast to the convention found in Table 3-1.

The wind direction and wind speed distributions of the measurement data employed in the analysis are depicted in Figure 4-44. These measurement data are used to statistically evaluate the error during normal operation. Simulation of the grid methods were also carried out to investigate the change in wake effects during down-regulation (Section 4.3.2).

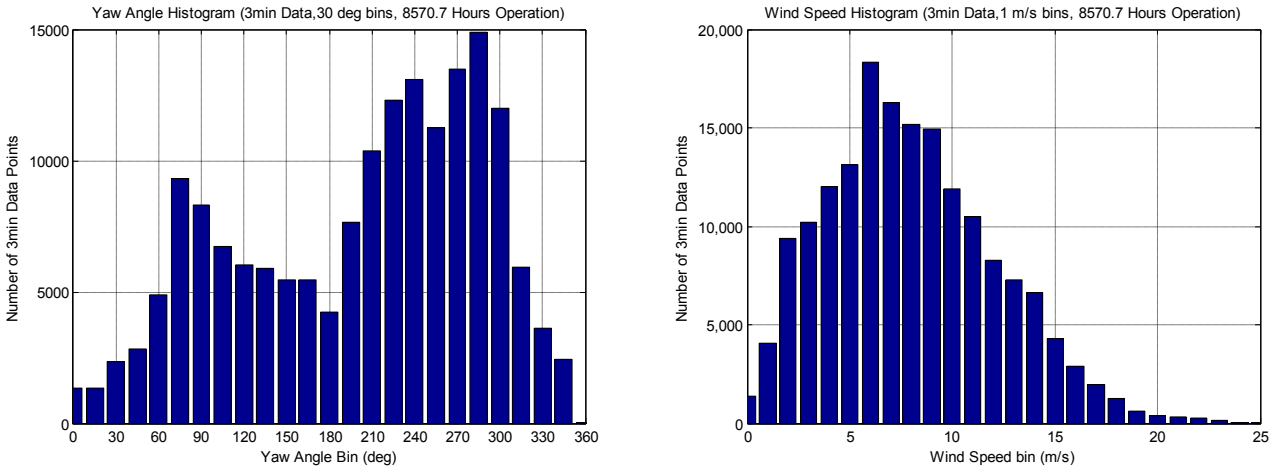

Figure 4-44: Wind Direction and Wind Speed Distributions for Measurement Data Analyzed (3 min measurement data points)

4.2.1 SPLIT GRID METHOD

The split grid method employs 2 separate grids determined by the principle alignment directions of the wind plant (see Figure 3-2). The 4 principle alignment directions investigated are depicted graphically in Figure 4-45. The basic idea of the split grid method is to choose grids based on a mean plant wind direction determined from the average yaw angles of all online turbines. The wind plant controller maintains the grid layout within a +/-45 deg window about the split direction. If the wind direction changes outside this window the wind plant controller switches the split grid layout to match the mean plant wind direction. with adequate hysteresis to avoid oscillation between different grid layouts.

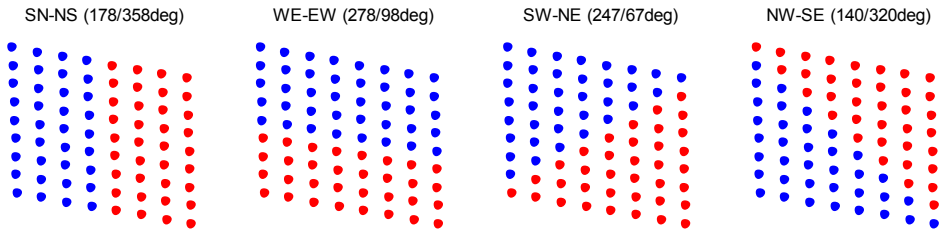

Figure 4-45: Different Split Grid Layouts

To assess the ability of the split grid method to accurately predict the total possible plant production, the power production of each grid during normal operation are compared. Analysis of the measurement data from Nysted indicates that the error between the split grids is less than 15% for all configurations , 90% of the total time analyzed. The analysis includes data from a +/- 45 degree yaw sector about the split grid axis (from both directions) and are limited to a minimum plant production level of 25% of rated. The mean and standard deviation of the error between grids is summarized in Table 4-4. Duration curves for the error between the split grids are depicted in Figure 4-49.

Grid Layout	**Mean Value**	**Confidence Interval of the Error Between Grid**		
		1 σ (68%)	2 σ (95%)	3 σ (99.7%)
North-South / South-North Split Grid	0.1%	6.0%	12.1%	18.1%
West-East / East-West Split Grid	1.6%	5.7%	11.5%	17.2%
South-West / West-South Split Grid	1.4%	6.6%	13.1%	19.3%
North-West / West-North Split Grid	-1.3%	7.1%	14.2%	21.3%
Interlaced Grid	*-0.2%*	*0.9%*	*1.8%*	*2.7%*

Table 4-4: Summary of Error Between Grids (Measurement Data)

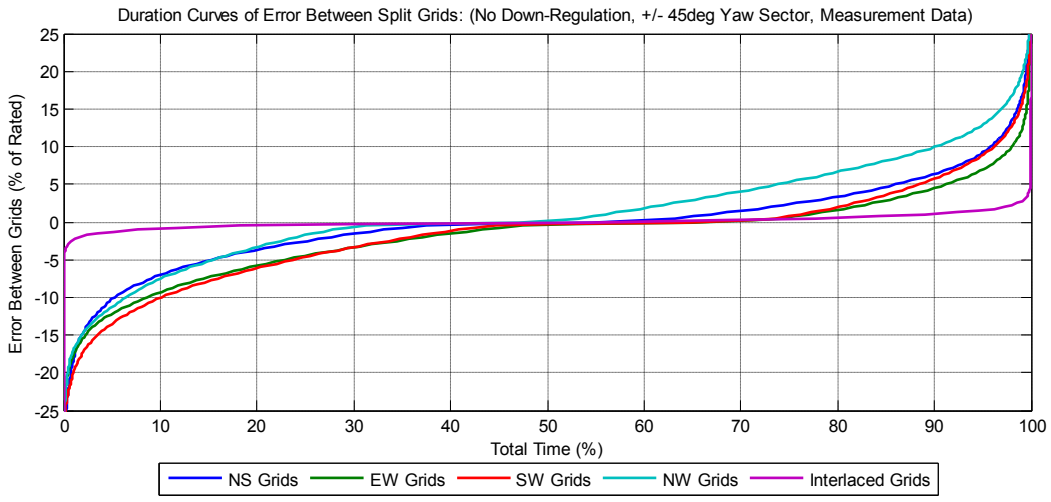

Figure 4-46: Duration Curves of Error Between Split Grids and Interlaced Grids (3 min measurement data points)

A 3 dimensional histogram of the error between the split grids for varying power levels is depicted for the 4 principle directions in Figure 4-47. The abscissa indicates the error between the grids as a percentage of rated power while the ordinate indicates the plant production level. The color of each square indicates the total amount of time at that error and power level. The sum of all the square equals 100%. Note that the scale is logarithmic.

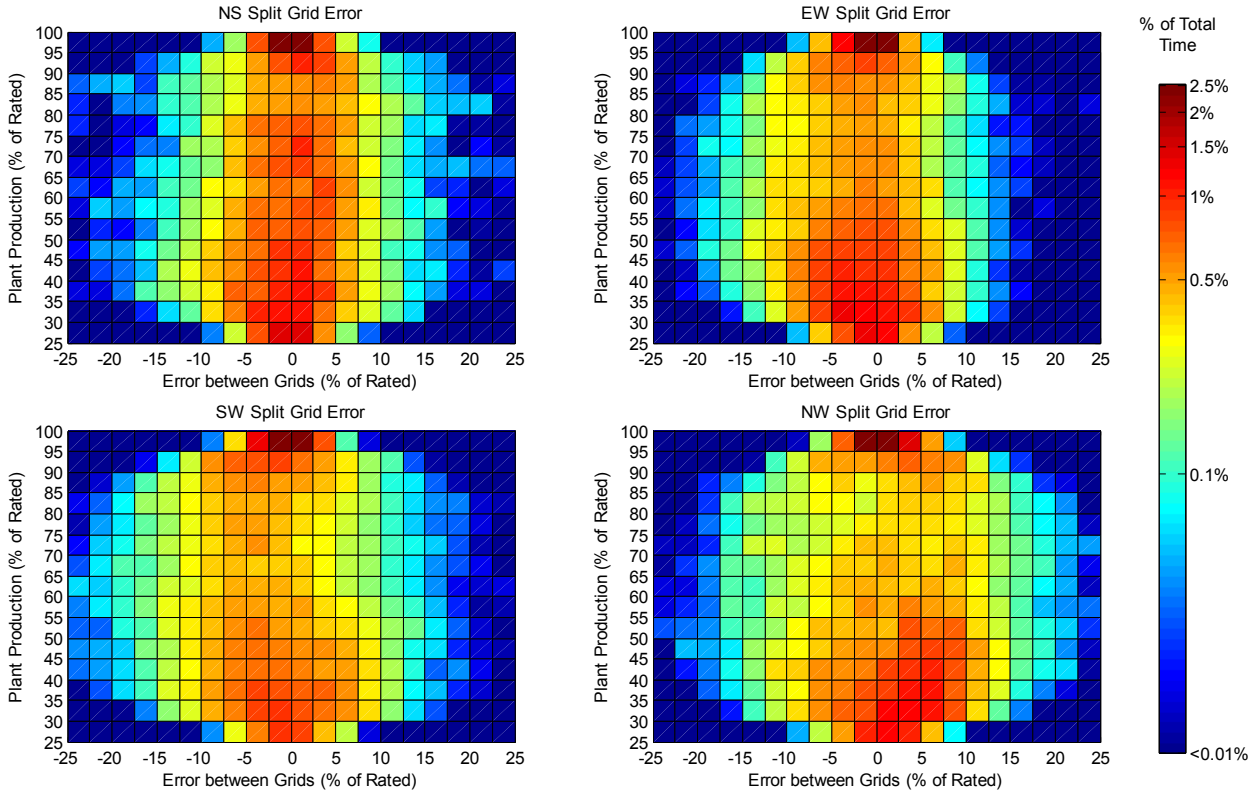

Figure 4-47: 3D Histogram of Error between Splits for the 4 Principle Directions (3 min measurement data points)

Overall, the results from analysis of the split grid method indicate significant scatter between the power output in each grid (Up to +/- 20%). However the mean value of the error for all configurations is close to zero indicating the method

could be useful during absolute limitation and balance control. For these types of regulations, the estimate of the possible production is used to predominately to calculate the financial cost of the lost production. Over a long period of regulated operation the estimate error of the measurement grid tends to zero so the lost production, and its subsequent financial cost, could be effectively calculated from the difference between the possible production estimate and the actual production. However, the analysis of the measurement data do not include any down-regulated operation which may induce an additional estimate error due to the altered wake effects of the down-regulated grid. This error may be significant for unfavorable wind directions where the measurement grid is down-wind of the control grid. The effect of down-regulation is investigated with simulations in Section 4.3.2.

4.2.2 INTERLACED GRID METHOD

A variation of the split grid method that gives better results during normal operation configures the control and measurement grids in the interlaced pattern depicted in Figure 4-48. In this layout spatial variations in the wind are effectively accounted for since the measurement and control turbines are evenly distributed throughout the wind plant.

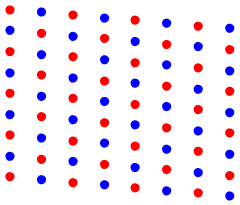

Figure 4-48: Interlaced Grid Layout

Analysis of approximately 1 year of 3min measurement data from Nysted indicates that the error between the interlaced grids for normal operation is less than 2% , 90% of the total time analyzed. For the interlaced grid the yaw sector is not limited, as is the case for the split grid method since the grids are independent of wind direction. However, the minimum plant production level is still limited to 25% of rated. The mean and standard deviation of the error between grids are summarized in Table 4-4.

The duration curve and 3D estimate error between the interlaced grids are depicted in Figure 4-49.

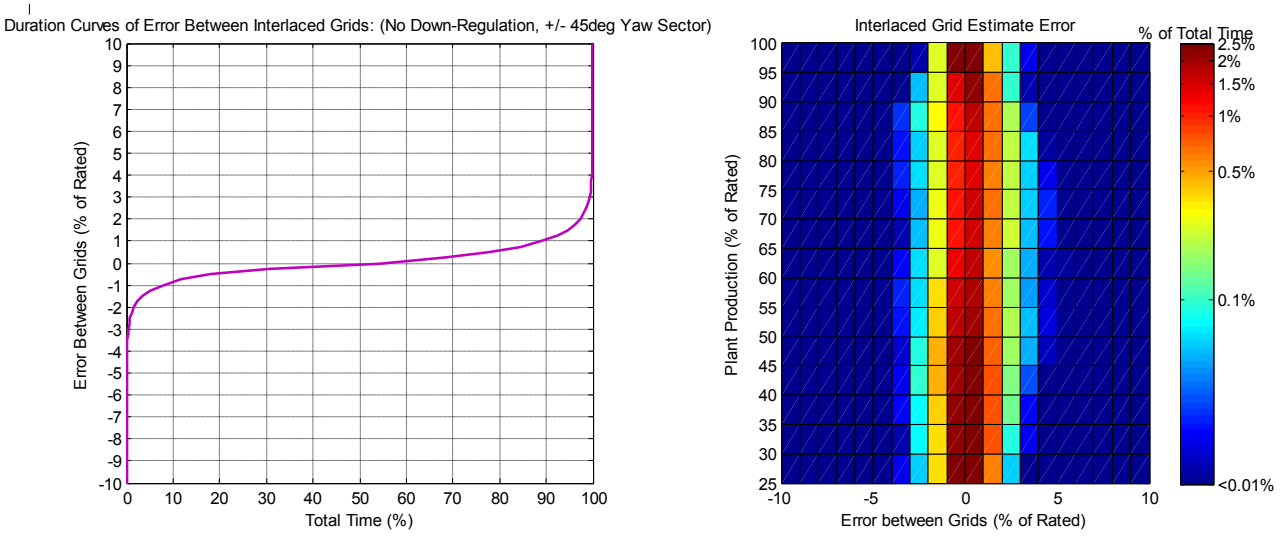

Figure 4-49: Duration Curve and 3D Histogram of Error between Interlaced Grids (3 min measurement data points)

The results indicate very good agreement between the interlaced grids. However, like the split grid analysis, no down-regulated operation is included. In this case the altered wake effects of the down-regulated control grid will interact with the measurement grid and induce an error. This is unavoidable. The magnitude of the error caused by the altered wakes is investigated with simulations in Section 4.3.2.

4.3 COMPARISON WITH SIMULATIONS

The power curve and grid estimation methods were implemented in the Wind Power Production Simulation Tool (WPPST, Section 5) to investigate their performance during down regulation. Simulations were run for both normal and 100% down-regulated operation using 546 hours of simulated wind direction and wind speed input data. For each case the simulated wind direction and wind speed input data were identical. Maximum down-regulation is not possible at Nysted, since down-regulation of individual turbines is limited to approximate 25% of rated production but this represents a worst case for investigation of the performance of the DWM. The distribution of the input data is depicted in Figure 4-50. Note that this distribution does not corresponds to the measurement data distribution depicted in Figure 4-44. In this present work, the wind direction was limited to a mean value of 178 degrees. The wind speed input values were generated by PARKSIMU, described in Section 5.3, for the Nysted wind plant layout with 178 degree wind direction and mean wind speed values of 7, 9, 11, 13 m/s. For all cases the estimate error is calculated as:

$$e_{estimate} = \left(\frac{P_{est} - P_{norm}}{P_{rated}}\right) * 100$$

Where P_{est} is the possible production estimate based on the power curve method or the grid method, P_{norm} is the simulated production during normal operation and P_{rated} is the rated plant production. P_{norm} represents the reference production from which P_{est} is compared during down-regulation.

All analysis was performed on 3 min mean values of the simulation data.

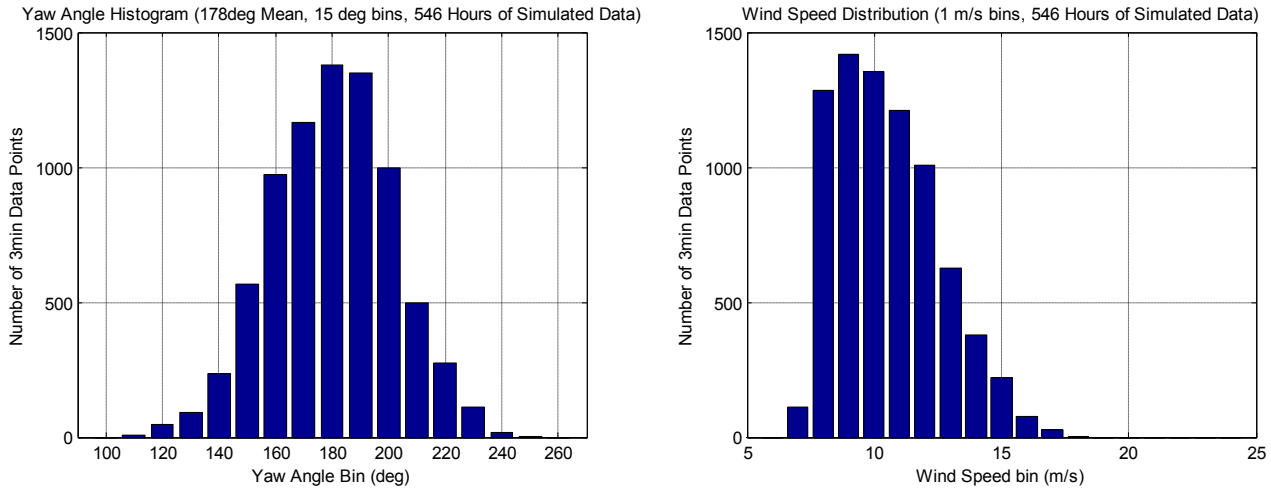

Figure 4-50: Wind Direction and Wind Speed Distributions for Simulation Data

4.3.1 SIMUALTION RESULTS: POWER CURVE METHOD

Simulations of the Power Curve Method were preformed for both normal and down-regulated operation. They were primarily intended to investigate the performance of the DWM. The NWS correction was not included in the simulation model since modeling of the local flow conditions about the NWS measurement are beyond the scope of this work. Details of the power curve model employed in the simulations are described in Section 5.4. In the case of down-

regulation, the estimated production was compared to the production during normal operation to determine the estimate error. This is possible because the wind direction and wind speed input for both cases are identical.

Overall the results indicate that the DWM performs as expected. During normal operation, the DWM makes essentially no correction since no down-regulation occurs. The estimate error for normal operation is depicted in Figure 4-51 and Figure 4-52, as a duration curve and a 3D histogram (left most plot), respectively. The estimate error for normal operation is significantly less than that from measurements since the model employs a "perfect" power curve derived from the wind turbine model, the wind speed inputs are exactly the same for the estimate and wind turbine model, and no NWS correction is required. For the case of 100% down regulation, i.e. all turbines down-regulated to zero power, the estimate error without the DWM under predicts the possible production since down-regulation further decreases the wind speed in each turbine's wake compared to normal operation. Inclusion of the DWM returns the mean estimate error to approximately zero but includes increased scatter compared to the no down-regulation case.

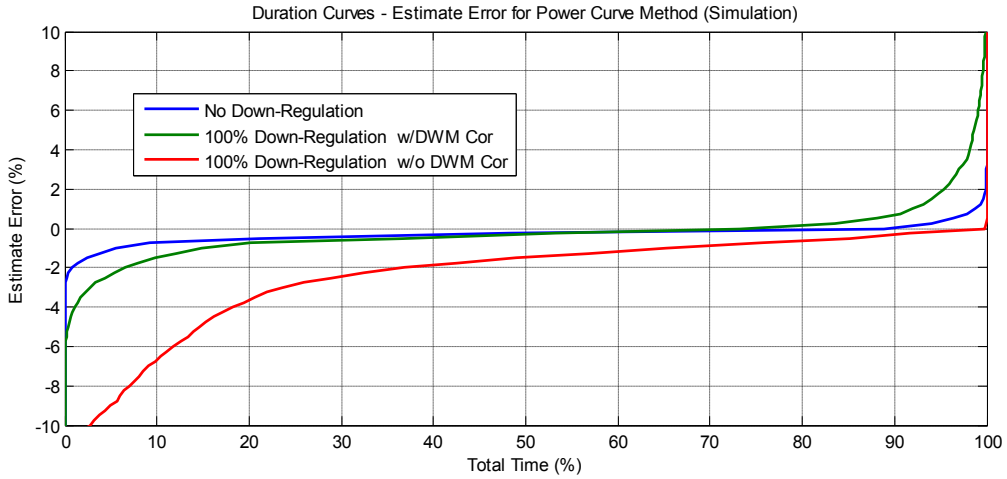

Figure 4-51: Duration Curves of Estimate Error for Power Curve Method (Simulation Data)

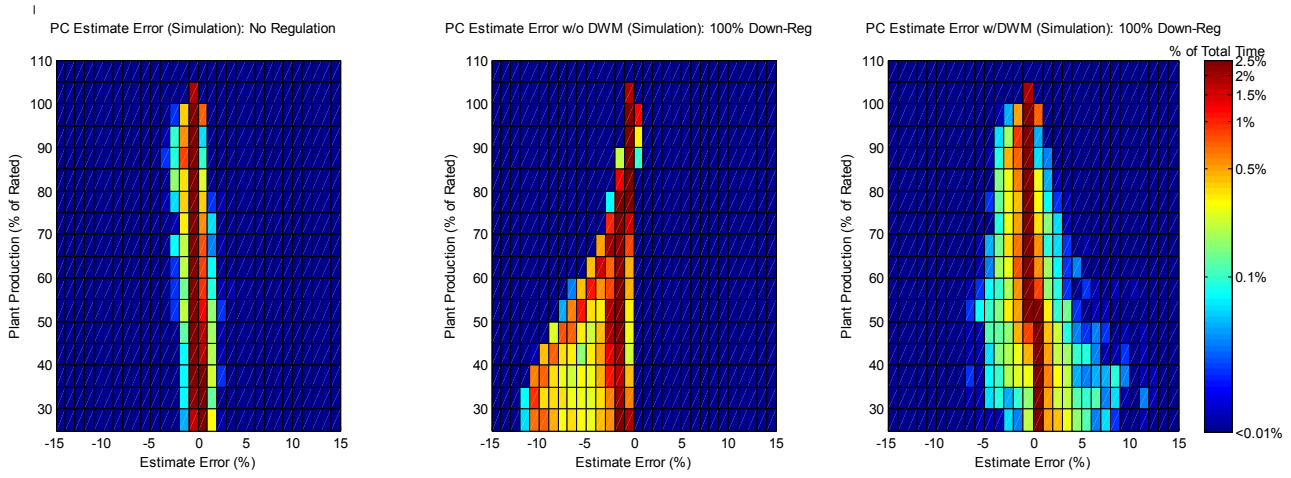

Figure 4-52: 3D Histogram of Estimate Error for Power Curve Method (Simulation Data)

The mean DWM adjustment for normal and down-regulated operation versus wind direction are depicted in Figure 4-53 and provides an indication of the DWM adjustment level. During normal operation the DWM should provide no correction since the estimate and the actual production are the same (left plot in Figure 4-53). The corrections visible during normal operation are due to discrepancies between the pitch angle trajectory for normal operation employed in the simulations (described in Section 5.4.1) and the commanded pitch angles of the individual wind turbine model controllers (described in Section 5.1). The discrepancies are exacerbated when the wind direction corresponds to the a

principle alignment direction (in this case 178 degrees) which corresponds to the greatest wind speed deficits. During down-regulation (right plot in Figure 4-53). the DWM provides a varying level of correction that is also heavily dependent on wind direction.

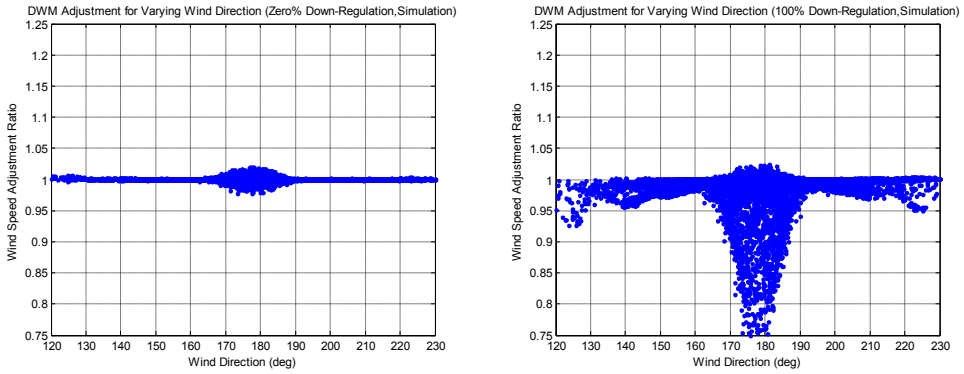

Figure 4-53: Overall DWM Adjustment for Varying Wind Direction for zero and 100% Down-Regulation (Simulation Data)

4.3.2 SIMUALTION RESULTS: GRID METHODS

Simulations of the North-South Split and Interlaced grid methods were preformed for both normal and down-regulated operation. The normal operating case provides a base line to validate the model against measurement data while the down-regulated case provides an estimation of the performance of the grid methods during down-regulation. In the case of down-regulation, the estimated production was compared to the production during normal operation to determine the estimate error. This is possible because the wind direction and wind speed input for both cases are identical. Note that the wind direction distribution is quite restricted for the simulations compared to the measurement data. This impacts the scatter primarily in the split grid case result since the large wind direction deviations from the principle split direction (178 degrees for North/South grids) produces larger errors. Future work should include a larger wind distribution. For simulations of down-regulated operation the control turbines were down-regulated 100% to ensure the worst case change in the wake effects of the down-regulated turbines. This represents a 50% delta regulation.

Overall the simulation results for the split and interlaced grid methods for normal operation indicate agreement with measurements in terms of the mean error value and scatter considering the limited wind direction distribution. A summary of the error between the grids is depicted in Table 4-5, the duration curves are depicted in Figure 4-54 and the 3D histograms are depicted in Figure 4-55 and Figure 4-56 for the split and interlaced grids, respectively.

Grid Layout	**Mean Value**	**Confidence Interval of the Error Between Grids**		
		1 σ (68%)	2 σ (95%)	3 σ (99.7%)
Interlaced Grid: No Down Regulation	0.0%	0.5%	1.0%	1.5%
Interlaced Grid: 100% Down Regulation	1.6%	2.0%	4.0%	5.9%
NS Split Grid: No Down Regulation	0.1%	4.1%	8.2%	12.4%
NS Split Grid: 100% Down Regulation	0.2%	4.2%	8.4%	12.6%

Table 4-5: Summary of Error Between Grids (Simulation Data)

The results of the split grid method indicates that the error between the grids does not change significantly during down regulation, implying that the interaction of the altered wake effects between grids tends to average out if the wind direction distribution is even about the principle split direction.

The error during down-regulation with the interlaced grid method becomes increasingly negative for decreasing power levels, reaching -7.5% at 35% of rated production. This is a result of wakes from control (down-regulated) turbines affecting the measurement turbines.

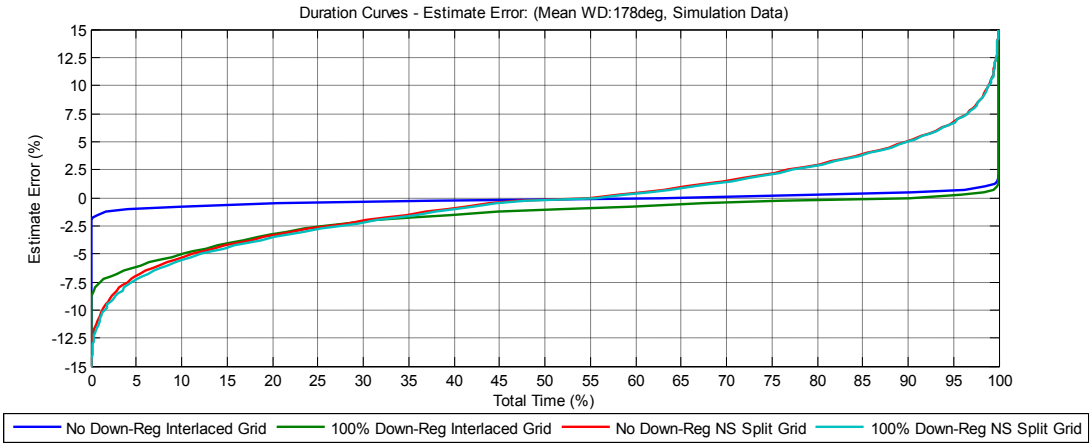

Figure 4-54: Duration Curves of Error Between North/South Split Grids and Interlaced Grids for zero% and 100% Down-Regulation (Simulation Data)

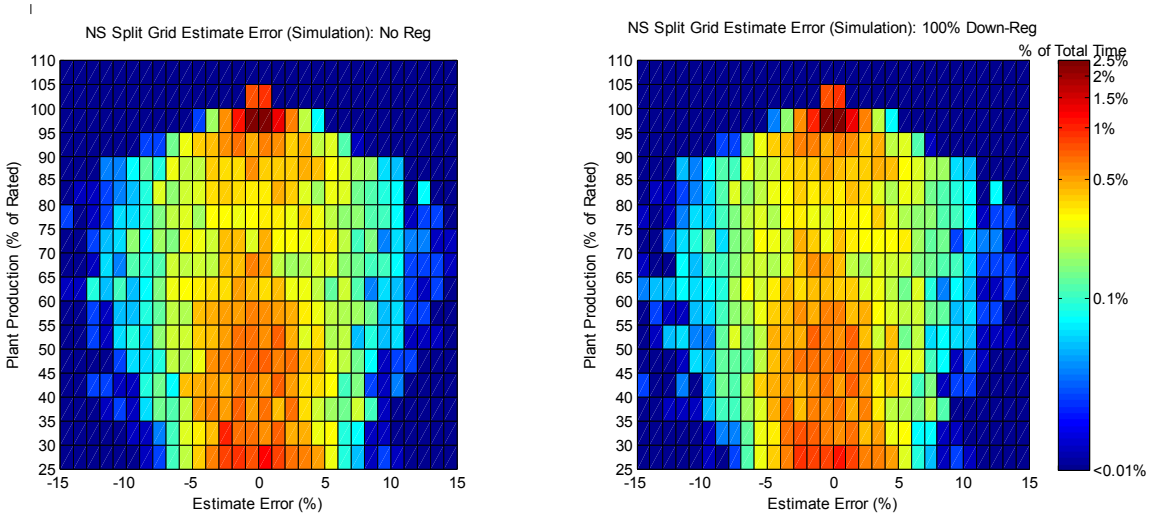

Figure 4-55: 3D Histogram of Error between North/South Split Grids for zero% and 100% Down-Regulation (Simulation Data)

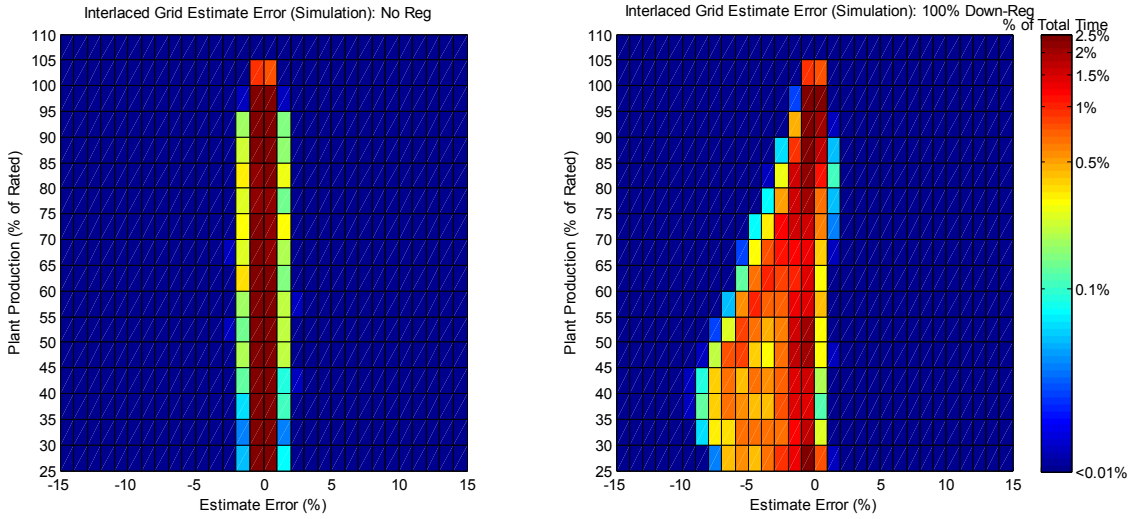

Figure 4-56: 3D Histogram of Error between Interlaced Grids for zero% and 100% Down-Regulation (Simulation Data)

5 WPPST SIMULATION MODEL

The Wind Plant Power Simulation Tool (WPPST) is intended for investigations of different wind plant control strategies and in this present work is configured for evaluation of the different possible production estimation methods described in the previous sections. It is primarily intended to represent the Nysted Wind Plant in terms of plant layout and turbine configuration but an alternative version, incorporating pitch regulated turbines, has also been developed. The pitch regulated turbine is based on the historic 2MW Tjaereborg turbine.

A significant feature of the WPPST is that each turbine is represented individually. The wind turbines have not been aggregated as is often the case in wind plant simulation models so that the interaction between the wind plant controller and the individual turbines can be incorporated. Additionally, the model can account for the wake effects from each turbine during normal and down-regulated operation.

The WPPST has been developed in Matlab® Simulink ®. It consists of the following major functional sub-models:

- Simulation Input Data
- Wind Turbine Model
  - Stall Regulated Turbine (Nysted Turbine)
  - Pitch Regulated Turbine (Tjaereborg Turbine)
- Wind Plant Controller Model
  - Power Curve Method
  - Grid Methods
- Wind Simulation Model
  - Park Scale Model
  - Rotor Wind Model
  - Wake Model
- Possible Plant Production Model
  - Power Curve Method
  - Grid Methods

Each of these sub-model are described in turn. The general layout of the WPPST is depicted in Figure 5-1 and highlights the data flow between sub models. Table 5-1 describes the salient data values.

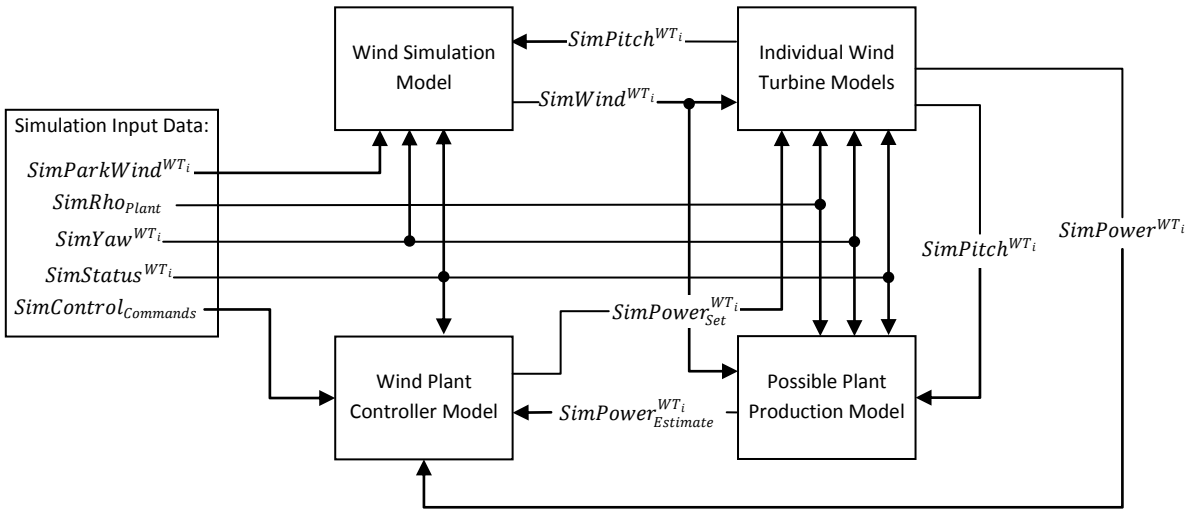

Figure 5-1: Simulation Model Layout

Simulation Input Data	Description
$SimParkWind^{WT_i}$	Simulated wind input at each turbine generated from (PARKSIMU).
$SimRho_{Plant}$	Simulated air density input of overall plant.
$SimYaw^{WT_i}$	Simulated yaw angle of each turbine.
$SimStatus^{WT_i}$	Simulated status of each turbine.
$SimControl_{Commands}$	Simulated plant control commands.
Model Data	
$SimPitch^{WT_i}$	Simulated pitch angle command from the each wind turbine model's pitch controller.
$SimPower_{Set}^{WT_i}$	Simulated power set-point command for each wind turbine model.
$SimPower_{Estimate}^{WT_i}$	Simulated possible power estimate of each wind turbine.
$SimPower^{WT_i}$	Simulated power output of each wind turbine model.

Table 5-1: Salient Data Employed in the WPPST

All input data are loaded at the start of the simulation. The simulated wind speed values at each turbine location are generated from the PARKSIMU program described in Section 5.3. The yaw angles are currently generated from a highly modified wind speed signal and are identical for all turbines. This approach provided a convenient way to produce a stochastic yaw angle signal. The status values in this present work have all been set to zero (indicating all turbines online as defined in Table 3-1). The wind plant controller commands vary depending on the simulation objective. The plant air density is set to 1.225.

The simulation model uses a fixed-step discrete solver with a 1 second time step. This approach is intended to represent the actual wind plant controller, which operates on fixed priority real time operating system (i.e. constant or fixed update rate). A one second time step might be considered insufficient in regards to power output fluctuations since the blade passing frequency of this size machine is on the order of 1 second but the focus of this tool is on the overall plant output, measured on the minutes time scale.

5.1 WIND TURBINE MODEL

The wind turbine model is configured as a standalone model called by the main simulation model during simulation. There are 72 identical wind turbine models called by the main simulation model. Each of these models has unique input data corresponding to its specific turbine number. The input data to the wind turbine model include the turbine status, turbine power reference (set-point command), nacelle wind speed and the air density. Input data values are updated at each simulation time step. Details of the model are provided in Appendix I.

5.1.1 STALL REGULATED TURBINE (NYSTED TURBINE)

The stall regulated wind turbine model is based on the Siemens 2.3MW turbine installed at Nysted described in Section 3.1. It incorporates Power and C_T lookup tables provided by Siemens which are intended to represent the as-built turbines. The lookup tables are depicted in Figure 5-2. The specific settings of the wind turbine controller are derived from the turbine parameter log file (18). In this present work the pitch controller does not include a below rated power optimization pitch schedule like the actual machine since it has little impact on the performance of the turbine during down-regulation

The behavior of the stall regulated turbine model is compared with measurements from one turbine at Nysted. Overall, the wind turbine model and measurements are in good agreement. Power curves and normal operating pitch angle trajectories from the model and measurements, respectively are depicted in Figure 5-3. Additionally, the response of the model during start-up, shut-down and down-regulation has been compared qualitatively with good results using actual measurement data to drive the turbine model. Figure 5-3 depicts an example of down-regulation of turbine A09. Both the measured and simulated power traces follow the commanded set-point as expected. The corresponding pitch angle traces have the same character (during the regulation) but are offset from each other, indicating that the power lookup tables do not correspond exactly to the as built turbine. Additionally, the simulated turbine uses the single point

NWS measurement to calculate the rotor power; whereas, the measured power is related to the average wind speed over the entire rotor disk.

Note the below rated pitch activity of the measured data in Figure 5-4 is not represented in the simulation data. Additionally, the measured pitch angle data has an 1 HZ square wave overlaid on it below rated operation (a saw tooth in Figure 5-4 due to a 1min moving average filter) which is intended for pitch bearing lubrication. This is not present in the wind turbine model.

Finally, the power and pitch angle during start-up and shut-down are compared in Figure 5-5. In the shut-down case (initiated when the status signal changes from 100 to 900) the measured and simulated power ramp-down to zero power show good agreement. For the start-up case the pitch angle traces are offset because the wind turbine model does not consider the rotor speed ramp up and generator synchronization. In this mode the actual wind turbine controller employs closed loop speed control. However, it is the power ramp up that is significant for the overall model and this shows good agreement.

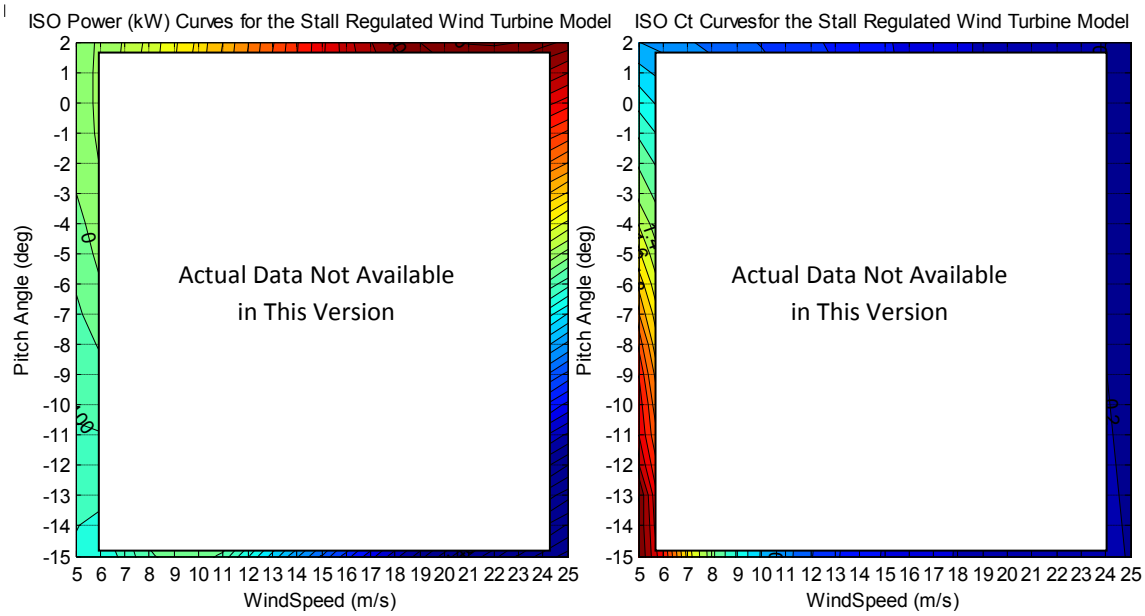

Figure 5-2: Power and C_T Maps for Siemens 2.3MW Turbine

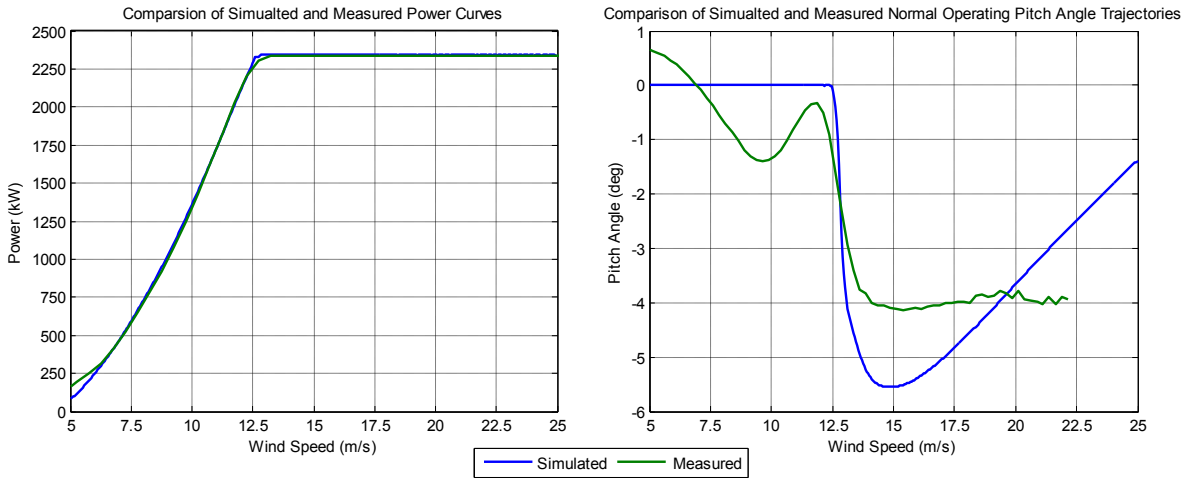

Figure 5-3: Comparison of the Simulated and Measured Power Curves and Pitch Angle Trajectories

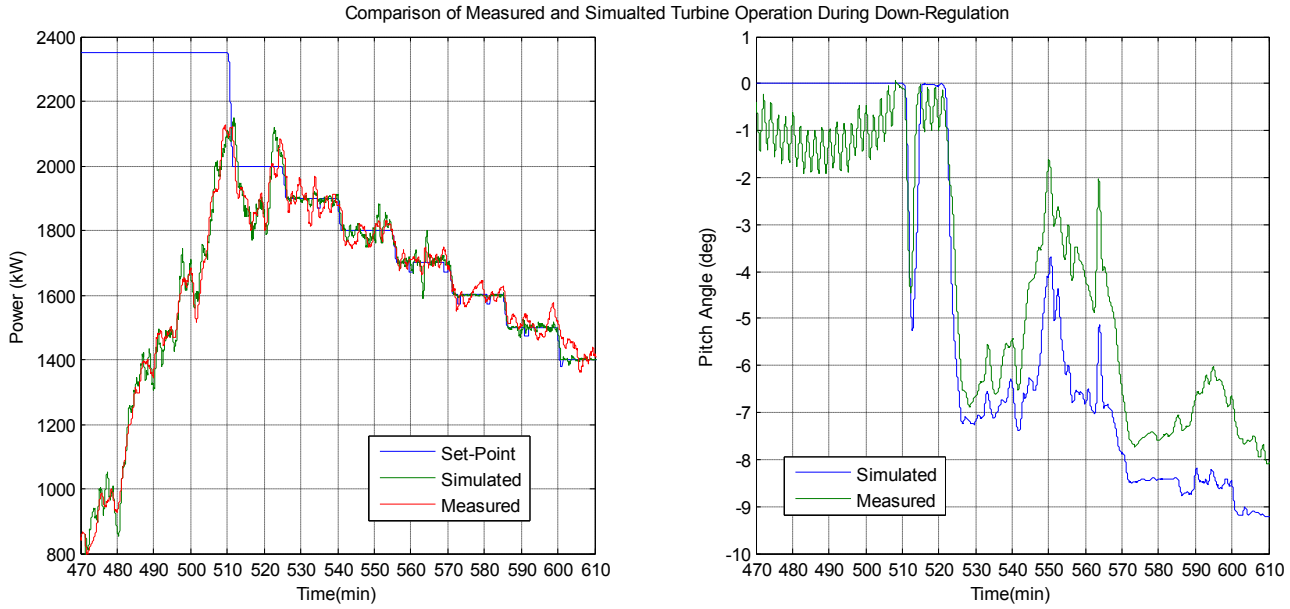

Figure 5-4: Comparison of Measured and Simulated Turbine Operation During Down-Regulation

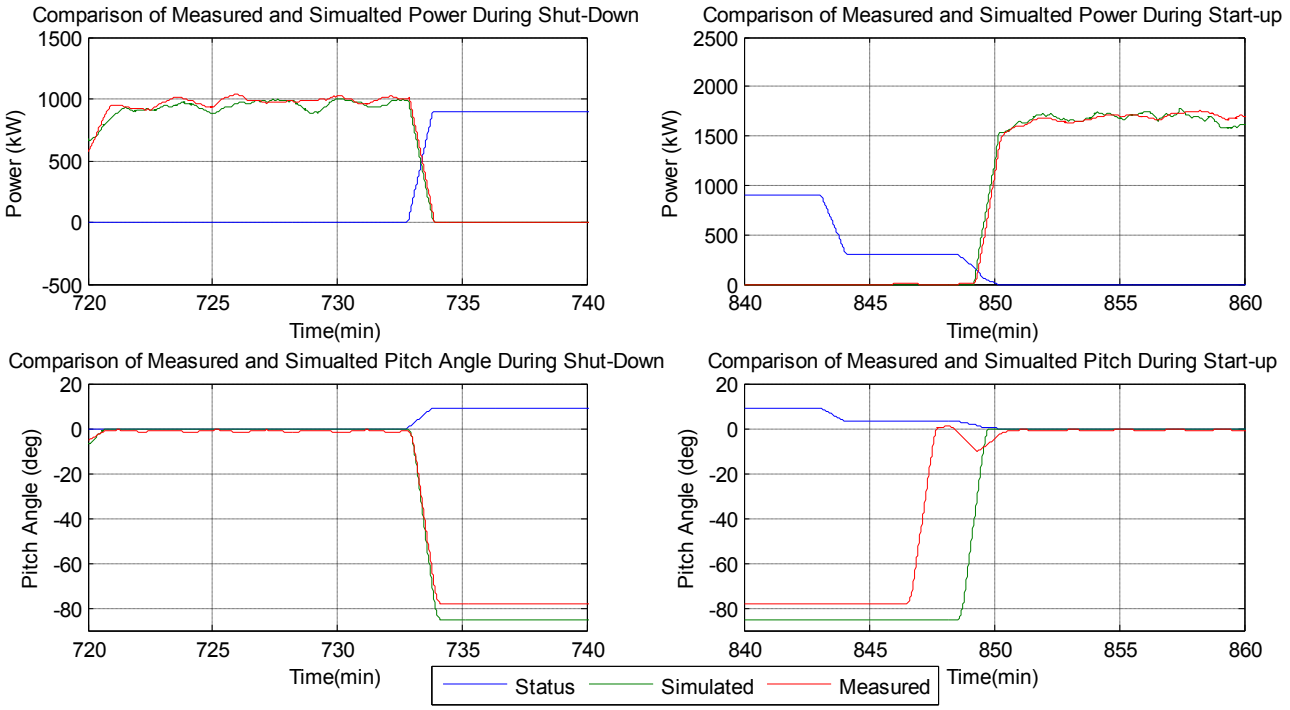

Figure 5-5: Comparison of Measured and Simulated Turbine Operation During Start-Up and Shut-Down

5.1.2 PITCH REGULATED TURBINE

The pitch regulated turbine is based on the 2MW Tjaereborg turbine. The power and C_T lookup tables were derived from application of a BEM code with appropriate aerodynamic and structural properties (19).The turbine controller is the same as that is employed in the stall-regulated turbine except for the controller gains and the pitch limits. A pitch-regulated turbine pitches increasingly positive to limit the power during normal operation above rater wind speed and during down-regulation. The controller gains were chosen visually by observing where the pitch activity was excessive

or became unstable and then they were reduced until stability returned. Figure 5-6 depicts the power curve, pitch activity and C_T for normal and varying levels of down-regulation. A significant feature of the pitch regulated turbine is that the C_T value decrease considerably during down-regulation in contrast to the stall regulated turbine. This implies that the wakes throughout the wind plant will also change considerably during down-regulation of a plant incorporating pitch-regulated turbines. Finally, the power and C_T maps for the pitch-regulated turbine are depicted in Figure 5-7.

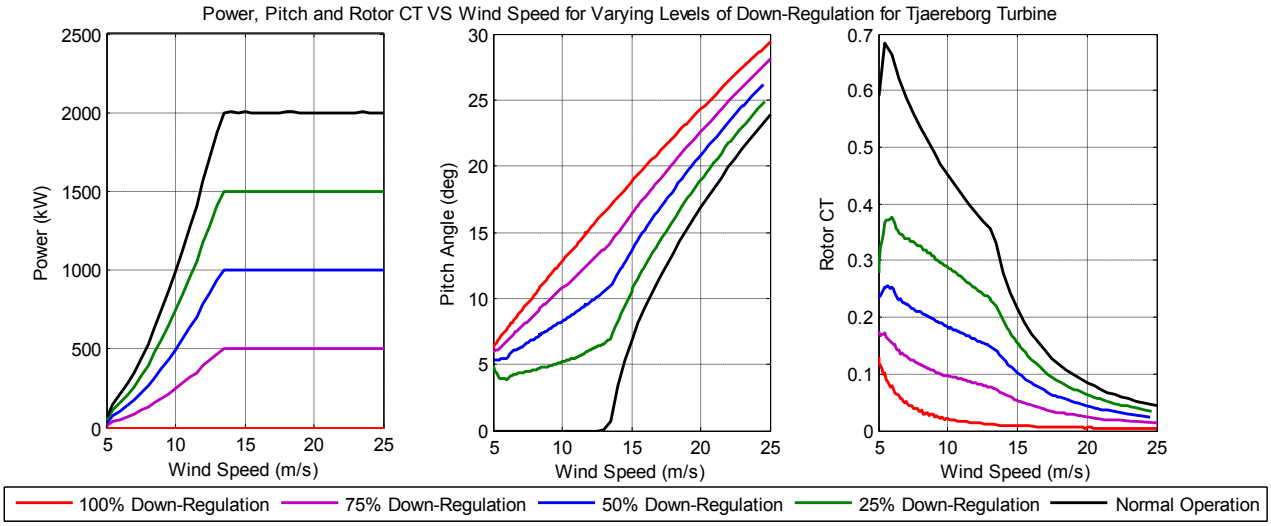

Figure 5-6: Power, Pitch and C_T for Varying Levels of Down-Regulation for Tjaereborg Turbine

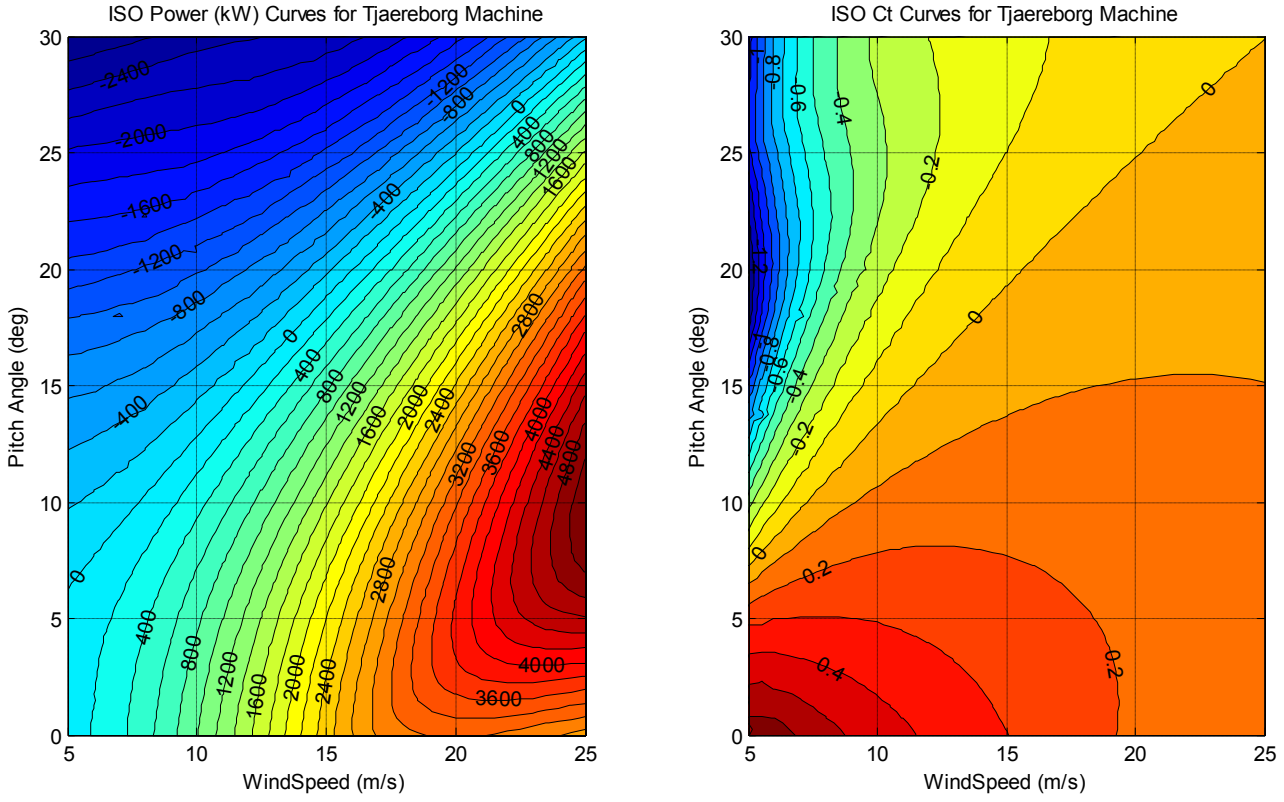

Figure 5-7: Power and C_T Maps for Tjaereborg Turbine

5.2 WIND PLANT CONTROLLER MODEL

Two different wind plant controllers (WPC) are employed in the simulation model depending on the possible power estimation method. The WPC employed for the power curve method is a simplified version of the as-built Nysted WPC. It is configured only for delta and absolute limitation control and employs the set-point distribution algorithm described in Section 3.2.

For the grid methods, the WPC can only adjust the set-points of the control turbines. Subsequently, the total plant set-point, P_{set}^{Plant} , is the sum of the production from the measurement turbines and the set-points from the control turbines as follows:

$$P_{set}^{Plant} = \sum_{i=1}^{N} P_{MT}^{WT_i} + \sum_{k=1}^{M} P_{Set}^{WT_k}$$

Where $P_{MT}^{WT_i}$ is the i[th] measurement turbine, *N* is the total number of measurement turbines, $P_{Set}^{WT_k}$ is the set-point of the control turbines, *M* is the total number of control turbines. The set-points of the control turbines in the grid method all take on the same value in contrast to the set-point distribution algorithm employed in the WPC for the power curve method. The set-point are determined as follows:

$$P_{set}^{WT_k} = \frac{P_{set}^{Plant} - \sum_{i=1}^{N} P_{MT}^{WT_i}}{\sum_{k=1}^{M} S_{CT}^{WT_k}}$$

Where $S_{CT}^{WT_k}$ is the status of the individual control turbines. Note that online turbines here are indicated by value 1 in contrast to the convention found in Table 3-1.The individual set-point, $P_{set}^{WT_k}$, are limited to the operating range of the individual turbine.

Calculation of the production from the measurement turbines is described in Section 5.4.2.

Details of both models are provided in Appendix I.1.

5.3 WIND SIMULATION MODEL

The primary input to the WPPST is a simulated time history file of wind speed values at each turbine throughout the wind plant if the wind plant did not exist. These “free” simulated wind speed values are then modified in the main simulation model to account for rotational sampling of the wind by the rotor blades and the wake effects throughout the wind plant. In this present work the wind simulation consists of the following elements:

- A park scale wind model (PARKSIMU)
- A rotor wind model
- A wake model

The park scale wind model is intended for simulation of power fluctuations in large wind farms and is implemented as a standalone application PARKSIMU (20). It simulates the hub-height wind speed at each turbine location in the wind plant and includes both the stochastic component of the wind caused by turbulence and the coherence between the turbulent structures at each turbine location in the plant. The stochastic component of the wind is important since the individual turbine power output is directly related to the wind speed below rated power. Additionally, the turbine control must respond to wind speed variations to maintain the desired power set point in both normal and down-regulated operation. The coherence is important to realistically represent power fluctuations from the entire plant output and is dependent on wind direction. These fluctuations have impact on the response of the wind plant controller (21).

The rotor wind model is included to account for rotational sampling of the wind speed field in the rotor area. It is implemented as a variable coefficient low pass filter that effectively smoothes the single hub height wind speed measurement to represents an equivalent rotor wind speed (ERWS) (21). In continuous time Laplace space the rotor wind model takes the following form (Eqn 36 in (21)):

$$H(s) = \frac{0.99 + 4.79ds}{1 + 7.35ds + 7.68(ds)^2} \; where \; d = {}^{R}/_{V_0}$$

Finally, the wake model is included to account for the effect of turbine wakes on the wind speed at each turbine position throughout the wind plant. It employs the static wake model (Section 4.1.3.1) with the simulated pitch, wind speed and yaw angles from each turbine to estimate the wind speed deficits at each turbine. The deficits are then added to the wind speeds estimated by the rotor wind model.

A block diagram of the simulated wind is depicted in Figure 5-8. Details of the model are provided in Appendix I.5.

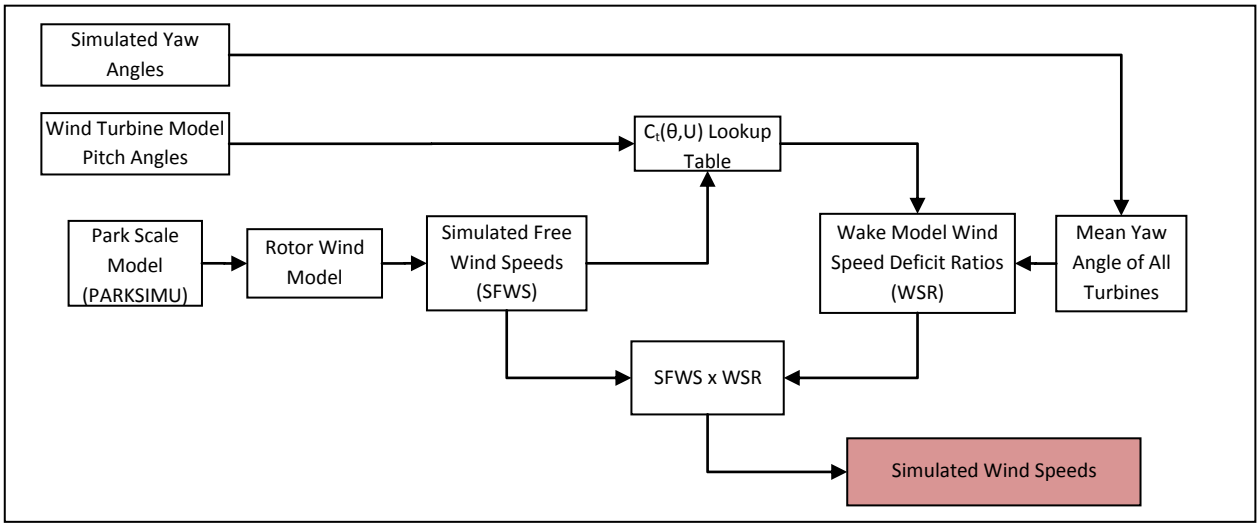

Figure 5-8: Block Diagram of Simulated Wind Model

5.4 POSSIBLE PLANT PRODUCTION MODEL

The plant production model employed in the WPPST can be configured for simulation of the power curve method or the grid methods.

5.4.1 POWER CURVE METHOD

The power curve method sub-model is a derivative of the model described in Section 4.1.5. It employs the DWM and a power curve, derived from the wind turbine model, to estimate the possible plant production. It does not include the air density or NWS corrections since the air density is assumed constant and the local flow conditions affecting the NWS measurement are not included in the WPPST. The power curve and static pitch angle trajectory for normal operation are derived from the wind turbine model ISO-Power Map assuming a constant pitch angle below rated power and a rated power set point of 2.35 MW. Details of the model are provided in Appendix I.9.

5.4.2 GRID METHODS

The grid method sub-model processes individual turbine production and status data to estimate the possible production. The possible plant production is determined from the mean production value of the measurement turbines multiplied by the total number of turbines online in the following way:

$$P_{estimate}^{Total} = \frac{\sum_{i=1}^{N} P_{MT}^{WT_i}}{\sum_{i=1}^{N} S_{MT}^{WT_i}} * \left(\sum_{i=1}^{N} S_{MT}^{WT_i} + \sum_{k=1}^{M} S_{CT}^{WT_k} \right)$$

This formulation facilitates accounting of both the measurement and control turbine statuses.

Details of the model are provided in Appendix I.8.

5.5 SELECTED SIMULATION RESULTS

The following figures depict selected simulation results for Nysted configured with both stall and pitch regulated turbines. They include both normal and down-regulated operation employing the power curve method for the estimations. The simulated wind speed and yaw angle data for all the simulation examples are depicted in Figure 5-9. All simulation data has had a 3min moving average filter applied.

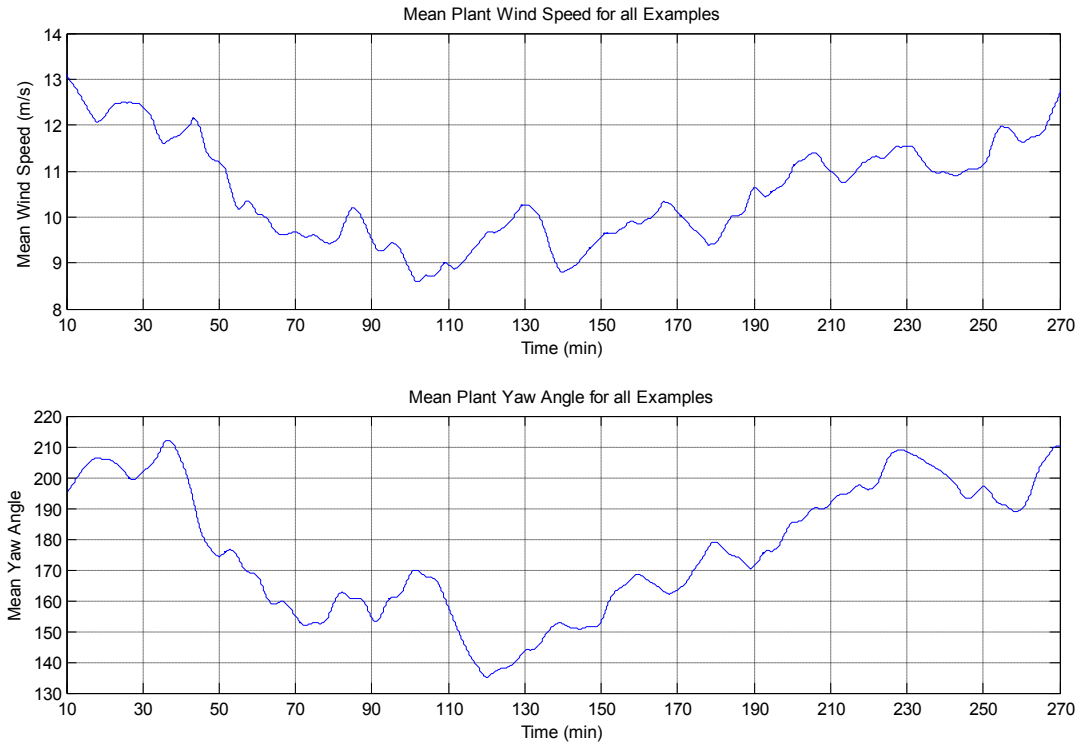

Figure 5-9: Mean Plant Wind Speed and Yaw Angle for Selected Simulation Examples

Figure 5-10 depicts normal operation. In this case the plant set-point is set to rated production. Note that the rated plant production with the stall or pitch regulated turbines is 169.2 MW and 144MW, respectively.

Figure 5-11 depicts a 20MW delta regulation between time 33 and 200 minutes. Note that the possible production estimate without the DWM under-predicts the possible production of the stall regulated configuration but over-predicts for the pitch regulated configuration.

Figure 5-11 depicts a 10MW absolute limitation regulation between time 33 and 200 minutes. Again the possible production estimate without the DWM under-predicts the possible production of the stall regulated configuration but over-predicts for the pitch regulated configuration.

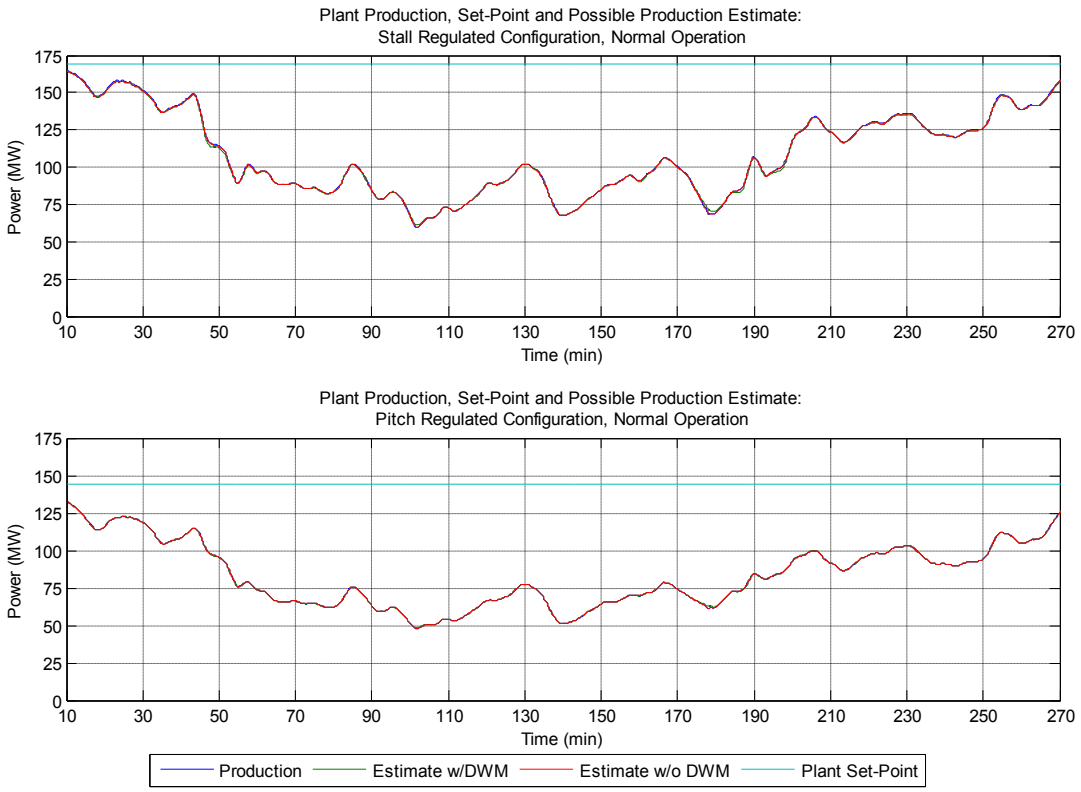

Figure 5-10: Plant Production for Nysted Configured with Stall (top plot) and Pitch (bottom plot) Regulated Turbines: Normal Operation

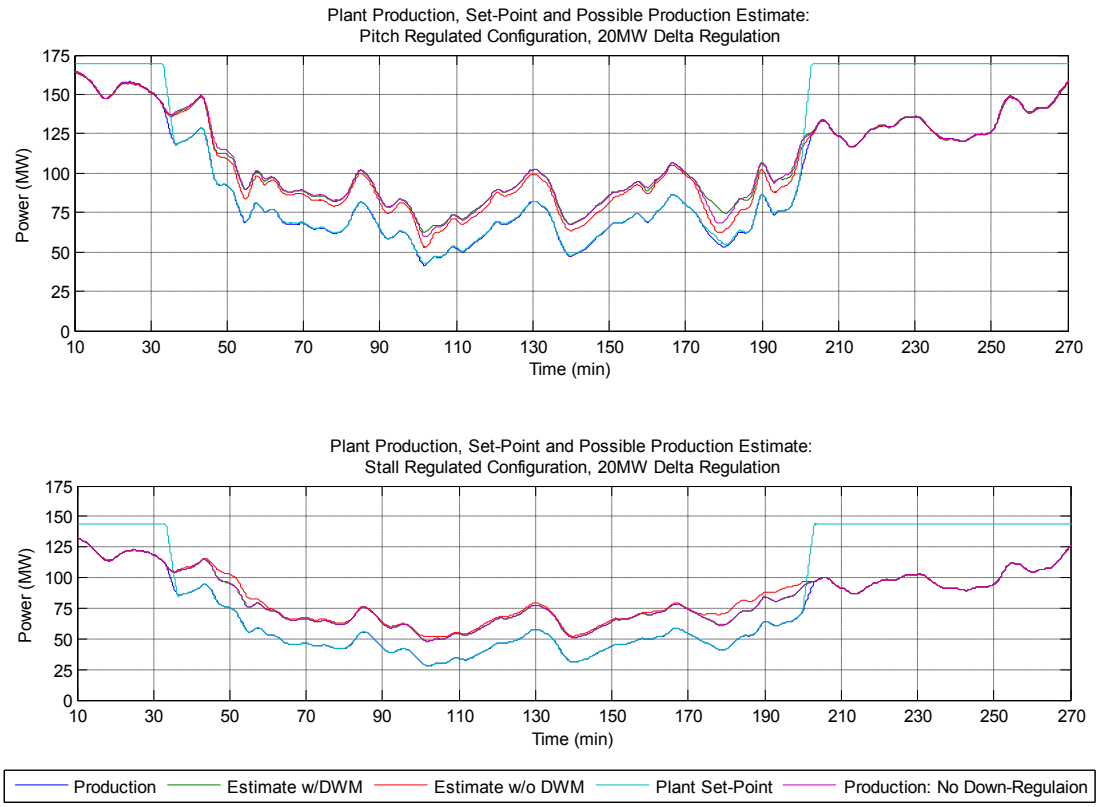

Figure 5-11: Plant Production for Nysted Configured with Stall (top plot) and Pitch (bottom plot) Regulated Turbines: 20MW Delta Operation

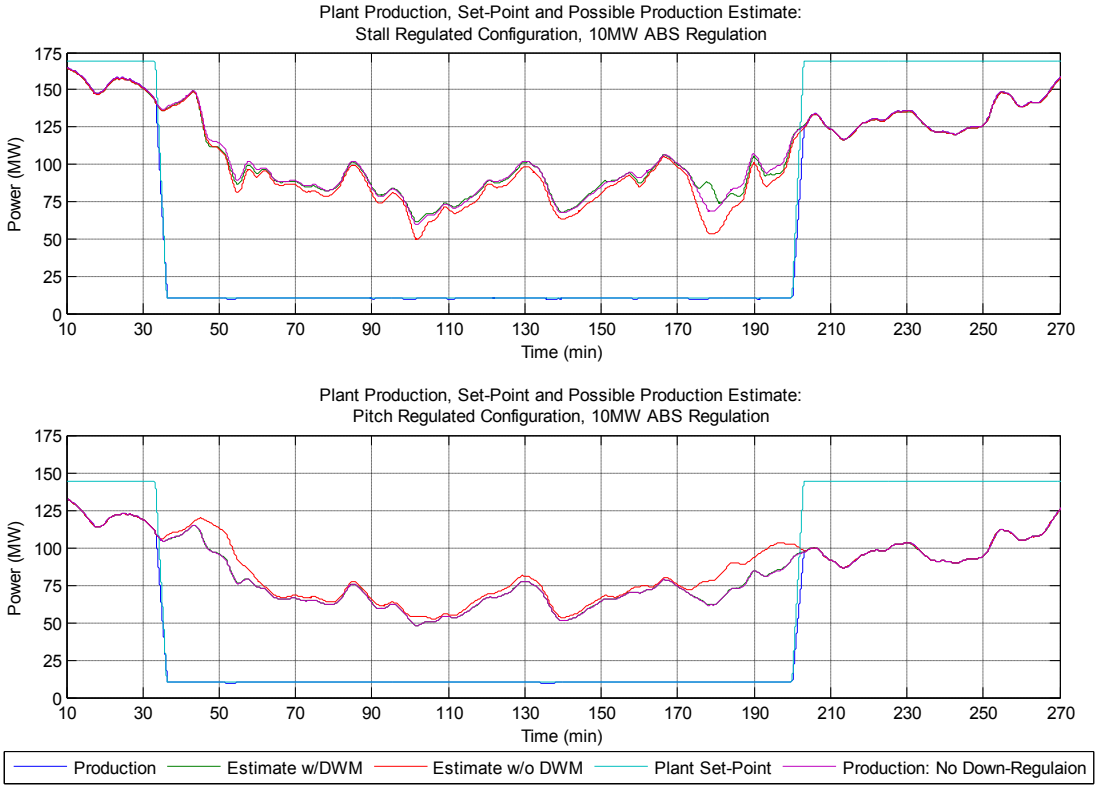

Figure 5-12: Plant Production for Nysted Configured with Stall (top plot) and Pitch (bottom plot) Regulated Turbines: 10MW Absolute Limitation

6 CONCLUSION

Two methods for estimating the possible production of a large wind plant during down-regulation have been investigated. The Power Curve Method, which is an extension of the current approach at Nysted, employs real time nacelle wind speed and turbine operation data to calculate corrections for the NWS measurement and wake effects during down-regulated operation. The corrections are applied to the NWS measurements to estimate the wind speeds at each turbine if no down-regulation had taken place. These wind speed are used with an appropriate power curve to determined the possible plant production. The Grid Method, which requires no wake model development or wind speed measurement error correction, divides the wind plant into two separate grids; one grid is used to estimate the total plant production while the other is down regulated to meet the desired plant control objective. Models of both methods have been developed and incorporated into a wind plant simulation tool, intended to represent Nysted.

Results from analysis of measurement and simulation data from application of the Power Curve Method indicate an improvement in the estimate of possible production during down-regulation over the currently employed method at Nysted. The largest improvement is gained from correction of the wind speed measurement error; whereas the dynamic wake correction contributes relatively little.

Results from analysis of simulations of the Grid Method indicate that both the split grid and interlaced grid variations could be successfully employed for estimation of the possible plant production and overall wind plant control. The split grid variation has zero mean estimate error but significant scatter. The scatter is due predominantly to spatial variations in the ambient wind throughout the wind plant and the down-wind effects of down-regulated turbines for unfavorable wind directions. The interlaced grid method has less scatter overall but interacting wakes during down-regulation include a bias error in the estimate. For low levels of down-regulation the bias error is small.

7 REFERENCES

1. Nysted Havmøllepark. [Online] www.nystedhavmoellepark.dk .

2. *The Horns Rev Wind Farm and the Operational Experience with the Wind Farm Main Controller.* **Kristoffersen, J.R.** 2005. Copenhagen Offshore Wind Conference, 26-28 October.

3. **ABB.** *Nysted Havemoellepark Teknisk Specifikation TS-2 as Built.* s.l. : ABB A/S, 2006. Doc No. 1KEL000129D0120 Internal DONG Document.

4. **Eltra.** *Wind Turbines Connected to Grid with Voltages above 100kV, Regulation TF 3.2.5.* s.l. : Eltra, 2004.

5. *Wind Turbine Generator Systems Part 12: Wind Turbine Power Performance Testing.* **IEC.** s.l. : IEC, 1998. IEC-61400-12:1998.

6. **Hansen & Henneberg.** *Notat Vedr. Undersøgelse Af Indflydelse Af Møllereguleringen På Målinger Fra Nacelleanemometer, 3908not006, Rev. 0.26.07.2005.* s.l. : Hansen & Henneberg, 2005.

7. **Jensen, N.O.** *A Note on Wind Generator Interaction.* Roskilde, DK : Risoe National Laboratory, 1983. RISOE-M-2411.

8. *A Simple Model for Cluster Efficiency.* **Katic, I., J. Højstrup and N.O. Jensen.** Rome, Italy : s.n., 1986. Proc. European Wind Energy Conference and Exhibition. pp. 407-410.

9. **Laboratories, Risoe National.** WAsP – the Wind Atlas Analysis and Application Program. [Online] www.wasp.dk.

10. **Burton, T.,Sharpe, D.,Jenkins, N. Bossanyi, E.** *Wind Energy Handbook.* s.l. : Wiley, 2001.

11. **Hansen, M. O. L.** *Aerodynamics of Wind Turbines.* London : James and James, 2000.

12. **Rathmann, Ole.** personal communication, Risoe.

13. **Weisstein, Eric W.** "Circle-Circle Intersection." From MathWorld--A Wolfram Web Resource. . [Online] http://mathworld.wolfram.com/Circle-CircleIntersection.html.

14. **Stoddard, F. S., Eggleston, D. M.** *Wind Turbine Engineering Design.* s.l. : Van Nostrand Reinhold, 1987.

15. *New Equations for Computing Vapor Pressure and Enhancement Factor.* **Buck, A. L.** 1981, J. Appl. Meteorol., Vol. 20, pp. 1527-1532. equation downloaded from: http://cires.colorado.edu/~voemel/vp.htm.

16. **Perstrup, Claus.** personal communication, DONG Energy.

17. *Array Efficiency at Horns Rev and the Effect of Atmospheric Stability.* **Jensen, Leo.** Milan, Italy : s.n., 2007. EWEC Proceedings.

18. **DONG Energy.** *WTC-3_INFO_CS_051031 R1.01.xls.* Internal DONG document.

19. **Eisen, S., Peroches, E.,.** *Wind Turbine Aerodynamics – 4131: Assignment #3.* Depatment of Wind Energy, Technical University of Denmark. Lyngby, Denmark : s.n., 2005.

20. *Power Fluctuations from Large Wind Farms.* **Sørensen, P., et al.** s.l. : IEEE Trans. Power Systems, 2007, Vol. 22, pp. 958-965 .

21. *Wind Models for Simulation of Power Fluctuations from Wind Farms.* **Sørensen, P., Hansen, A.D., Carvalho Rosas, P.E.,.** 90:, 2002, Journal of Wind Engineering and Industrial Aerodynamics, pp. 1381–1402.

8 FURTHER READING

- Sørensen, P., Hansen, A.D., Iov, F., Blaabjerg, F.,Donovan, M.H., (2005), Wind Farm Models and Control Strategies, Risø National Laboratory, DK-4000 Roskilde, Denmark, Risø-R-1464.
- Sørensen, P., et al, (2005), Operation and Control of Large Wind Turbine and Wind Farms – Final Report, Risø National Laboratory, DK-4000 Roskilde, Denmark, Risø-R-1532.
- Frandsen, S. (1992), On the Wind Speed Reduction in The Center of Large Clusters of Wind Turbines, Jour. of Wind Engineering and Industrial Aerodynamics, 39, pp. 251-265
- Barthelmie, R., Frandsen, S., Jensen, L., Mechali, M., Perstrup, C. (2005), Verification of an efficiency model for very large wind turbine clusters". Copenhagen Offshore Wind Conference, 26-28 October, Copenhagen, Denmark.
- Rathmann, O., Barthelmie, R., Frandsen, S. (2006), Turbine Wake Model for Wind Resource Software, Risø National Laboratory, Proc. European Wind Energy Conference and Exhibition, Athens, Greece.
- Frandsen, S. et al. (2006), Analytical Modeling of Wind speed Deficit in Large Offshore Wind Farms, Wind Energy 9, 39-53.
- Frandsen, S. (2007), Turbulence and Turbulence Generated Structural Loading in Wind Turbine Clusters, Risø National Laboratory, DK-4000 Roskilde, Denmark, Risø-R-1188.
- Sørensen, P., Hansen, A.D., Carvalho Rosas, P.E., (2002), Wind models for simulation of power fluctuations from wind farms, Journal of Wind Engineering and Industrial Aerodynamics, 90:1381–1402.
- *Elsam. Havmøller.Horns Rev.Blokleder.Design Dokument,* 236493 Bloklederdokumentation.DOC, Internal DONG document.
- E-On Netz GmbH, Grid Code, High and Extra High Voltage, August 2003.
- Jauch, C.; Hansen, A.D.; Sørensen, P.; Blaabjerg, F., *Simulation Model of an Active-Stall Fixed-Speed Wind Turbine Controller*. Wind Eng. (2004) 28 , 177-198.
- Tripod Wind Energy A/S(2005), *Nysted Offshore Wind Farm: Park Regulation*, internal DONG Report.
- Tripod Wind Energy A/S(2005), *Single Row Turbulence Intensity versus Atmospheric Stability: Nysted Offshore Wind Farm*, internal DONG Report.
- Tripod Wind Energy A/S(2005), *Wind Sheer and Turbulence Intensity: Nysted Offshore Wind Farm*, internal DONG Report.
- Spera, D.A. (editor, 1994), *Wind Turbine Technology*, ASME Press
- Ackermann, T. (editor, 2005), *Wind Power in Power Systems*, Wiley.
- Eisen, S, *Wind Plant Simulation Tool for Operation and Control of Large Wind Plants,* Special Course DTU, 2007.

9 APPENDICES

Appendices are found in the separate document:

Real_Time_Estimation_of_Possible_Power_APPENDICES.pdf